Paleozoic magmatism and syngenetic massive sulphide deposits of the Eagle Bay assemblage, Kootenay terrane, southern British Columbia[1,2]

Suzanne Paradis

Geological Survey of Canada, 9860 West Saanich Road,
Sidney, British Columbia, V8L 4B2, Canada, suparadi@NRCan.gc.ca

Sean L. Bailey

687 McAllister Loop SW, Edmonton, Alberta, T6W 1M6, Canada

Robert A. Creaser

Department of Earth and Atmospheric Sciences, University of Alberta,
Edmonton, Alberta, T6G 2E3, Canada

Stephen J. Piercey

Mineral Exploration Research Centre, Department of Earth Sciences,
Laurentian University, 933 Ramsey Lake Road, Sudbury, Ontario, P3E 6B5, Canada

Paul Schiarizza

B.C. Geological Survey, P.O. Box 9333, Stn Prov Govt,
Victoria, British Columbia, V8W 9N3, Canada

Abstract

The Eagle Bay assemblage of Kootenay terrane includes Lower Cambrian and Devonian-Mississippian metavolcanic, metaplutonic and metasedimentary rocks that host a variety of volcanic- and sediment-hosted, polymetallic massive sulphide deposits. The Lower Cambrian succession consists of continental-slope siliciclastic rocks that are overlain by alkalic (OIB) to subalkalic (MORB) mafic volcanic rocks, interlayered with marble inferred to correlate with the

---

archaeocyathid-bearing Tshinakin limestone. Alkalic basalts have εNd_{540} values of +4.3 to +5.7, and MORBs have εNd_{540} values of +8.2 and +8.3. These Cambrian basalts formed in a continental rift setting along the ancient continental margin of North America.

The Devonian-Mississippian succession comprises metamorphosed clastic sedimentary rocks and mafic to felsic volcanic and synvolcanic intrusive rocks. Mafic volcanic rocks of the Tsalkom Formation have N-MORB geochemical characteristics identical to mafic volcanic rocks of the Upper Devonian-Middle Permian Fennell Formation, which suggests similar genesis within a back-arc oceanic basin. Devonian mafic flows of unit EBM are alkalic (OIB), whereas Upper Devonian-Lower Mississippian mafic tuffs of unit EBA are subalkalic, transitional andesites/basalts typical of an arc environment. Their evolved Nd isotopic signature (εNd_{360} values = −6.5 to −6.8) indicates input of crustal material. Devonian-Mississippian intermediate to felsic volcanic flows, tuffs and intrusions of units EBA, EBF and EBAF have arc affinities, and evolved Nd isotopic signatures (εNd_{360} = −3.3 to −13.7). These rocks record deposition within an evolving continental arc along the western edge of ancestral North America.

Rocks of the Eagle Bay assemblage record a tectonically active continental margin in Early Cambrian and Late Devonian-Mississippian. Continental extension and rifting occurred in Early Cambrian and generated small volcanic-hosted massive sulphide deposits in OIB-type mafic volcanic rocks, and volcanic-sediment hosted massive sulphide deposits in associated clastic sedimentary rocks. Volcanic arc and back-arc development, and rifting of that arc in Late Devonian-Mississippian, produced a variety of stratabound, polymetallic, volcanic-hosted massive sulphide deposits.

Résumé

L'assemblage de Eagle Bay du terrane de Kootenay comprend des roches métavolcaniques, métaplutoniques et métasédimentaires du Cambrien inférieur ainsi que du Dévonien au Mississipien, qui renferment une variété de gisements de sulfures massifs polymétalliques au sein de roches volcaniques et sédimentaires. La succession du Cambrien inférieur est constituée de roches siliciclastiques de pente continentale surmontées par des roches volcaniques mafiques alcalines (OIB) à subalcalines (MORB) interstratifiées avec des marbres, dont on présume qu'ils correspondent au calcaire à archéocyathes de Tshinakin. Les basaltes alcalins ont des valeurs εNd_{540} de +4.3 à +5.7, et les MORB ont des valeurs εNd_{540} de +8.2 et +8.3. Ces basaltes cambriens se sont formés dans un milieu d'ouverture de fosse tectonique continental le long de l'ancienne marge continentale de l'Amérique du Nord.

La succession dévonienne à mississipienne comprend des roches sédimentaires clastiques métamorphisées ainsi que des roches volcaniques mafiques à felsiques et des roches intrusives synvolcaniques. Les roches volcaniques de la Formation de Tsalkom ont des caractéristiques géochimiques N-MORB identiques aux roches volcaniques mafiques de la Formation Fennell du Dévonien supérieur au Permien moyen, ce qui indique des conditions de genèse semblables aux bassins d'arrière-arc. Les coulées dévoniennes de l'unité EBM sont alcalines (OIB), alors que les tufs du Dévonien supérieur à Mississipien inférieur de l'unité EBA sont des andésites/basaltes subalcalins de transition qui sont typiques d'un milieu d'arc insulaire. Leurs signatures isotopiques Nd (valeurs εNd_{360} = −6.5 à −6.8) indiquent qu'il y a eu apport de matériaux crustaux. Du Dévonien au Mississipien, les coulées volcaniques de composition intermédiaire à felsique, les tufs et les intrusions des unités EBA, EBF et EBAF sont d'affinité d'arc insulaire, et ont généré des signatures isotopiques Nd (εNd_{360} = −3.3 à −13.7) évoluées. Ces roches témoignent d'un milieu de dépôt d'arc insulaire continental en évolution, le long de la bordure ouest de l'ancienne marge de l'Amérique du Nord.

Les roches de l'assemblage de Eagle Bay témoignent d'un milieu de marge continentale active au Cambrien inférieur ainsi qu'au Dévonien supérieur jusqu'au Mississipien. Une extension continentale et l'ouverture d'un fossé tectonique se sont produites au Cambrien inférieur, et cela a entraîné la formation de petits gisements de sulfures massifs au sein de roches volcaniques mafiques de type OIB, ainsi que de gisements de sulfures massifs volcano-sédimentaires dans les roches sédimentaires clastiques associées. Le développement de milieux de volcanisme d'arc et d'arrière-arc, et l'ouverture d'une fosse tectonique dans cet arc, du Dévonien supérieur au Mississipien, a entraîné la formation d'une variété de gisements de sulfures massifs, stratiformes, polymétalliques et contenus dans des roches volcaniques.

INTRODUCTION

The Eagle Bay assemblage of the Kootenay terrane in south-central British Columbia, Canada (Fig. 1) includes variably deformed and metamorphosed Lower Cambrian and Upper Devonian to Mississippian volcanic, intrusive and sedimentary rocks that host several polymetallic precious and base metal massive sulphide deposits (Fig. 2). A number of these, including Rea Gold, Homestake and Samatosum, have had limited past production, and others (*e.g.*, Mount Armour, Harper Creek) have had extensive exploration and some development.

Since the discovery of the sulphide deposits in the Eagle Bay assemblage, several studies have been undertaken to understand its stratigraphy and tectonic history. Regional geological mapping was done by Campbell (1964), Campbell and Okulitch (1973), Okulitch (1974, 1975), and Schiarizza and Preto (1987). However, limited petrochemical studies have been completed on the volcanic and plutonic rocks of the Eagle Bay assemblage (Höy, 1987, 1999; Bailey *et al.*, 2001; Hughes, 2001). More recently, a metallogenic and mineral deposit study conducted under the auspices of the Ancient Pacific Margin NATMAP (National Mapping Program), a multi agency,
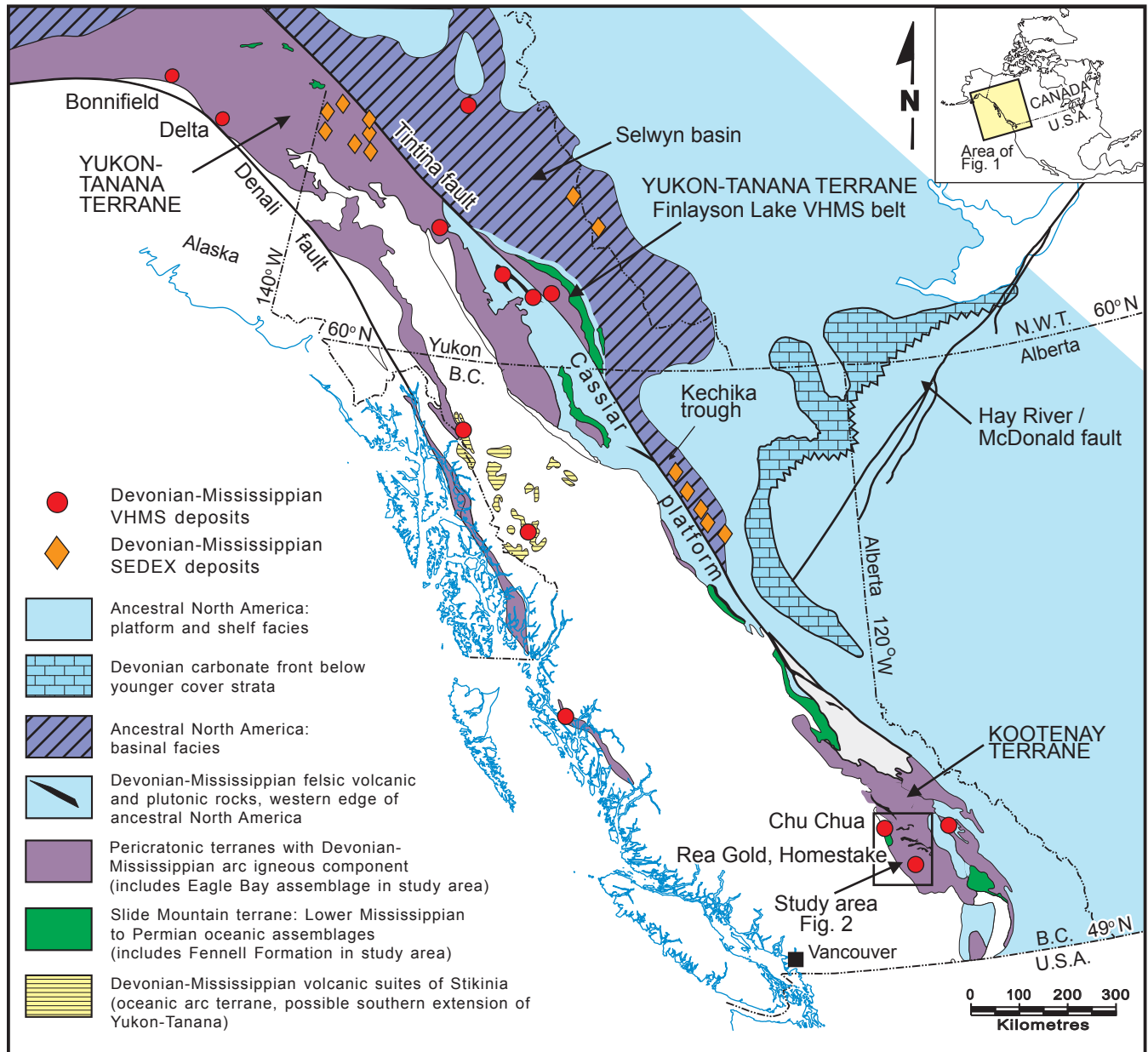
Figure 1. *Location of the study area within the Eagle Bay assemblage of the Kootenay terrane in southern British Columbia (modified from Nelson* et al*., 2002). Note the trend of the Devonian–Mississippian volcanic-hosted massive sulphide (VHMS) deposits in the pericratonic terranes (Kootenay and Yukon-Tanana terranes) and the sedimentary exhalative (SEDEX) deposits in continent-margin basins and in the pericratonic Yukon-Tanana terrane.*
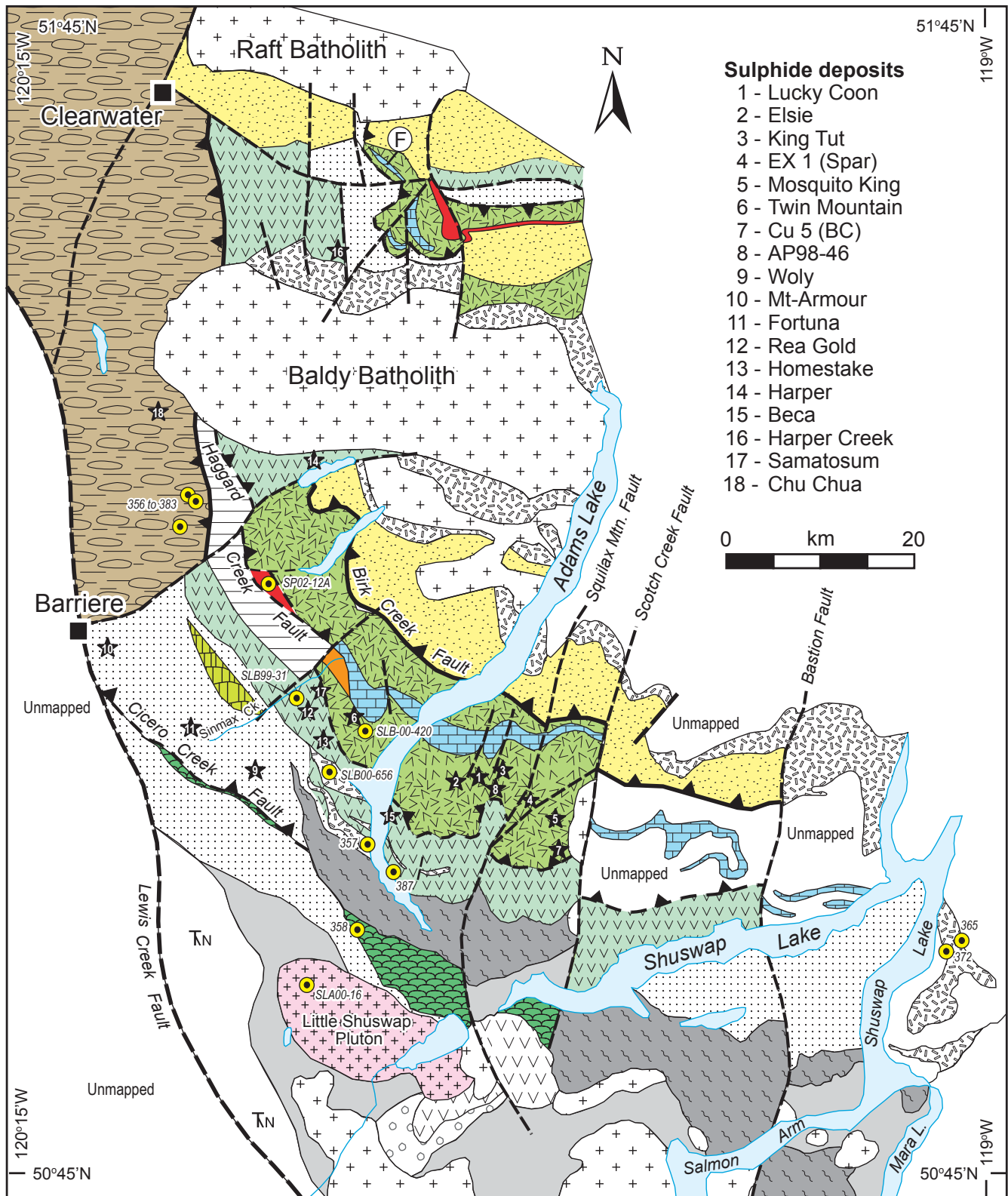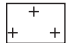
Figure 2. *Simplified geological map of the Eagle Bay assemblage with location of some of the major massive sulphide deposits (modified from Schiarizza and Preto, 1987; Thompson and Daughtry, 1998; Hughes, 2001; Bailey, 2002). For description of sulphide deposits, see Table 1.*
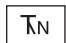
Legend

Eocene

Kamloops Group: volcanic flows, breccia, tuff, conglomerate

Jurassic-Cretaceous

granite to granodiorite and quartz monzonite pluton

Upper Triassic

Nicola Group (Quesnel terrane): augite-phyric flows, breccia, and tuff; volcanic sandstone, siltstone, and mudstone
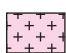
Devonian-Permian

Fennell Formation (Slide Mountain terrane): mafic volcanic rocks, gabbro, diorite, chert, argillite, and minor limestone, conglomerate, and quartz-feldspar-phyric rhyolite

Eagle Bay assemblage (Kootenay terrane)

Devonian-Mississippian

EBP: phyllite, slate, grit

granodiorite, granite, and diorite pluton (Upper Devonian)

granite to diorite sill and dike (Upper Devonian-Lower Mississippian)

EBAF: feldspar-phyric and quartz-feldspar-phyric felsic tuff

EBA-EBF: felsic to intermediate volcanic flow and tuff; minor mafic tuff, phyllite, siltstone, grit

EBM: mafic volcanic rocks; minor sedimentary rocks

EBS: clastic sedimentary rocks, limestone, mafic tuff and flows

EBL ~ Sicamous Formation: calcareous black phyllite and argillaceous limestone

Tsalkom Formation: mafic volcanic rocks

Silver Creek Formation: micaceous quartzite, marble, calc-silicate, amphibolitic schist

Chase Formation: calcareous quartzite

Lower Cambrian

EBG: mafic volcanic rocks (alkalic basalt) and Tshinakin limestone; [   ] subalkalic basalt

Paleozoic (age unknown)

EBQ/EBH: clastic sedimentary rocks

undivided

★ Sulphide deposit

Normal fault

Thrust fault, defined

Thrust fault, assumed

Ⓕ Archaeocyathid fossil locality

⊙ Geochronology sample site

cooperative bedrock mapping project, was initiated in 1999 (Thompson *et al.*, 2000).

This paper presents regional lithogeochemical and isotopic datasets from the volcanic and synvolcanic intrusive rocks of the Eagle Bay assemblage. The geochemistry of the mafic volcanic rocks of the Tsalkom Formation is also presented and compared to mafic volcanic rocks of the Fennell Formation of south-central British Columbia. The petrogenesis of these rocks provides insights into: (1) the Paleozoic tectonic evolution of the western North American continental margin; and (2) the local- and regional-scale volcanic and tectonic controls on sulphide mineralization.

REGIONAL GEOLOGY

The pericratonic Kootenay terrane in the southeastern Canadian Cordillera (Fig. 1) hosts volcanic, intrusive and sedimentary rocks of the Eagle Bay assemblage. The Kootenay terrane lies within the Omineca belt, one of five morphological belts of the Canadian Cordillera (Schiarizza and Preto, 1987; Wheeler and McFeely, 1991; Monger, 1993). The Omineca belt refers to variably deformed and metamorphosed rocks of continental affinity, that are exposed east of Mesozoic arc and back-arc sequences (*i.e.*, Intermontane belt) and west of deformed Paleozoic continental margin sedimentary rocks (*i.e.*, Foreland belt). The Kootenay terrane comprises dominantly lower to mid-Paleozoic sedimentary and volcanic rocks deposited on the distal western edge of ancestral North America (Gabrielse *et al.*, 1991; Colpron and Price, 1995; Logan and Colpron, this volume).

The Eagle Bay assemblage, as described by Schiarizza and Preto (1987), consists of deformed and metamorphosed (greenschist to lower amphibolite facies) Lower Cambrian to Mississippian sedimentary and volcanic rocks (Fig. 2). They are intruded by Upper Devonian-Lower Mississippian foliated granite to diorite sills and dikes and by Middle to Upper Jurassic and Cretaceous hornblende-biotite granite to granodiorite, biotite-muscovite granite and biotite monzogranite of the Raft and Baldy batholiths; and they are overlain by Eocene volcanic rocks of the Kamloops Group (Schiarizza and Preto, 1987; Logan and Mann, 2000). The Eagle Bay assemblage is flanked by high-grade metamorphic rocks of the Shuswap metamorphic complex to the east, and by low-grade metamorphic rocks of the Fennell Formation of the Slide Mountain terrane to the west. The Upper Devonian to Middle Permian Fennell Formation was thrust over rocks of the Eagle Bay assemblage in Early Mesozoic time (Schiarizza and Preto, 1987; Monger *et al.*, 1991; Monger, 1993). Rocks of the Eagle Bay assemblage and Fennell Formation were deformed and metamorphosed during the Jurassic-Cretaceous orogeny (Schiarizza and Preto, 1987; Gabrielse *et al.*, 1991). Despite regional deformation and metamorphism, rocks of the Eagle Bay assemblage commonly preserve original igneous and sedimentary textures. For this reason, sedimentological and igneous terminology is used where appropriate in this paper.

Schiarizza and Preto (1987) divided the Eagle Bay assemblage into four northeast-dipping thrust sheets that collectively contain a succession of Lower Cambrian rocks overlain by a succession of Devonian-Mississippian rocks. Within the successions, the strati-

graphic relationship between the various units is conformable; however, west-verging thrust faults emplaced the Lower Cambrian succession over the Devonian-Mississippian succession during the Jurassic-Cretaceous orogeny (Schiarizza and Preto, 1987; Gabrielse *et al.*, 1991).

The older stratigraphic succession of the Eagle Bay assemblage consists of Upper Proterozoic-Paleozoic clastic sedimentary rocks (units EBH and EBQ of Schiarizza and Preto, 1987) overlain by Lower Cambrian mafic volcanic rocks (unit EBG of Schiarizza and Preto, 1987) that contain a sparsely fossiliferous, shallow-water carbonate unit, the archaeocyathid-bearing Tshinakin limestone (Figs. 2, 3). This succession is overlain by a Devonian-Mississippian succession that consists of mafic to felsic volcanic rocks (units EBM, EBA and EBF of Schiarizza and Preto, 1987), clastic sedimentary rocks (units EBS, EBL, EBK and EBP of Schiarizza and Preto, 1987), and synvolcanic granitic to dioritic sills, dikes and plutons (Figs. 2, 3). In the study area, we include mafic volcanic rocks of the Tsalkom Formation, carbonaceous limestone of the Sicamous Formation, clastic sedimentary rocks of the Silver Creek Formation and calcareous quartzite of the Chase Formation in the Eagle Bay assemblage.

Sulphide deposits of the Eagle Bay assemblage include stratabound, volcanic-sediment-hosted massive sulphide (VSHMS) and volcanic-hosted massive sulphide (VHMS) deposits in unit EBG, and polymetallic precious and base metal VHMS deposits in units EBA and EBF (Table 1). Small, polymetallic massive sulphide lenses also occur in mafic volcanic rocks and clastic sedimentary rocks of unit EBS. Disseminated Cu-Au-Ag sulphides and massive to semi-massive magnetite-sulphide layers occur in mafic to felsic tuffs and clastic sedimentary rocks of units EBA and EBQ in close proximity to Late Devonian-Early Mississippian granite to diorite sills and dikes.

STRATIGRAPHY OF THE EAGLE BAY ASSEMBLAGE

Stratigraphic descriptions and observations are from Schiarizza and Preto (1987), Hughes (2001), Bailey (2002) and the first author. Stratigraphic nomenclature follows Schiarizza and Preto (1987), who assigned each map unit a combination of letters such as EBG, where EB represents Eagle Bay assemblage and G the lithologic unit (*i.e.*, greenstone; Fig. 3). In this paper, we describe volcanic rocks of units EBG, EBM, EBA, EBF and EBAF (new unit), and the Tsalkom and Fennell formations, which were sampled for geochemical analysis. Protoliths of map units consist of mafic to felsic volcanic and intrusive rocks interlayered with sedimentary rocks (Fig. 2).

Unit EBG consists predominantly of calcareous chlorite-sericite-quartz schist and chlorite-sericite schist derived from massive basaltic flows, flow breccias, fine-grained basaltic tuffs, and rare vesicular and (or) amygdaloidal pillowed flows (Schiarizza and Preto, 1987; Hughes, 2001; Bailey, 2002). The volcanic rocks are typically fine-grained, aphyric, well foliated and platy; some tuffs and flows are feldspar-phyric (~ 5 vol.%). They are composed of chlorite, actinolite, epidote, albite, calcite, iron oxides and minor amounts of quartz, titanite and magnetite. Millimetre- to centimetre-wide veins

of quartz and calcite are common, and distinguish these rocks from other mafic volcanic rocks of the Eagle Bay assemblage. The volcanic rocks are interlayered with limestone (assumed to belong to the Lower Cambrian Tshinakin limestone), phyllite, chert, quartzite, grit and conglomerate (Schiarizza and Preto, 1987; Bailey, 2002). Age constraint on the succession is based on the Lower Cambrian, archaeocyathid-bearing Tshinakin limestone (*ca.* 530 Ma) that is interlayered with the mafic volcanic rocks north of the Baldy batholith (Schiarizza and Preto, 1987). A similar, thick limestone succession is interlayered with mafic volcanic rocks south of the Baldy batholith; it also is inferred to be the Tshinakin limestone. The structural top and basal section of unit EBG are in thrust contact with various units of the Devonian-Mississippian succession and unit EBH/EBQ (Fig. 2). The mafic volcanic rocks host several small showings of massive to semi-massive sulphide lenses and sulphide-bearing quartz veins along faults. Siliceous, carbonaceous and calcareous phyllites on the Adams Plateau, east of Adams Lake, host several thin sheets of stratabound massive sulphide Zn-Pb-Ag (±Cu, ±Au) deposits and occurrences, such as Lucky Coon, King Tut, Spar and Mosquito King (Höy, 1999; Fig. 3, Table 1, Table DR1 [see footnote 2]).

Unit EBM (Fig. 3) is dominated by chlorite schist derived from mafic, unpillowed and pillowed volcanic flows. Quartzite, phyllite and bedded chert are interlayered with the volcanic rocks. Unit EBM is exposed in a NW-SE belt north of Sinmax Creek, where it stratigraphically overlies Devonian sedimentary rocks of unit EBS in the core of a west-verging syncline. Schiarizza and Preto (1987) described another belt of unit EBM south of the northeast-dipping Cicero Creek fault; however, the petrographic and chemical differences between them (this study) suggest the latter belt represents the northwest extension of the Tsalkom Formation. Mafic volcanic rocks of unit EBM are fine-grained, weakly foliated, vesicular and/or amygdaloidal, massive basaltic flows and pillowed and pillow-brecciated flows. The rocks are completely recrystallized and consist of an assemblage of chlorite, plagioclase and calcite with minor amounts of epidote, magnetite and quartz. The age of unit EBM is not known, but is presumed Devonian-Mississippian based on stratigraphic relationships (Schiarizza and Preto, 1987; Thompson *et al.*, this volume).

Unit EBA forms prominent cliffs on the slopes northeast of Sinmax Creek and on the shores of Adams Lake. It is dominated by light silvery to yellowish grey, fissile, quartz-sericite schist, ankerite-sericite schist, and chlorite-sericite schist derived from mafic to felsic volcanic tuffs and rare coherent flows (Schiarizza and Preto, 1987; Bailey *et al.*, 2000, 2001; Bailey, 2002). Bands of dark grey argillite and phyllite, pyritic chert and chert breccia are interlayered with the volcanic tuffs towards the stratigraphic top of the unit. In thin section, the quartz-sericite schist shows relict quartz and/or feldspar phenocrysts (1 to 10%) in a recrystallized matrix of quartz, sericite and minor chlorite, carbonate and albite. The Late Devonian age of unit EBA is based on a U-Pb zircon age of 387 ± 4 Ma (upper concordia intercept; Preto, 1981; Schiarizza and Preto, 1987) for a felsic volcanic rock collected on the east shore of Adams Lake (Fig. 2, geochronological site 387 Ma). Rusty to yellowish weathered quartz-sericite schist hosts the Homestake polymetallic precious and base
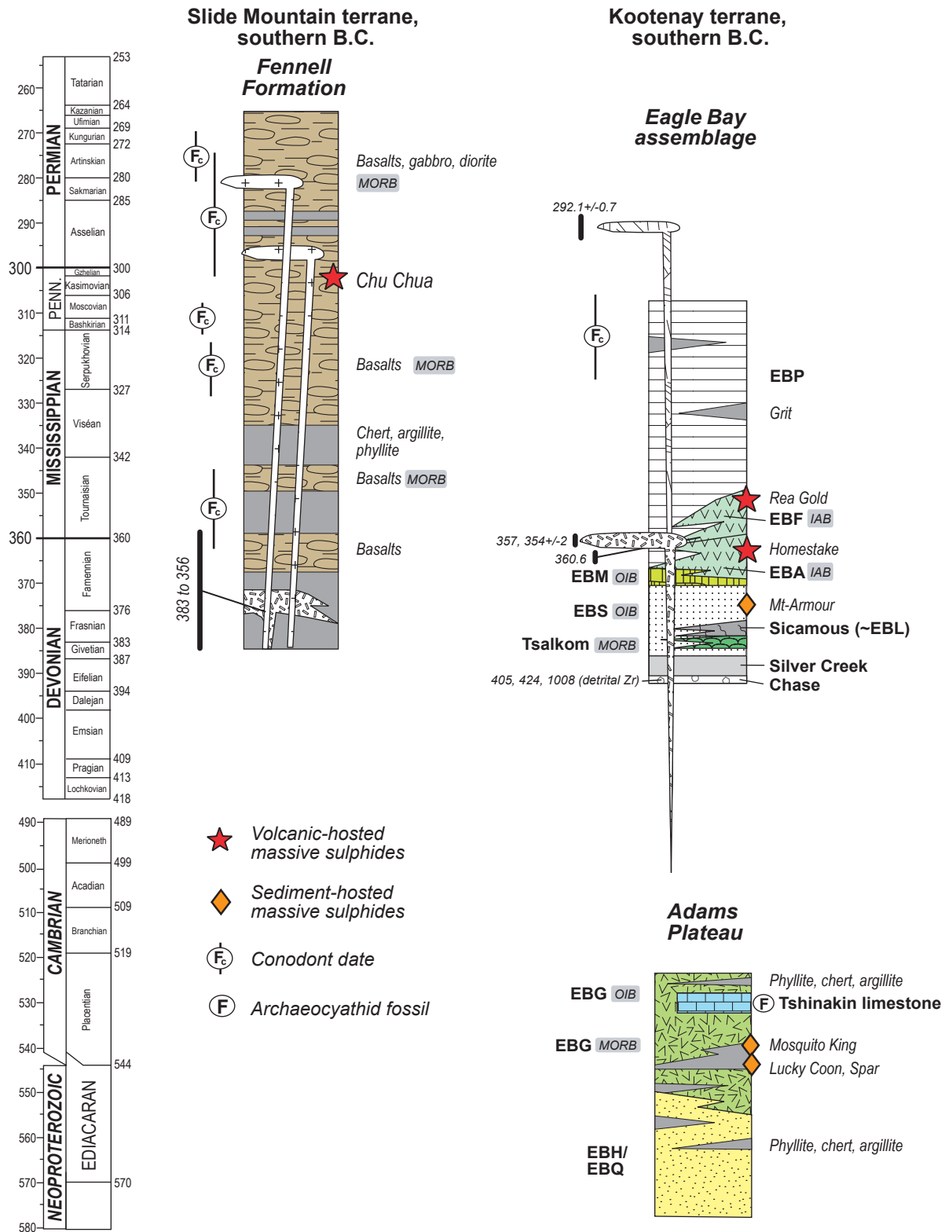
Figure 3. *Schematic stratigraphy of the Eagle Bay assemblage within the Kootenay terrane with location of some of the volcanic-hosted and sediment-hosted sulphide deposits (adapted from Schiarizza and Preto, 1987; Höy, 1991; Bailey* et al.*, 2000). See Figure 2 for legend. Penn = Pennyslvanian.*

Table 1. Major sulphide deposits of the Eagle Bay assemblage and Fennell Formation, southern British Columbia.

	Deposit	BC Minfile #	UTM[1] zone	UTM Northing	UTM Easting	Deposit Classification Class[2]/Type[3]	Status[4]	Formation / Unit	Lithology	Tonnage / grades	Comments[5]
1	Lucky Coon	082M 012	11	5661183	317276	VSHMS or SEDEX	Past-producer	EBG	Siliceous, carbonaceous, calcareous and sericitic phyllite, chloritic schist and grey limestone (unit EBG5 of Höy, 1999)	Production 1956, 1975, 1977: 30 tonnes of 264,131 g Ag, 744 kg Au, 3,822 kg Cd, 140,068 kg Pb, and 51,176 kg Zn. Inferred reserves are 68,033 tonnes.	Conformable layers, lenses and pods of semi-massive to massive sulphides. Intense deformation has caused discontinuity and marked variability in the widths of the sulphide horizons which tend to thicken in the hinge zones of folds.
2	Elsie	082M 213	11	5660607	316087	VSHMS or SEDEX	Developed Prospect	EBG	Siliceous, carbonaceous, calcareous and sericitic phyllite, chloritic schist and grey limestone (unit EBG5 of Höy, 1999)	A 0.75 m sample from an adit assayed 357 g/t Ag, 26% Pb, and 10.2% Zn.	Semi-massive layers, lenses, pods of sulphides within a siliceous gangue of the chloritic phyllite; well-banded and conformable to the schistosity and bedding.
3	King Tut	082M 013	11	5662054	318865	VSHMS or SEDEX	Showing	EBG	Siliceous band within dark phyllite (unit EBG5 of Höy, 1999)	A 60 cm sample assayed 295 g/t Ag, 7.6% Pb, and 21.5% Zn. A 90 cm sample assayed 2.7 g/t Au, 1118 g/t Ag, 28.8% Pb, and 8.4% Zn.	Sulphides occur across two one-metre thick siliceous bands within dark phyllite.
4	EX 1 (Spar)	082M 017	11	5659482	321698	VSHMS or SEDEX	Past-producer	EBG	Sericitic and siliceous calc-silicate phyllite within dark carbonaceous phyllite	Production 1952-53, 1955, 1976: 274 tonnes of 249,383 g Ag, 435 g Au, 291 kg Cu, 4,953,594 kg Pb, and 891,766 kg Zn. Indicated reserves are 11,157 tonnes at 4.83% Zn, 10.56% Pb, 187.6 g/t Ag.	Massive sulphides occur at the crests of several superimposed monoclinal folds averaging 3 m thick along a strike length of 365 m in a NE trend. The central portion of the zone is primarily massive ga bordered by a "fringe" zone of ga, sph, py, and po.
5	Mosquito King	082M 016	11	5657844	324370	VSHMS or SEDEX	Past-producer	EBG	Sericitic and siliceous calc-silicate bands within dark carbonaceous phyllite	Production 1972-73: 419 tonnes of 232,154 g Ag, 218 g Au, 42 kg Cd, 22,721 kg Pb, and 18,328 kg Zn. Indicated reserves (1985) are 33,744 tonnes at 13.3 g/t Ag, 0.83% Pb, and 2.09% Zn.	Several showings of separate discrete massive to poorly banded sulphide layers, discontinuous stringers, and disseminations over an area about 1000 m by 500 m. Sulphides are fine-grained banded ga, sph, and minor po, cp and mt in layers up to 30 cm in thickness. Immediate host rocks contain disseminated po.
6	Twin Mountain	082M 020	11	5667133	306784	VHMS / Mafic type or veins	Prospect	EBG	Pyritic and calcareous chlorite-sericite-quartz schist enclosed in chlorite schist	Average value of 11 samples is 0.90% Pb, 2.15% Zn, 8.9 g/t Ag, 0.18% Cu, and 0.17 g/t Au.	Sulphides (py, po, minor ga, sph, cp) occur within conformable carbonate-quartz-barite lenses and veins containing disseminations and massive sulphide pods.
7	Cu5 (BC)	082M 139	11	5653850	323649	VHMS / Mafic type	Developed Prospect	EBG	Siliceous phyllite, chlorite schist and amphibolite	Indicated reserves are 181,000 tonnes grading 54.9 g/t Ag, 0.2% Cu, 1.0% Pb, and 2.72% Zn.	Numerous zones of massive ga, sph, po, py and mt with minor cp occur in conformable chlorite- and/or epidote-rich layers of the chlorite schist and amphibolite.
8	AP98-46	082M 269	11	5560323	322429	VHMS / Mafic type	Prospect	EBG	Amphibolite, chlorite schist	Two samples from the massive sulphide layer returned 0.48% and 0.23% Cu, with low Pb and Zn content and traces of Ag and Au.	Small pod of rusty-weathering massive sulphides, which are banded, swirled, and cut by late cp veinlets.
9	Woly	No Minfile	11	5662951	294926	VSHMS	Showing	EBS	Pillow basalts interlayered with clastic rocks and limestone	New showing; no assay	Stringers of mal, mt, hm (±cp) and disseminations in interstices of pillow basalts
10	Mt-Armour	092P 051	10	5671390	702600	SHMS	Prospect	EBS	Phyllite, wacke and bedded chert	Drill core with best values of 0.73% Cu over 1.44 m and 4.1% Zn over 1.04 m.	Two separate stratabound and conformable sulphide layers; massive, disseminated and stockwork sulphides.
11	Fortuna	092P 044	10	5664350	708815	SHMS	Prospect	EBS	Sericite-talc schist (±ankerite, ±chlorite, ±chloritoid); quartz-eye sericite grit and quartzite	Grab samples: 1.2% Cu, 0.33% Zn, 14.6 g/t Ag, 0.45 g/t Au, and 0.47% Pb	Three alteration zones of pyritic sericite-talc schist containing discontinuous, semi-massive sulphide lenses and pods conformable to schistosity.
12	Rea Gold	082M 191	11	5669758	302798	VHMS / Bimodal-felsic type	Developed Prospect	EBF	Siliceous phyllite, chlorite schist and chert (stratigraphic footwall); tuffaceous argillite, phyllite, siltstone and wacke (stratigraphic hanging wall)	Indicated reserves for the northern and southern lenses are 376,000 tonnes grading 0.33% Cu, 2.2% Pb, 2.3% Zn, 6.1g/t Au, and 69.4 g/t Ag.	Rea Gold, Twin 3 and K-7 lenses are potentially located along the same stratigraphic level, the "Rea Zone". They consist of several thin, tabular-shaped, continuous, stratabound massive sulphide lenses underlain by a stratigraphic footwall feeder and alteration zone, and locally overlain by massive barite.
13	Homestake	082M 025	11	5665766	302061	VHMS / Bimodal-felsic type	Past-producer	EBA	Quartz-sericite schist, ankerite-sericite schist, chlorite-sericite schist; lesser argillite, phyllite, pyritic chert and chert breccia	Production 1926-27, 1935-37, 1941: 6,962 tonnes of 9,138 kg Cu, 203,310 kg Zn, 141,295 kg Pb, 8,750,829 g Ag, and 11,259 g Au.	At least 3 stratabound lenses of sulphides associated with massive and banded barite and/or quartz veins.

Table 1. continued.

	Deposit	BC Minfile #	UTM zone	UTM Northing	UTM Easting	Deposit Classification Class[2]/Type[3]	Status[4]	Formation / Unit	Lithology	Tonnage / grades	Comments[5]
14	Harper	082M 060	11	5691481	300920	VHMS / Bimodal-felsic type	Prospect	EBA	Sericite-quartz schist and calc-silicate schist	A grab sample returned 2.1% Cu, 24 g/t Ag, and 0.37g/t Au; another one returned 0.41% Cu, 6.86 g/t Ag, and 0.14 g/t Au. 1-2 metre drill intersection assayed 0.93% Zn and 0.18% Cu; and 0.15% Cu over 7.9 metres to 0.84% Cu over 4.9 metres.	Several stratabound bands of massive po and py and lesser cp, sph and ga.
15	Beca	082M 055	11	5658370	309575	VHMS / Bimodal-felsic type	Past-producer	EBA	Chloritic and siliceous schist	Production 1926: 5 tonnes of 1,498 kg Pb, 2,395 g of Ag, and 31 g Au.	Massive pods and lenses of fine-grained sulphides within a conformable lens of rusty siliceous schist.
16	Harper Creek	082M 009	11	5711134	304581	Porphyry Cu (±Au, ±Ag, ±Mo) or disseminated VHMS	Developed Prospect	EBA	Quartz-sericite schist; lesser chloritic phyllite, carbonaceous phyllite and sericitic quartzite; locally quartz-feldspath orthogneiss	Indicated open pit reserves: 53 million tonnes grading 0.37% Cu and 0.016% Mo. Bench-scale tests indicated 2.8 g/t Au and 88.4 g/t Ag. Calculated geological resources: 96 million tonnes grading 0.41% Cu, 0.045 g/t Au, and 2.5 g/t Ag.	Sulphide disseminations form discontinuous tabular-shaped zones that are slightly discordant to bedding and foliation. Massive to semi-massive lenses of mt (±cp, ±py) seem to be parallel to bedding and foliation.
17	Samatosum	082M 244	11	5669419	303562	Veins or VSHMS	Past-producer	EBG or EBF	Mafic volcanic rocks, clastic rocks and chert	Production 1989-1992: 353,129 tonnes of 3,678,016 kg Cu, 9,538,263 kg Zn, 5,069,127 kg Pb, 429,356,776 kg Ag, and 639,118 g Au.	Stratabound deformed quartz vein system with massive to disseminated sulphides; may represent the stockwork of VHMS lens.
18	Chu Chua	092P 140	10	5696070	704555	VHMS / Mafic type	Developed Prospect	Fennell Formation / upper structural division	Massive and pillow basalts	Indicated open pit reserves: 1,043,165 tonnes at 2.98% Cu, 0.3 % Zn, 0.54 g/t Au, and 10.2 g/t Ag	Two major and several minor stratiform massive sulphide lenses associated with pyritic cherty rock and lenses of mt-talc.

[1]Coordinates are given in Universal Transverse Mercator (UTM) projection, North American Datum 1983.
[2]Classes: VHMS = Volcanic-hosted massive sulphides; SHMS = Sediment-hosted massive sulphides; VSHMS = Volcanic-sediment-hosted massive sulphides; SEDEX = Sedimentary exhalative.
[3]Type is defined according to classification of Barrie and Hannington (1999).
[4]Past producer = deposits that are not currently being mined but have recorded production; Developed prospect = deposits on which exploration and development have progressed to a stage that allows a reasonable estimate of the amount (s) of one or more of the potentially mineable commodities; Showing = occurrences hosting minor *in-situ* mineralization; Prospect = occurrences documented as containing mineralization which warrants further exploration; Occurrences = uneconomic but still anomalous concentrations of minerals that are common to ore minerals elsewhere (B.C. Ministry of Energy and Mines, MINFILE; http://www.em.gov.bc.ca/Mining/Geolsurv/Minfile/manuals/coding/codeocc.htm#3.4%20STATUS).
[5]Mineral abbreviations: asp=arsenopyrite, cp=chalcopyrite, ga=galena, hm=hematite, mal=malachite, mt=magnetite, po=pyrrhotite, py=pyrite, sph=sphalerite, td=tetrahedrite, tn=tennantite.

metal sulphide/barite deposit (Fig. 3) and numerous small stratiform polymetallic precious and base metal massive to semi-massive sulphide showings (Table 1; Paradis *et al.*, 2003b).

Unit EBF consists predominantly of fragmental feldspar-phyric or quartz-feldspar-phyric schist and chlorite schist derived from intermediate to felsic volcaniclastic rocks and rare volcanic flows (Schiarizza and Preto, 1987; Bailey *et al.*, 2000, 2001; Bailey, 2002). They are interlayered with minor phyllite and quartz wacke. The volcaniclastic rocks are crystal-lithic tuffs and volcanic breccias of mainly trachytic andesite, andesite and dacite composition. Sericitic quartzo-feldspathic clasts of 1-15 cm in size make up 5 to 60% of the rock; they are flattened and stretched in the foliation plane. The rock matrix is composed of fine-grained quartz, feldspar and phyllosilicates. Unit EBF hosts the Rea Gold polymetallic precious and base metal massive sulphide deposit (Paradis *et al.*, 2003b). Schiarizza and Preto (1987) assigned unit EBF a Devonian and (or) Mississippian age, based on its stratigraphic position between Upper Devonian-Lower Mississippian unit EBA and Mississippian unit EBP. A new U-Pb zircon date of 360.6 ± 4.7 Ma (Bailey, 2002) established its age as Upper Devonian-Lower Mississippian (see the section on Geochronology).

Unit EBAF (new unit, this study) consists chiefly of fragmental feldspar-phyric and quartz-feldspar-phyric schists that are carbonatized, sericitized and chloritized. The schists are derived from dacitic ash and lapilli tuffs. They are exposed north of the Baldy batholith, where they form thin bands on the limbs of a west-verging fold-nappe cored by the Tshinakin limestone and unit EBG mafic volcanic rocks (Hughes, 2001). They also outcrop south of the Baldy batholith, where they are in fault contact with units EBP and EBG. The schists consist of chloritized, sericiticed, and carbonatized ash- and lapilli-sized fragments (<2 cm) in a fine-grained quartz, sericite, chlorite and calcite-rich matrix that contains embayed quartz phenocrysts (<10%) and/or feldspar phenocryts (≤20%). Calcite generally comprises 15-20% of the rock, and small Fe-carbonate grains are common, which give an orange speckled appearance to the schists upon weathering. New U-Pb isotopic data from magmatic zircons indicate an age of 345.8 ± 5.3 Ma (see section on Geochronology). Hughes *et al.* (2003) also reported a Late Devonian age of *ca*. 360 Ma.

In the study area, the Tsalkom Formation forms a northwest-trending, discontinuous belt that extends for approximately 62 km from south of Shuswap Lake to the town of Barriere (Fig. 2). It is dominated by dark grey chloritic schist derived from unpillowed and pillowed volcanic flows, and also includes a thin band of

serpentinite that occurs along the Cicero Creek fault. The mafic volcanic rocks are fine-grained, commonly vesicular and amygdaloidal, and consist of chlorite, albite and calcite with variable amounts of epidote, magnetite, quartz and biotite. In the study area, the Tsalkom Formation is stratigraphically overlain by calcareous phyllite of the Sicamous Formation, and is in structural contact with clastic sedimentary rocks of unit EBS along the Cicero Creek fault. The Bruen phyllite (informal name; Thompson *et al.,* this volume), which is time-equivalent to the Tsalkom and Sicamous formations, contains a rhyolitic sill that has yielded an U-Pb zircon age of *ca.* 359 Ma (Thompson *et al.,* this volume). This suggests that the Tsalkom Formation is older than latest Devonian-earliest Mississippian.

The Fennell Formation, which is part of the Slide Mountain terrane, was comprehensively described by Schiarizza and Preto (1987) and Schiarizza (1989) who divided it into lower and upper structural divisions. The lower structural division consists of a heterogeneous assemblage of bedded chert, gabbro, diabase, pillow basalt, clastic sedimentary rocks, and rare quartz-feldspar-phyric rhyolite and conglomerate. The upper structural division comprises primarily pillowed and massive basalts with minor amounts of bedded chert and gabbro. The basalts are aphanitic to fine-grained medium to dark grey or green in colour, and rarely display a tectonic foliation. Microscopically, they consist of relict clinopyroxene and plagioclase variably altered to an assemblage of chlorite, actinolite, epidote, leucoxene, titanite, and minor carbonates and quartz (Schiarizza and Preto, 1987). The diabase and gabbro are coarser grained than the volcanic rocks, but they have the same composition. Conodonts extracted from the bedded chert range in age from Early Mississippian to Middle Permian, and the quartz-feldspar-phyric rhyolite yielded U-Pb zircon ages between *ca.* 356 Ma and *ca.* 383 Ma (Schiarizza and Preto, 1987). Based on the distribution of dated units, Schiarizza and Preto (1987) suggested that the Fennell Formation was imbricated during easterly-directed thrusting over rocks of the Eagle Bay assemblage in Early Mesozoic time. Unpillowed and pillowed basalt flows of the upper structural division host the stratabound Chu Chua Cu-Zn-Au-Ag sulphide deposit (Table 1).

Upper Devonian-Lower Mississippian felsic to intermediate intrusive rocks, called granitic orthogneiss by Schiarizza and Preto (1987), occur as sill-like bodies and dikes that intruded the sedimentary and volcanic rocks of the Eagle Bay assemblage, most commonly units EBQ and EBA. The dominant lithologies are medium-grained, variably foliated sericite-feldspar-quartz and chlorite-sericite-feldspar-quartz (±epidote) schist and gneiss that display a relict granitic texture (Schiarizza and Preto, 1987). The more mafic components comprise quartzo-feldspathic lenses alternating with foliae of biotite, hornblende, chlorite and sericite (Schiarizza and Preto, 1987). The sills and dikes intrude unit EBA along both sides of Adams Lake (Fig. 2). The margins of the intrusions are fine-grained and resemble the felsic volcanic tuffs of unit EBA, whereas coarser phases with better preserved igneous textures are found in the interior of the intrusions. Similarities in composition and chemistry (see section on Lithogeochemistry), and their shallow emplacement at the base of unit EBA, suggest that these rocks are intrusive equivalents of unit

EBA volcanic rocks. They yield a Late Devonian-Early Mississippian U-Pb zircon age of *ca.* 357 Ma (Höy and Friedman, personal communication, 2001) from a foliated felsic intrusion on the western side of Adams Lake (location 51°01'08.6"N and 119°45'05.1"W; Fig. 2, geochronological site 357 Ma). Near this locality, V. Preto (1981; as R.L. Armstrong, personal communication, 1980) mentioned 367 to 379 Ma U-Pb zircon ages from a felsic synvolcanic intrusion. The latter dates are considered approximate, because laboratory procedures and precision have improved significantly since the sample collected by Preto was analyzed. The Little Shuswap pluton (Fig. 2, geochronological site SLA00-16) gives an age of 354.3 ± 2.2 Ma (S. Acton, personal communication, 2003; see section on Geochronology). A deformed quartz-feldspar-phyric dike or sill (Fig. 2, geochronological site SLB00-656) that intruded the synvolcanic granitic intrusion on the western side of Adams Lake yields an age of 291.5 ± 2.8 Ma (see section on Geochronology).

Foliated hornblende diorite and quartz diorite (not shown on Fig. 2) occur as sills and dikes within volcanic rocks of unit EBG and clastic sedimentary rocks of units EBS and EBQ; internal foliation and lineations parallel the host schistosity. U-Pb geochronology done on a diorite dike/sill that intrudes volcanic rocks of unit EBG yielded discordant zircon populations of 411 Ma, 778 Ma and 1217 Ma (Fig. 2, geochronological site SLB00-420). The $^{207}Pb/^{206}Pb$ dates likely represent minimum ages for the zircon xenocrysts (see following section).

GEOCHRONOLOGY

New U-Pb zircon ages of geological units from the Eagle Bay assemblage are presented here. The analytical procedures for U-Pb geochronology are explained in Appendix 1, and the results are listed in Table 2.

A quartz-feldspar-phyric schist from unit EBF (Fig. 2, sample and geochronological site SLB99-31) yielded a Late Devonian-Early Mississippian U-Pb zircon age of 360.6 ± 4.7 Ma (Fig. 4A). Five fractions of zircons were identified (Table 2), but only 4 are presented on Figure 4A. Fraction 1, which has low uranium content (171 ppm), consists of a single, colourless, slightly resorbed zircon prism, with a possible tip overgrowth interpreted to be a xenocryst. The older $^{207}Pb/^{206}Pb$ date of ~750 Ma for this fraction is consistent with the presence of a Precambrian inherited Pb component. Fraction 2 is made of 9 tan coloured euhedral prisms with a length-to-width ratio ranging from 2:1 to equant. Fraction 3 consists of 15 tan euhedral zircons that are slightly resorbed. Fraction 4 is a single angular tan zircon fragment, and fraction 5 consists of 11 angular, transparent, tan zircon fragments. Fractions 2, 3 and 5 are discordant, indicating that some Pb may have been lost during deformation and metamorphism. Linear regression of these fractions yields an age of 360.6 ± 4.7 Ma, which is interpreted to be the crystallization age of unit EBF. The reverse discordance displayed by fraction 4 may be related to incomplete zircon dissolution and was not used in the age calculation.

A coherent quartz-feldspar-phyric flow from unit EBAF (Fig. 2, sample and geochronological site SP02-12A) yielded abundant zircons that varied in shape, size (30-200 μm) and colour. Most zircon

crystals were very rounded, pink to brown equant to elliptical grains. Some of these had the appearance of detrital or xenocrystic zircon. A smaller proportion of large subhedral prismatic grains and tiny euhedral colourless prismatic grains (2:1 aspect ratio) were also present. The U-Pb results for three single pink subhedral equant grains are presented in Table 2 and on a concordia diagram in Figure 4B. The chemistry of these three zircon grains is similar, with consistent uranium contents (165-242 ppm), Th/U (0.35-0.47) and $^{207}Pb/^{206}Pb$ dates (345.7 to 368.7 Ma). The $^{206}Pb/^{238}U$ date of 344.1 ± 1.0 Ma (2 sigma) obtained for concordant fraction #1 provides a minimum constraint on the emplacement age of unit EBAF. The similarity in the $^{207}Pb/^{206}Pb$ dates for fractions #1 and #3 (345.7 and 345.8 Ma, respectively) is strong support for the interpretation that the weighted average $^{207}Pb/^{206}Pb$ date of 345.8 ± 5.3 Ma (2 sigma) is the best current estimate for the crystallization age of unit EBAF.

A variably foliated granodiorite (Fig. 2, sample and geochronological site SLA00-16) from the Little Shuswap pluton gives an age of 354.3 ± 2.2 Ma (S. Acton, personal communication, 2003). Two zircon populations were recovered from the samples. Population 1 was made of subhedral to euhedral colourless prisms with 3:1 length:width ratios; the larger grains in this population contained tiny fluid/mineral inclusions and fractures, and a few of these grains displayed visible core/overgrowth relationships. Population 2 was a subordinate population of larger equant colourless grains of poor quality typically containing numerous fractures and turbid regions. The U-Pb results for five zircon fractions are presented in Table 2 and on a concordia diagram in Figure 4C. The selected zircon fractions are all from population 1 and varied from single colourless prismatic grains (fractions #1 and #2) to small multi-grain fractions consisting of morphologically distinct grain types (e.g., fragments, resorbed prisms and equant grains). This zircon population 1 contains moderate to high uranium contents (423-881 ppm), similar Th/U (0.42-0.54) and similar $^{206}Pb/^{238}U$ dates (349-357 Ma). The best estimate of the emplacement age for the Little Shuswap pluton is the lower intercept date of 354.3 ± 2.2 Ma, based on a regression of three zircon analyses (fractions #1, #3 and #4).

A foliated quartz-feldspar-phyric felsic dike or sill (Fig. 2, sample and geochronological site SLB00-656) that intruded a Devonian-Mississippian synvolcanic granitic intrusion on

Table 2. U-Pb zircon analyses of samples from the Eagle Bay assemblage.

Sample Description[1]	Location[2]	Weight (ug)	U (ppm)	Th (ppm)	Pb (ppm)	Th/U	Total common Pb (pg)	$^{206}Pb/^{204}Pb$	Atomic Ratios[3] $^{206}Pb/^{238}U$	$^{207}Pb/^{235}U$	$^{207}Pb/^{206}Pb$	Apparent Age (Ma) $^{206}Pb/^{238}U$	$^{207}Pb/^{235}U$	$^{207}Pb/^{206}Pb$	% Disc.
SLB99-31 - Quartz-feldspar-phyric flow from unit EBF															
1 resorbed prism col possible tip overgrowth NM4	301799E / 5669140N	3.7±1.6	171	20	10	0.1	17	95	0.0336±4	0.297±24	0.0643±49	212.8±2.4	264.4±19.0	750.4±158.4	72.8
9 prisms (2:1 to equant) tan eu sl res NM (4)		3.7±1.8	879	547	55	0.6	10	1159	0.0555±2	0.411±3	0.0538±3	348.4±1.4	348.1±1.4	361.6±10.6	3.8
15 prisms (2:1) tan eu NM (4) sl res		2.6±0.6	1348	943	82	0.7	6	2035	0.0543±2	0.402±2	0.0537±2	340.8±1.4	340.8±1.4	358.6±8.0	5.1
1 angular piece tan NM (4)		1.0±0.2	1227	806	78	0.7	8	548	0.0551±3	0.399±6	0.0525±7	345.7±1.6	340.7±4.4	306.7±31.0	-13.0
11 angular tan trans fracs n/incl 4NM		13.3±0.5	964.9	727.5	59.98	0.8	16	2789	0.0547±3	0.405 ± 2	0.0538±1	343.0±0.8	345.3±0.8	360.7±2.5	5.0
SP02-12A - Quartz-feldspar-phyric flow from unit EBAF															
1 z, lt pink equant subhedral 0NM (1)	297486E / 5680028N	14	165	78	10.2	0.47	13	606	0.05483±8	0.40368±146	0.05340±18	344.1±0.5	344.3±1.1	345.7±7.6	0.5
2 z, lt pink equant subhedral 0NM (1)		17	185	65	10.8	0.35	5	2171	0.05712±8	0.42488±93	0.05394±9	358.1±0.5	359.5±0.7	368.7±3.8	3.0
3 z, lt pink equant subhedral 0NM (1)		18	242	108	14.2	0.45	5	2925	0.05640±8	0.41526±75	0.05340±7	353.7±0.5	352.7±0.5	345.8±2.9	-2.3
SLA00-016 - Granodiorite from Little Shuswap Pluton															
1 z, larger euh pr (1)	301778E / 5642270N	2	881	472	54	0.54	4	1371	0.05652±11	0.4180±16	0.05364±16	354.4±0.7	354.6±1.1	356.1±6.8	0.5
2 z, col pr (1)		1	723	322	44	0.45	5	535	0.05568±19	0.4253±69	0.05539±75	349.3±1.2	359.8±5.3	428.2±30.0	18.9
3 z, larger tan frags 0NM (5)		27	450	213	27	0.47	16	2712	0.05694±20	0.4250±15	0.05413±5	357.0±1.2	359.6±1.1	376.5±2.1	5.3
4 z, col res pr 0NM (14)		30	384	196	23	0.51	5	7513	0.05682±9	0.4247±7	0.05421±3	356.3±0.6	359.4±0.5	379.8±1.3	6.4
5 z, tiny col eq 0NM (14)		24	423	176	25	0.42	20	1841	0.05580±9	0.4235±8	0.05505±6	350.1±0.5	358.6±0.6	414.1±2.5	15.9
SLB00-656 - Quartz-feldspar-phyric dike or sill crosscutting Dev-Miss synvolcanic granitic intrusion															
1 z, col prisms 0NM (18)	302385E / 5662360N	20	229	101	11	0.44	10	1312	0.04624±9	0.3433±9	0.05384±10	291.4±0.5	299.6±0.7	364.2±4.1	20.4
2 z, tiny col prisms 0NM (15)		12	314	131	19	0.42	43	263	0.04639±35	0.3567±103	0.05576±146	292.3±2.2	309.7±7.7	443.0±57.1	34.8
SLB00-420 - Foliated diorite dike or sill crosscutting unit EBG															
1 z, tiny col eq 10NM (12)	307590E / 5667520N	12	398	40	28	0.1	13	1541	0.06848±13	0.7631±16	0.08082±8	427.0±0.8	575.79±0.9	1217.1±2.0	67.1
2 z, larger col irreg 10NM (6)		16	246	81	21	0.33	6	3236	0.08459±12	0.7595±13	0.06512±6	523.5±0.7	573.7±0.7	778.2±1.9	34.1
3 z, lg tan euh 10NM (1)		7	174	93	12	0.53	16	270	0.05219±9	0.3956±32	0.05497±43	328.0±0.5	338.4±2.3	410.9±17.2	20.7

[1]col. colourless, eq: equant, eu: euhedral, frags: fragments, incl: inclusions, irreg: irregular, pk: pink, pr: prism, sm: small, sl res: slightly resorbed, trans: transparent, z: zircon, Disc: dissolution
#NM = degrees of non-magnetic fraction; 0NM = non-magnetic fraction at 0 degree side tilt on a Frantz Isodynamic Separator
Number in parentheses refers to the number of grains per fraction
[2]Coordinates are given in Universal Transverse Mercator (UTM) projection, zone 11, North American Datum 1983.
[3]All error are reported at one sigma (except sample SLB99-31, which is reported at 2 sigma)
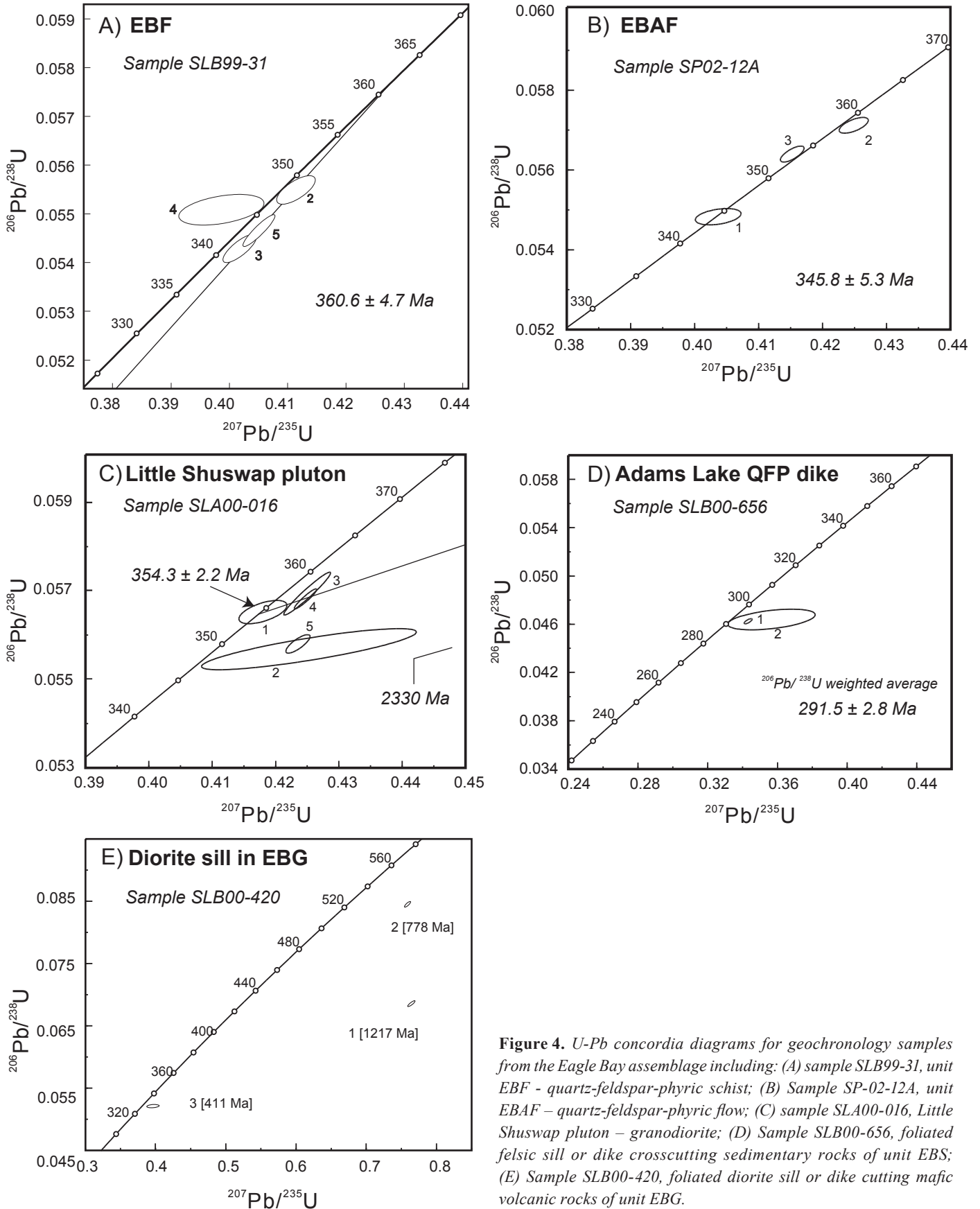
Figure 4. *U-Pb concordia diagrams for geochronology samples from the Eagle Bay assemblage including: (A) sample SLB99-31, unit EBF - quartz-feldspar-phyric schist; (B) Sample SP-02-12A, unit EBAF – quartz-feldspar-phyric flow; (C) sample SLA00-016, Little Shuswap pluton – granodiorite; (D) Sample SLB00-656, foliated felsic sill or dike crosscutting sedimentary rocks of unit EBS; (E) Sample SLB00-420, foliated diorite sill or dike cutting mafic volcanic rocks of unit EBG.*

the western side of Adams Lake yields an age of 291.5 ± 2.8 Ma. The sample contains a modest amount of colourless zircons that likely form part of a single zircon population. The U-Pb results for two small multi-grain zircon fractions are presented in Table 2 and on a concordia diagram in Figure 4D. Zircons in this sample contain moderate uranium contents (229-314 ppm), similar Th/U (0.42-0.44) and virtually identical $^{206}Pb/^{238}U$ dates of 291.4 and 292.3 Ma, respectively. The weighted average $^{206}Pb/^{238}U$ date of 291.5 ± 2.8 Ma is considered a good estimate for the emplacement age of this quartz-feldspar-phyric dike or sill.

A foliated diorite sill or dike (Fig. 2, geochronological site SLB00-420), which crosscuts the mafic volcanic rocks of unit EBG, yields zircon populations of 411 Ma, 778 Ma and 1217 Ma (Fig. 4E and Table 2). A total of 61 zircons were recovered from the three least magnetic mineral splits. Each zircon crystal has a distinctive colour (range from colourless to dark pink) and/or morphology (euhedral prisms to round balls): they do not appear to be part of a single zircon population, and more likely they represent individual xenocrysts. The three zircon fractions display a range in uranium content (174 to 398 ppm), Th/U (0.10 to 0.53) and $^{207}Pb/^{206}Pb$ dates (411, 778 and 1217 Ma). All three fractions are discordant (21-67%) and the $^{207}Pb/^{206}Pb$ dates likely represent minimum ages for zircon xenocrysts. If all zircons in this sample are inherited, then the youngest zircon fraction (#3, 411 Ma) represents a maximum date for the emplacement age of this dike or sill.

SYNGENETIC SULPHIDE DEPOSITS

Volcanic and sedimentary rocks of the Eagle Bay assemblage contain numerous syngenetic sulphide deposits of several types and settings (Table 1). The deposits are classified using the nomenclature of the British Columbia mineral deposit profiles (Lefebure and Ray, 1995; Lefebure and Höy, 1996) and they have been grouped into three classes that include: Class 1 — volcanic-sediment hosted massive sulphide (VSHMS) deposits; Class 2 — volcanic-hosted massive sulphide (VHMS) deposits; and Class 3 — sediment-hosted massive sulphide (SHMS) deposits.

Class 1 — VSHMS Deposits

These Zn, Pb, Ag (±Cu, ±Au) deposits have been described by Höy (1999), who classified them as sediment-hosted massive sulphide (SHMS) or SEDEX deposits. Here they are tentatively classified as VSHMS because they are hosted in fine-grained clastic sedimentary rocks enclosed in mafic volcanic rocks of unit EBG on Adams Plateau, southeast of Adams Lake (Figs. 2, 3). The deposits include Mosquito King, Lucky Coon, EX 1, Elsie, King Tut, and several others (Table 1). The host rocks consist of a heterogeneous clastic sedimentary succession of thin bedded carbonaceous, calcareous and sericitic phyllite interlayered with chlorite or calcareous phyllite, thin impure grey limestone and calc-silicate gneiss. The sulphide mineralization occurs as deformed thin layers, lenses, and pods of semi-massive to massive sulphides crudely to well banded and conformable to schistosity and bedding. The host sedimentary rocks also contain abundant fine disseminated and lamellae of pyrrhotite. Intense deforma-

tion of the host rocks has caused discontinuity and marked variability in the widths of the sulphide mineralization, which tend to thicken in the hinge zones of folds (Höy, 1999). Overall, the sulphide layers have a high aspect ratio (*i.e.,* the ratio of lateral extent of the sulphide layer to its maximum thickness) and occur discontinuously over of strike length of few tens of metres to several hundreds of metres (Dickie, 1983; Höy, 1999). Pyrite, sphalerite and galena comprise over 95% of the sulphides; pyrrhotite, magnetite, arsenopyrite, argentite, tetrahedrite and chalcopyrite account for most of the remaining sulphides. Sulphides are enclosed in an alteration envelope of sericite, quartz and minor carbonates. The most common alteration types consist of sericitization and silicification in hanging wall and footwall phyllitic rocks.

Class 2 — VHMS Deposits

Two types of VHMS deposits, mafic and bimodal-felsic, have been recognized in volcanic rocks of the Eagle Bay Assemblage. The mafic type deposits, such as the Twin Mountain, Cu5, AP98-46 and Woly (Table 1), occur as volcanic-hosted, thin, discontinuous, concordant massive sulphide lenses and layers; and disseminated sulphides hosted by chlorite-sericite schists and amphibolites of unit EBG, which were derived from massive basaltic lavas, flow breccias and tuffs. The sulphides consist of small pods of massive to disseminated galena, sphalerite, pyrrhotite, pyrite and magnetite with minor chalcopyrite, and layers of banded pyrrhotite with minor chalcopyrite and sphalerite. At Twin Mountain, the sulphides occur as disseminations and pods within carbonate-quartz-barite lenses. Another mafic-type deposit, Woly (new occurrence), occurs as stringers and disseminations of sulphides and oxides in thin discontinuous pillowed flows interlayered with limestone and clastic sedimentary rocks of unit EBS. The sulphides and oxides, enclosed in a chlorite and epidote-rich gangue, form stringers crosscutting the pillowed flows and are disseminated in the pillow selvages.

The bimodal-felsic type deposits, such as Homestake, Beca, Rea Gold and Harper (Table 1), are hosted by Devonian-Mississippian aphyric and feldspar (± quartz)-phyric schists and chlorite schists of units EBA and EBF derived from mafic to felsic volcaniclastic and rare lava flows (Figs. 2, 3). The deposits are polymetallic precious and base metal-bearing stratabound massive sulphide lenses and disseminations locally overlain or enclosed by massive barite (Höy and Goutier, 1986). Within individual deposits, the bulk of the sulphides are typically contained in tabular lenses of stratiform sulphides up to a few metres in thickness and more than a few tens of metres in length, and as thin bands and laminae of semi-massive sulphides within 1 to 2 m-thick siliceous pyritic schist intervals. Multiple lenses are generally present along one or several stratigraphic levels. For example, Rea Gold, Twin 3 and K-7 consist of at least five massive sulphide lenses along a continuous, well-defined stratigraphic horizon within unit EBF, called the "Rea Zone", which has a strike length of approximately 7 km (Carmichael, 1991). Homestake is comprised of at least three sulphide-bearing barite lenses and veins within highly altered sericite-quartz schists of unit EBA (Höy and Gouthier, 1986). The deposits of unit EBA occur near the stratigraphic top of a 450-500 m-thick section of altered light

silvery to yellowish grey, fissile, sericite-quartz schists that derived from felsic tuffs. This zone of alteration outcrops on the cliffs along Sinmax Creek for up to 7 km from Squaam Bay northwest.

Class 3 – SHMS Deposits

SHMS deposits, such as Mount Armour and Fortuna (Table 1, Figs. 2, 3), occur in a thick and varied succession of clastic sedimentary rocks interlayered with limestone and mafic volcanic rocks of unit EBS. The clastic sedimentary rocks, which comprise sericite-talc schist (±ankerite, ±chlorite, ±chloritoid), calcareous argillite, grit, phyllite, chert and quartzite host the Cu-Zn-Pb (±Au, ±Ag) sulphide deposits. The deposits consist of small conformable sulphide layers and lenses, locally accompanied by brecciated quartz-pyrite stockwork zones. The Mount Armour deposit has two sulphide lenses that consist of massive fine to coarse-grained banded pyrite, pyrrhotite and minor chalcopyrite up to 2 m thick that are enclosed in a sericitized, pyritized and carbonate-rich horizon. The stratigraphic and structural relationships suggest that the two sulphide lenses represent stacked horizons and not a folded single horizon (Rimfire Minerals Corp., personal communication, 2001). The Fortuna deposit consists of discontinuous zones of semi-massive pyrite (±chalcopyrite) lenses and pods and pyrite-chalcopyrite stringers (Table 1). The mineralized zones are enclosed in three prominent alteration zones that vary in size from 100 to 500 m in length and 50 to 200 m in width, and are parallel to the regional foliation. The alteration mineralogy consists of an assemblage of sericite, quartz, talc, kaolinite and gypsum with varying amount of ankerite, chlorite and chloritoid. In addition, the zones contain weathered fine- to coarse-grained disseminated pyrite (up to 5 vol.%).

LITHOGEOCHEMISTRY AND NEODYMIUM ISOTOPE GEOCHEMISTRY

Sampling and Analytical Methods

Representative samples were taken from archival material (Schiarizza and Preto, 1987), as well as samples collected by S. Paradis, S.L. Bailey and N.D. Hughes during NATMAP geological investigations between 1999 and 2002. Representative major and trace element analyses of each unit and formation are presented in Tables 3 and 4. The complete geochemical data set is given in Tables DR2 and DR3 (see footnote 2). Nd isotopic values are listed in Table 5. Analytical methods are described in Appendix 2.

Alteration, Metamorphism and Element Mobility

Least altered samples were selected for geochemical analysis and characterization of the volcanic and intrusive rocks; however all samples exhibit the effects of greenschist facies regional metamorphism and some hydrothermal alteration. Primary igneous textures may be preserved at outcrop and thin section scales, however the primary mineralogy has been replaced. The matrix of mafic rocks has been replaced by chlorite, actinolite, epidote, quartz, plagioclase, sericite and carbonates. The matrix of intermediate to felsic varieties has been replaced by sericite, quartz, plagioclase, and minor chlorite

and biotite. Plagioclase and pyroxene phenocrysts have been replaced by sericite, quartz, carbonate and chlorite; quartz phenocrysts are rounded, embayed and mantled by sericite.

Under the hydrothermal alteration conditions outlined above, most major elements (SiO_2, Na_2O, K_2O, CaO, MgO and iron) and low field strength elements (LFSE: Cs, Rb, Ba, Sr, U) are mobile (*e.g.*, Ishikawa *et al.*, 1976; Saeki and Date, 1980; Date *et al.*, 1983; MacLean, 1990; Lentz, 1999; Large *et al.*, 2001). In contrast, some major elements (Al_2O_3, TiO_2), transition elements (V, Ni, Cr, Co), high field strength elements (HFSE: Nb, Ta, Zr, Hf, Y, Sc, Ga), rare earth elements (REE: La, Ce, Pr, Nd, Sm, Gd, Tb, Dy, Er, Yb, Lu) and Th are relatively immobile under low to medium hydrothermal alteration (Loughman, 1969; Floyd and Winchester, 1978; Whitford *et al.*, 1989; Pearce, 1996; Barrett and MacLean, 1999). They can be mobile; however, during intense hydrothermal alteration and high water-rock ratios (Campbell *et al.*, 1984; Whitford *et al.*, 1989; Valsami and Cann, 1992; Barrett and MacLean, 1999). Except for samples picked in close proximity to sulphide mineralization, the HFSEs and REEs in the Eagle Bay suite behave coherently and appear to be immobile. The same is observed in metamorphosed (greenschist to mid-amphibolite facies) and polydeformed rocks of the Yukon-Tanana terrane (Dusel-Bacon and Cooper, 1999; Piercey *et al.*, 2001, 2002, this volume), another pericratonic terrane, which contains rocks of similar lithologies and ages, and hosts syngenetic base metal sulphide deposits. They are used therefore to assess the original petrological attributes and geochemical affinities of the volcanic and intrusive rocks. The protolith composition of volcanic and intrusive rocks is identified by using the modified Winchester and Floyd (1977) Zr/TiO_2 *vs.* Nb/Y diagram of Pearce (1996), in which the Zr/TiO_2 ratio serves as a fractionation index and the Nb/Y ratio serves as an alkalinity index. In the following sections, the geochemistry of the mafic volcanic units is first described, followed by a description of the intermediate to felsic volcanic units.

Geochemistry of Mafic Volcanic Rocks

Unit EBG

Mafic volcanic rocks of unit EBG have the composition of alkalic to subalkalic basalt of within-plate and mid-ocean ridge basalt (MORB) affinities. On the Zr/TiO_2 *vs.* Nb/Y diagram (Fig. 5A), unit EBG forms two groups: (1) alkalic basalts with high Nb/Y (0.5-1.8) and Zr/TiO_2 (50.8-123.5) ratios; and (2) subalkalic basalts with lower Nb/Y (0.03-0.1) and Zr/TiO_2 (28.6-66.0) ratios.

The alkalic basalts volumetrically predominate in unit EBG. They contain P_2O_5 (0.16-0.64%) and TiO_2 (1.19-2.4%) concentrations that are typically higher than those determined from other mafic volcanic units of the Eagle Bay assemblage. The alkalic basalts also have high Ti/Sc and Ti/V ratios, and plot in the MORB to ocean-island basalt (OIB) fields in the Ti *vs.* V diagram (Fig. 5B). The Al_2O_3/TiO_2 ratios (5.25-14.71; average 9.01) are lower than those of primitive mantle (~21) and they have the lowest Zr/Nb ratios (3.8-11.7) of all mafic units, which place them in the fields for within-plate rocks (Fig. 6A) and OIB (Fig. 6B) on various discrimination diagrams. The primitive mantle-normalized plots for the alkalic basalts (Fig. 7A)

are characterized by LREE-enrichment (La/Yb$_n$ = 3.68-34.87), and positive Nb anomalies (Nb/Nb* = 0.93-1.56), similar to average OIB and to Nb-enriched basalts found in modern and ancient arc and back-arc environments (*e.g.*, Kepezhinskas *et al*., 1997; Hollings and Kerrich, 2000; Hollings, 2002). Their Nd isotopic composition yielded εNd$_{540}$ values between +4.3 and +5.7, with model ages of 0.96 to 1.09 Ga (Table 5).

The subalkalic basalts (Fig. 5A) are tholeiitic basalts that form a distinctive band 4.2 km in length and 800 m in width in the central western part of the study area (Fig. 2). Their TiO$_2$ content is low to moderate (0.68-1.3) and is accompanied by moderate Al$_2$O$_3$/TiO$_2$ values (10.5-23.14; average 19.44), which are within the range of values for primitive mantle (~21; Sun and McDonough, 1989), and are slightly higher than values for normal mid-ocean ridge basalt (N-MORB ~ 11; Sun and McDonough, 1989). On the Ti-V diagram, most of the samples plot within the MORB-BABB (back-arc basin basalt) field (Fig. 5B). On the Zr-Nb-Y plot (Fig. 6A), these basalts lie within the field for N-MORB, which is consistent with their low

Eagle Bay Assemblage

△ Unit EBG - Alkalic basalt   ■ Unit EBM - Alkalic basalt   ✳ Tsalkom Formation

▲ Unit EBG - Subalkalic basalt   ○ Unit EBA - Subalkalic andesite/basalt   + Fennell Formation
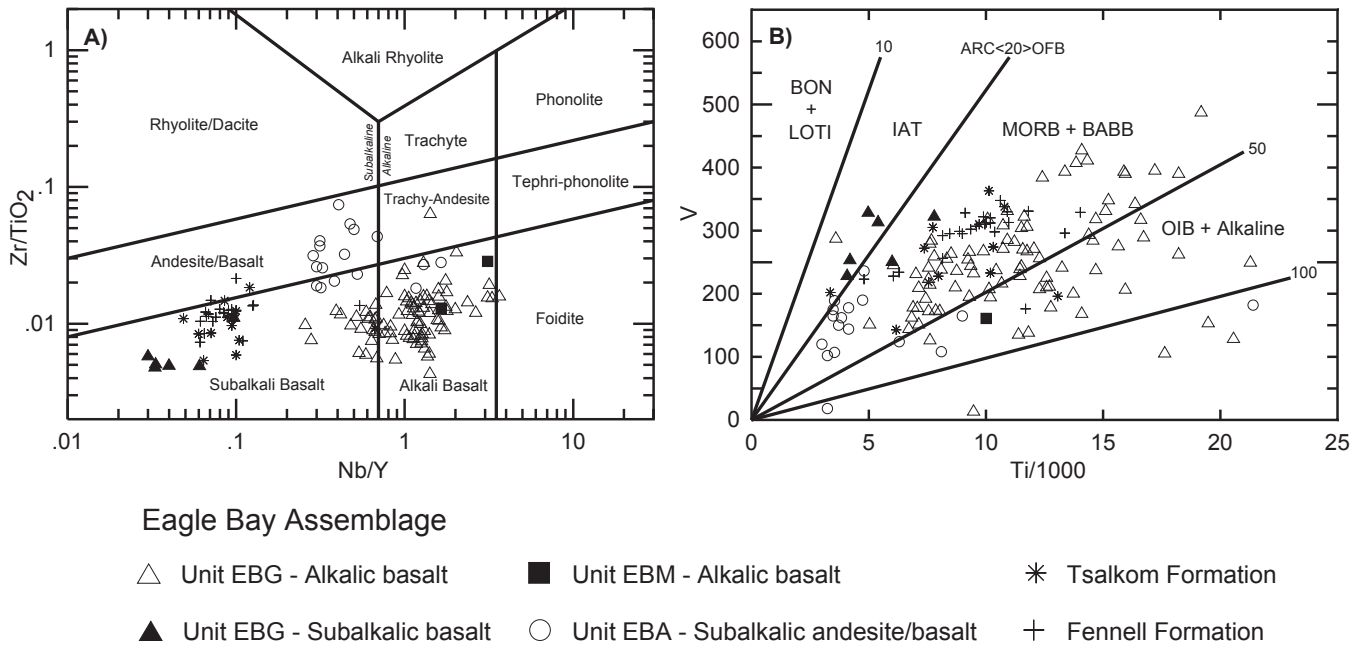
Figure 5. *(A) Diagram of Pearce (1996; modified Winchester and Floyd, 1977) for mafic volcanic rocks of the Eagle Bay assemblage and the Fennell Formation. (B) Ti-V diagram of Shervais (1982), values of Ti/V given: Ti/V = 20 is characteristic of arc-related basalts, Ti/V = 50 is characteristic of alkalic (within-plate) basalts, and Ti/V = 20-50 is characteristic of MORB. ARC = arc-related basalt; BABB = back-arc basin basalt; BON = boninite; IAT = island-arc tholeiite; LOTI = low-Ti tholeiite; MORB = mid-ocean-ridge basalt; OFB = ocean-floor basalt; OIB = ocean-island basalt.*

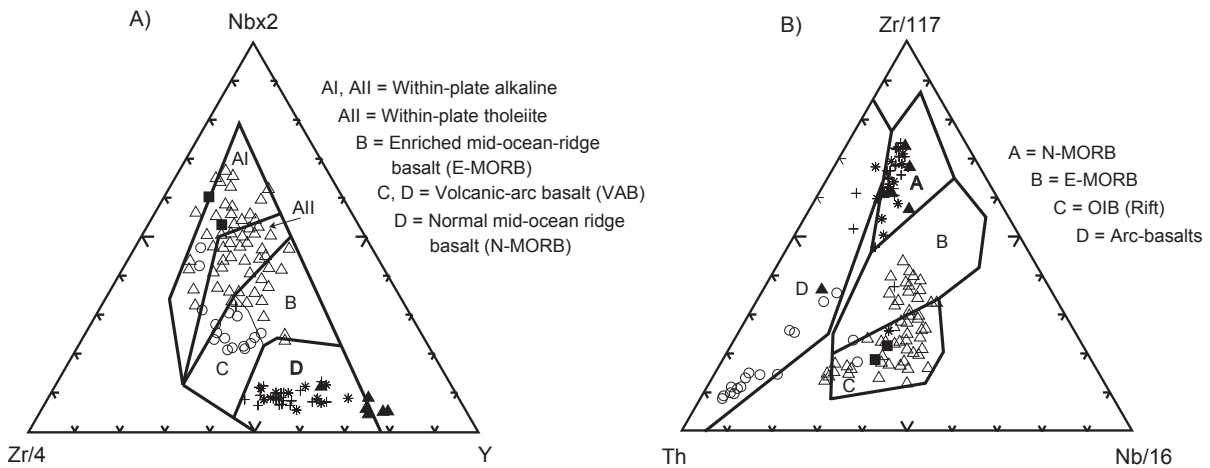**Figure 6.** *Discrimination diagrams for mafic volcanic rocks of the Eagle Bay assemblage and the Fennell Formation. (A) Zr-Nb-Y plot of Meschede (1986). (B) Th-Zr-Nb plot of Wood (1980). Symbols as in Figure 5.*

Table 3. Representative analyses of mafic volcanic rocks of the Eagle Bay assemblage and Fennell Formation.

Sample	SLB99-17C	SLB99-39	PS85-130	SP00-039	MC78-047	MC78-091	VP80-042	SP00-024	SLA-01-313	SP00-005	MC78-016	SP00-023	SP00-010	SP00-012
Unit	EBG	EBG	EBG	EBG	EBM	EBM	EBA	EBA	Tsalkom Fm	Tsalkom Fm	Fennell Fm-LSD	Fennell Fm-LSD	Fennell Fm-USD	Fennell Fm-USD
Lithology	Chloritic schist	Calcareous chloritic schist	Mafic tuff	Massive metabasaltic flow	Metabasaltic flow	Amygdaloidal metabasaltic flow	Mafic metavolcanic flow	Mafic to intermediat tuff	Metabasaltic flow	Metabasaltic flow	Metabasaltic flow	Metabasaltic flow	Pillow metabasaltic lfow	Metabasaltic flow
Affinity	N-MORB	N-MORB	OIB	OIB	OIB	OIB	CAB	CAB	N-MORB	N-MORB	N-MORB	N-MORB	N-MORB	N-MORB
SiO_2(wt.%)	42.90	46.70	57.20	45.30	41.30	47.90	57.30	53.30	45.30	49.10	52.50	54.20	49.40	50.90
TiO_2	0.90	0.83	1.70	1.55	4.21	1.67	0.59	0.64	1.03	1.33	2.23	1.95	1.97	1.67
Al_2O_3	18.10	16.30	15.80	12.90	14.60	11.50	15.00	16.80	16.90	17.20	14.20	15.70	14.20	14.50
Fe_2O_3T	13.10	9.40	10.80	12.80	15.80	11.30	6.80	9.00	11.20	10.30	13.60	11.60	11.50	11.30
Fe_2O_3	1.60	2.80	3.35	1.90	3.35	2.29	0.80	1.22	0.60	4.41	2.26	2.48	1.60	2.07
FeO	10.30	6.00	6.70	9.80	11.20	8.10	5.40	7.00	9.60	5.30	10.20	8.20	8.90	8.30
FeO*	11.74	8.52	9.71	11.51	14.21	10.16	6.12	8.01	10.14	9.27	12.23	10.43	10.34	10.16
MnO	0.25	0.14	0.14	0.16	0.29	0.14	0.20	0.12	0.14	0.17	0.22	0.19	0.17	0.17
MgO	11.91	9.16	3.50	13.85	5.32	8.13	3.11	3.62	7.32	6.59	4.56	3.46	7.15	7.71
CaO	5.06	13.43	2.20	6.64	6.29	12.08	3.51	5.11	5.47	10.45	7.06	7.06	5.87	8.04
Na_2O	2.60	1.50	5.80	2.40	3.70	2.90	3.30	3.90	4.70	3.80	4.80	4.10	3.20	4.50
K_2O	0.73	0.16	0.40	0.28	1.11	0.59	2.87	1.40	0.03	0.12	0.25	0.30	0.80	0.20
P_2O_5	0.05	0.05	0.29	0.19	2.06	0.37	0.17	0.20	0.21	0.13	0.27	0.32	0.20	0.17
H_2O	6.40	3.40	2.90	5.30	4.50	2.90	2.20	3.60	4.70	2.80	2.50	3.00	4.90	2.90
CO_2	0.40	0.10	1.20	0.50	2.70	2.40	6.10	3.90	3.70	0.20	0.20	0.20	3.00	0.20
LOI	-	-	-	-	-	-	-	-	-	-	-	-	-	-
S	0.00	0.00	0.02	0.06	0.03	0.02	0.46	0.00	0.03	0.00	0.01	0.00	0.07	0.13
Total	101.30	100.80	101.20	100.90	100.50	100.90	101.00	100.80	99.60	101.60	101.40	101.30	101.50	101.50
Cr (ppm)	592	497	102	684	16	391	92	19	359	331	42	5	212	240
Ni	230	162	23	457	9	241	9	5	85	107	22	5	53	101
Co	60	40	24	66	27	51	13	22	45	51	34	25	38	46
Sc	53	42	18	24	7	18	19	23	18	40	25	24	39	38
V	313	328	194	195	165	161	107	162	143	228	296	176	331	313
Cu	68	67	26	74	9	55	55	5	24	88	66	46	35	60
Pb	0.5	0.5	7.0	2.0	7.0	8.0	12.0	5.0	2.0	2.0	0.5	0.5	0.5	0.5
Zn	86	52	103	120	230	96	112	154	106	172	121	117	105	106
Cd	0.1	0.1	0.1	0.3	0.3	0.2	0.1	0	0.1	0	0.2	0	0	0
Sb	0.1	0.5	0.2	1.8	0.4	0.7	0.5	1.6	0.7	0.6	0.1	0	3.3	0.2
Rb	17.0	2.7	12.0	5.7	21.0	7.2	68.0	40.0	1.0	1.4	4.1	5.0	5.4	2.0
Cs	0.61	0.11	0.44	0.34	1.50	0.08	2.10	1.10	0.17	0.05	0.17	0.73	1.50	0.33
Ba	240	78	210	110	630	230	1300	710	48	72	200	620	570	60
Sr	76	75	160	110	460	890	200	220	159	250	96	210	120	130
Ga	18	23	18	19	28	19	17	18	21	15	17	22	14	15
Ta	0.07	0.07	3.2	1.1	12.0	1.5	0.87	0.38	0.6	0.19	0.41	0.45	0.21	0.23
Nb	0.75	0.90	56.00	18.00	180.00	28.00	18.00	6.60	10.00	2.50	5.90	6.60	3.20	3.30
Hf	0.95	0.81	3.20	2.10	13.00	2.10	4.80	1.90	1.60	1.30	4.10	5.30	2.60	3.10
Zr	31	25	210	82	720	130	190	100	57	47	180	250	150	120
Y	25	27	32	18	58	17	38	22	15	25	47	66	34	39
Th	0.05	0.08	8.6	1.3	16	2.2	14	2.1	0.78	0.24	0.43	0.57	0.25	0.34
U	0	0.04	1.8	0.35	3.9	0.51	3.4	0.7	0.2	0.12	0.17	0.22	0.1	0.31
La	0.9	1.7	47.0	13.0	160.0	20.0	42.0	16.0	8.2	3.4	7.1	9.7	4.8	4.9
Ce	3.1	5.2	89.0	28.0	340.0	44.0	97.0	35.0	18.0	10.0	21.0	29.0	14.0	15.0
Pr	0.6	0.9	10.0	3.6	41.0	5.5	13.0	4.5	2.6	1.8	3.5	4.6	2.2	2.4
Nd	4.0	5.2	39.0	16.0	160.0	23.0	51.0	19.0	13.0	9.6	18.0	24.0	12.0	13.0
Sm	1.7	1.9	7.8	4.0	28.0	5.3	10.0	4.1	3.2	3.0	5.7	7.3	4.0	3.9
Eu	0.58	1.00	2.20	1.40	7.90	2.30	1.50	1.10	1.30	1.10	1.70	2.10	1.30	1.40
Gd	2.9	2.9	7.0	4.3	21.0	5.2	8.6	4.0	3.6	3.8	7.2	9.5	5.3	5.5
Tb	0.57	0.56	1.10	0.67	2.70	0.74	1.20	0.62	0.54	0.66	1.30	1.70	0.93	0.97
Dy	3.9	3.8	5.9	3.7	12.0	3.6	6.9	3.6	3.0	4.3	7.9	11.0	6.0	6.1
Ho	0.87	0.83	1.20	0.67	2.10	0.64	1.30	0.74	0.54	0.91	1.70	2.40	1.20	1.30
Er	2.4	2.5	3.0	1.8	4.6	1.4	3.6	1.9	1.3	2.5	4.5	6.4	3.4	3.6
Tm	0.38	0.40	0.42	0.24	0.60	0.18	0.54	0.31	0.19	0.36	0.70	1.00	0.52	0.55
Yb	2.5	2.6	2.5	1.4	3.3	1.0	3.4	2.0	1.1	2.3	4.5	6.4	3.3	3.6
Lu	0.37	0.43	0.39	0.21	0.50	0.13	0.54	0.31	0.16	0.34	0.70	0.99	0.49	0.55
NTS	82M04	82M04	82M05	82M04	82M04	82M04	82M04	82M04	82L13	82L13	92P01	92P01	92P01	92P08
Easting[1]	303423	304006	322668	309375	290669	293311	304747	306143	308284	316487	706432	703528	699501	699486
Northing	5672249	5672284	5707168	5664950	5676262	5670747	5660634	5662093	5649546	5643351	5680769	5677018	5679551	5701922

[1]Universal Transverse Mercator projection, North American datum (NAD83), zone11; except for samples within NTS 92P01 and 92P08 = UTM zone 10.
LSD = Lower structural division, USD = Upper structural division, FP = Feldspar-phyric, Fm = formation, N-MORB = Normal mid-ocean ridge basalts, OIB = Ocean island basalts, CAB = Calc-alkaline basalts, - = not analysed

Table 4. Representative analyses of intermediate to felsic volcanic and intrusive rocks of the Eagle Bay assemblage.

Sample	VP80-153	SLB00-588	SLB99-142D	SLB99-31	SLB99-161	SLB99-192	SP-01-10	nh-00-088a	nh-00-115a	nh-00-228b	VP80-155	SP00-006
Unit	EBA	EBA	EBF	EBF	EBF	EBF	EBAF	EBAF	EBAF	EBAF	D-M intrusion	D-M intrusion
Lithology	QP sericite-quartz schist	Sericite-quartz schist	QFP felsic lithic tuff	QFP felsic metavolcanic flow	FP lithic tuff	FP metavolcanic flow	QFP ankerite-sericite lithic tuff	QFP lithic felsic tuff	FP lithic felsic tuff	FP sericite-chlorite tuffaceous sandstone (?)	Foliated granite/granodiorite sill	Foliated granite/granodiorite sill
Affinity	Volcanic Arc	Volcanic Arc	Volcanic Arc	Volcanic Arc	Volcanic Arc	Volcanic Arc	Volcanic Arc	Volcanic Arc	Volcanic Arc	Volcanic Arc	Volcanic Arc	Volcanic Arc
SiO_2 (wt.%)	70.10	74.90	65.50	67.20	59.90	63.20	60.80	62.80	62.30	72.60	68.30	73.20
TiO_2	0.30	0.14	0.32	0.25	0.58	0.34	0.41	0.51	0.62	0.54	0.31	0.35
Al_2O_3	14.30	13.60	15.90	13.00	17.10	15.80	14.50	15.40	16.20	12.90	15.40	14.20
Fe_2O_3T	3.30	1.60	4.00	2.70	7.40	5.30	5.20	6.00	6.40	5.60	3.80	2.10
Fe_2O_3	0.96	1.38	2.30	1.10	2.80	1.30	0.80	1.00	3.18	1.49	1.35	1.54
FeO	2.10	0.20	1.50	1.40	4.10	3.60	3.90	4.50	2.90	3.70	2.20	0.50
FeO*	2.96	1.44	3.57	2.39	6.62	4.77	4.62	5.40	5.76	5.04	3.41	1.89
MnO	0.05	0.01	0.07	0.05	0.07	0.05	0.08	0.09	0.05	0.03	0.05	0.01
MgO	1.61	0.38	1.03	0.72	3.52	1.22	2.28	3.39	2.01	1.66	1.11	0.65
CaO	2.01	1.01	2.67	4.91	0.70	3.95	5.33	2.69	1.92	0.08	0.62	0.78
Na_2O	0.30	3.40	2.20	3.30	6.60	3.20	2.10	3.80	6.70	1.80	3.10	2.20
K_2O	4.82	2.78	4.14	3.05	2.26	2.63	2.49	1.59	1.49	2.37	5.52	3.97
P_2O_5	0.09	0.04	0.20	0.16	0.45	0.21	0.09	0.11	0.16	0.08	0.06	0.07
H_2O	2.40	1.40	2.20	1.40	2.40	2.40	2.70	2.90	1.70	2.40	1.80	1.80
CO_2	1.60	0.80	2.40	4.10	0.20	2.90	4.00	1.90	1.30	0.30	0.50	0.60
LOI	0.00	0.00	0.00	0.00	0.00	0.00	0.00	0.00	0.00	0.00	0.00	0.00
S	0.01	0.01	0.00	0.00	0.00	0.00	0.01	0.01	0.01	0.09	0.09	0.00
Total	100.70	100.10	101.10	101.00	100.90	101.00	99.60	100.80	100.60	100.10	100.20	99.90
Cr (ppm)	79	8	18	12	14	14	26	33	21	89	69	5
Ni	9	8	8	8	8	8	9	9	9	35	9	5
Co	4	4	9	4	17	4	17	15	10	10	4	2
Sc	5.3	2.1	8	6.1	14	6.2	17	20	20	11	6.6	7.6
V	26	10	89	63	147	68	103	128	152	71	24	22
Cu	9	8	12	8	15	8	9	37	15	18	27	17
Pb	2	2	4	4	8	3	6	4	9	10	317	4
Zn	44	25	41	19	98	60	60	66	126	87	318	93
Cd	0.1	0.1	0.1	0.1	0.1	0.1	0.1	0.2	0.1	0.1	0.6	0
Sb	0.1	0.3	0.4	0.2	0.3	0.2	0.1	0.6	0.3	0.1	0.1	0
Rb	150	86	170	82	73	72	120	48	42	100	160	100
Cs	2.9	3.1	5.4	2.6	7.9	2.4	3.3	1.6	1.4	2.3	2.1	1.9
Ba	700	740	3400	810	1200	1600	620	770	1400	550	1700	1100
Sr	35	45	96	240	278	205	183	160	110	36	100	38
Ga	16	15	18	13	17	17	15	16	19	19	20	23
Ta	1.50	0.89	1.1	1.2	0.63	1.3	0.8	0.84	1.1	0.83	1.6	1.5
Nb	14	9.7	17	16	15	20	10	11	15	11	22	23
Hf	4.0	3.8	3.6	3.5	3.6	3.8	3.8	3.8	4.5	6.9	7.6	10.0
Zr	140	150	130	130	140	140	160	150	200	230	240	270
Y	16.0	14	19	22	25	19	17	17	23	17	34	48
Th	14.0	21.0	25.0	22.0	20.0	27.0	7.8	7.5	9.8	13.0	26.0	30.0
U	2.8	3.9	5.4	1.2	4.0	1.3	1.9	2.0	2.5	2.4	4.0	4.8
La	39.0	43.0	72.0	61.0	91.0	81.0	24.0	23.0	22.0	34.0	71.0	118.0
Ce	68.0	71.0	140.0	110.0	170.0	150.0	47.0	44.0	47.0	70.0	120.0	270.0
Pr	7.1	6.6	15.0	12.0	19.0	17.0	5.1	4.9	5.4	8.0	14.0	28.0
Nd	24.0	20.0	54.0	42.0	68.0	58.0	19.0	18.0	20.0	28.0	47.0	92.0
Sm	4.1	3.0	8.8	7.7	11.0	9.2	3.4	3.5	4.4	4.9	8.4	16.0
Eu	0.82	0.50	2.00	1.60	2.60	2.20	0.84	0.81	0.89	0.85	0.92	2.00
Gd	3.2	2.3	6.1	5.5	7.2	6.0	3.1	3.2	4.1	3.7	6.7	12.0
Tb	0.47	0.36	0.75	0.75	0.95	0.74	0.47	0.47	0.60	0.52	1.00	1.70
Dy	2.6	1.9	3.4	3.8	4.4	3.5	2.7	2.6	3.7	3.0	5.6	8.5
Ho	0.49	0.38	0.60	0.67	0.80	0.56	0.58	0.55	0.77	0.60	1.10	1.70
Er	1.4	1.2	1.6	1.6	1.9	1.4	1.6	1.6	2.1	1.5	3.0	4.4
Tm	0.24	0.20	0.25	0.26	0.29	0.23	0.26	0.26	0.34	0.25	0.48	0.72
Yb	1.6	1.5	1.6	1.6	1.9	1.4	1.8	1.8	2.4	1.7	3.2	4.7
Lu	0.28	0.25	0.27	0.27	0.31	0.25	0.28	0.29	0.39	0.27	0.52	0.72
NTS	82M04	82M04	82M04	82M04	82M04	82M04	82M12	82M12	82M12	82M12	82M04	82M04
Easting[1]	319258	307571	302878	301799	302875	301613	313590	309780	309000	317000	319168	306930
Northing	5654691	5662476	5668394	5669140	5667882	5668582	5714279	5710980	5715260	5710920	5652831	5655589

[1]Universal Transverse Mercator projection, North American datum (NAD83), zone 11
QP = Quartz-phyric, FP = Feldspar-phyric, QFP = Quartz-feldspar-phyric, D-M = Devonian-Mississippian

HFSE content. The Th-Zr-Nb plot (Fig. 6B) also illustrates the N-MORB signature of these basalts. On this plot, one sample with higher Th content lies within the field for arc basalt, which suggests either increased contribution from an arc or crustal contamination. The basalts are LREE-depleted (La/Sm$_n$ = 0.32-0.85; Table 6) and are similar to N-MORB. Primitive mantle-normalized plots (Fig. 7B) are also similar to N-MORB, with the exception of one sample with enriched Th content. The Nd isotopic composition of these samples has yielded εNd$_{540}$ values of +8.2 and +8.3 and low concentrations of Nd (1.73 ppm; Table 5).

Unit EBM

Only two samples of unit EBM were analyzed. Both are alkalic basalts (Fig. 5A) that plot in the fields for within-plate rocks and OIB on various discrimination diagrams (Figs. 6A, B). They have high Th/Yb, Ta/Yb, Nb/Yb and Zr/Yb values (Table 6) that are consistent with OIB in continental rift environments (Fig. 8A; *e.g.*, Goodfellow *et al.*, 1995; Logan and Colpron, this volume) and Nb-enriched basalts in arc and back-arc environments (Kepezhinskas *et al.*, 1997; Hollings

and Kerrich, 2000; Hollings, 2002). Their primitive mantle-normalized plots are characterized by slightly positive Nb anomalies (Nb/Nb* = 1.2 and 1.4; Fig. 9A) and low Th/Nb values (0.08 and 0.09). No EBM alkalic basalts were analysed for Nd isotopic composition.

Unit EBA

Most EBA mafic tuffs have the composition of subalkalic andesite-basalt (Fig. 5A). The tuffs have Zr/Y values (4.0-10.7; average 6.0) that are transitional in character, *i.e.,* between calc-alkalic and tholeiitic affinities, which according to Lentz (1998) are >7 in calc-alkaline rocks, <4 in tholeiitic rocks and between 7 and 4 in transitional rocks. They occupy the arc basalt-andesite field in the Zr-Nb-Y and Th-Zr-Nb diagrams of Wood (1980) (Figs. 6A, B). On primitive mantle-normalized multi-element plots (Fig. 8B), they exhibit pronounced negative Nb anomalies (Nb/Nb* = 0.05-1.19; average 0.41) relative to Th and La, and a slight negative Ti anomaly. Their Nd isotopic composition yields εNd$_{360}$ values of -6.5 and -6.8 (Table 5), much lower than those for a depleted mantle (DM) reservoir at 360 Ma, which has a value of εNd$_{360}$ = +9.5 (Goldstein *et al.*, 1984).

Table 5. Neodymium isotopic data for the rocks of the Eagle Bay assemblage and the Fennell Formation.

Sample	Formation/unit	Location[1]	Lithology[2]	Sm ppm	Nd ppm	[147]Sm/[144]Nd	[143]Nd/[144]Nd	uncert.[3] 2σ$_m$ +/-	T$_{DM}$[3] (Ga)	εNd$_T$[4]	~TMa
MC78-12	Fennell Formation	704016 E / 5680020 N	MORB; metabasalt	4.42	13.33	0.201	0.513	0.000	N/A	+8.1	300
PS78-51	Fennell Formation	706897 E / 5686163 N	MORB; metabasalt	5.35	16.12	0.201	0.513	0.000	N/A	+8.7	300
SLA-01-315B	Tsalkom Formation	312559 E / 5645973 N	MORB; amphibolite	1.13	2.95	0.231	0.513	0.000	N/A	+8.1	360
SP00-05	Tsalkom Formation	316487 E / 5643351 N	MORB; porphyritic metabasalt	4.51	13.68	0.200	0.513	0.000	N/A	+6.5	360
SLA-01-313	Tsalkom Formation	308284 E / 5649546 N	MORB; metabasalt	3.15	10.98	0.174	0.513	0.000	N/A	+5.0	360
SP00-002	Tsalkom Formation	707549 E / 5664274 N	MORB; porphyritic metabasalt	6.06	17.31	0.212	0.513	0.000	N/A	+7.6	360
SP00-008	Tsalkom Formation	701320 E / 5671488 N	MORB; pillowed metabasalt	4.58	13.48	0.205	0.513	0.000	N/A	+7.7	360
SLB99-39	Unit EBG	304006 E / 5672284 N	MORB; calcareous chloritic schist	2.35	5.44	0.261	0.513	0.000	N/A	+8.2	540
SLB99-09	Unit EBG	304198 E / 5672322 N	MORB; chlorite & epidote-rich metavolcanic flow	0.81	1.73	0.283	0.513	0.000	0.46	+8.3	540
SLB99-6A	Unit EBG	304000 E / 5671700 N	Alkaline within-plate metabasalt flow breccia	2.83	11.66	0.147	0.513	0.000	1.09	+4.3	540
SLB99-6B	Unit EBG	304000 E / 5671700 N	Alkaline within-plate metabasalt	4.66	20.52	0.137	0.513	0.000	0.99	+4.6	540
SLB99-61	Unit EBG	304152 E / 5671079 N	Alkaline within-plate chloritic & calcareous metabasalt	2.34	9.39	0.151	0.513	0.000	0.96	+5.7	540
SLB99-108	Unit EBG	305641 E / 5668240 N	Alkaline within-plate metabasaltic flow breccia	1.79	7.11	0.153	0.513	0.000	1.02	+5.3	540
SP01-10	Unit EBAF	313590 E / 5714279 N	QFP ankerite-sericite lithic tuff	3.32	17.45	0.115	0.512	0.000	1.93	-10.40	360
SP00-031B	Unit EBAF	309212 E / 5715240 N	QFP schist (felsic tuff)	4.8	24.92	0.116	0.512	0.000	1.88	-9.60	360
SP00-16	Unit EBAF	297641 E / 5679910 N	QFP sericite-ankerite schist (~ felsic tuff)	3.3	17.28	0.115	0.512	0.000	1.77	-8.50	360
SP02-07	Unit EBA	353010 E / 5664080 N	Transitional to calc-alkaline andesitic tuff	2.17	8.95	0.146	0.512	0.000	N/A	-6.80	360
SP00-24	Unit EBA	306143 E / 5662093 N	Transitional to calc-alkaline FP andesite tuff	3.65	16.4	0.135	0.512	0.000	1.93	-6.50	360
SLB00-588	Unit EBA	307571 E / 5662476 N	Sericite-quartz schist (rhyolite tuff)	2.47	16.58	0.090	0.512	0.000	1.43	-7.50	360
DF80-140	Unit EBA	312389 E / 5655746 N	Sericite-quartz schist (rhyolite tuff)	4.4	24.8	0.107	0.512	0.000	1.83	-10.60	360
MC79-002	Unit EBA	296132 E / 5690149 N	QP sericite-quartz schist (rhyolite tuff)	3.21	16.23	0.120	0.512	0.000	1.84	-8.40	360
SP-01-08	Unit EBA	319000 E / 5720139 N	FP sericite-quartz schist (dacite tuff)	7.48	39.6	0.114	0.512	0.000	2.17	-13.70	360
HSP-00-006	Unit EBA	301455 E / 5666349 N	Sericite schist (rhyolite tuff)	1.43	6.52	0.133	0.512	0.000	1.71	-4.70	360
PS-78-325	Unit EBA	309822 E / 5658680 N	Sericite-quartz schist (rhyolite tuff)	3.83	22.79	0.102	0.512	0.000	1.58	-8.1	360
SLB99-33	Unit EBF	300904 E / 5670565 N	QFP felsic tuff	9.54	57.60	0.100	0.512	0.000	1.30	-4.2	360
SLB99-86	Unit EBF	301712 E / 5668897 N	QFP schist (felsic tuff)	13.37	72.95	0.111	0.512	0.000	1.36	-3.7	360
SLB99-182	Unit EBF	301500 E / 5667500 N	FP chloritic andesite tuff	12.14	74.73	0.098	0.512	0.000	1.22	-3.3	360
SP02-08	Synvolcanic intrusion	304882 E / 5661513 N	Foliated granite/granodiorite	6.1	31.08	0.119	0.512	0.000	1.5	-4.40	360
SP02-09	Synvolcanic intrusion	307217 E / 5657927 N	Foliated granodiorite	3.76	22.46	0.101	0.512	0.000	1.5	-7.0	360
SP02-11	Synvolcanic intrusion	307143 E / 5657093 N	Foliated granodiorite	1.66	8.25	0.122	0.512	0.000	1.74	-6.90	360
SLB99-165	Unit EBP	298610 E / 5669348 N	Phyllite	4.63	25.37	0.110	0.512	0.000	1.46	-5.4	340

Notes:

[1]Coordinates are given in Universal Transverse Mercator (UTM) projection, North American Datum 1983. Most samples are in UTM zone 11; samples MC78-12, PS78-51, SP00-002 and SP00-008 are in UTM zone 10.

[2]Abbreviations: QFP = quartz-feldspar-phyric, QP = quartz-phyric, FP = feldspar-phyric, N/A = not available.

[3]Estimated [143]Nd/[144]Nd uncertainties in brackets at the 2σ level.

[4]εNd$_f$ is the initial [143]Nd/[144]Nd ratio, expressed in epsilon notation, calculated at the time given by the value of ~T Ma.

[5]T$_{DM}$ is the depleted mantle model age calculated using the linear model of Goldstein *et al.* (1984). It is not calculated for samples with [147]Sm/[144]Nd ratios greater than 0.1500.
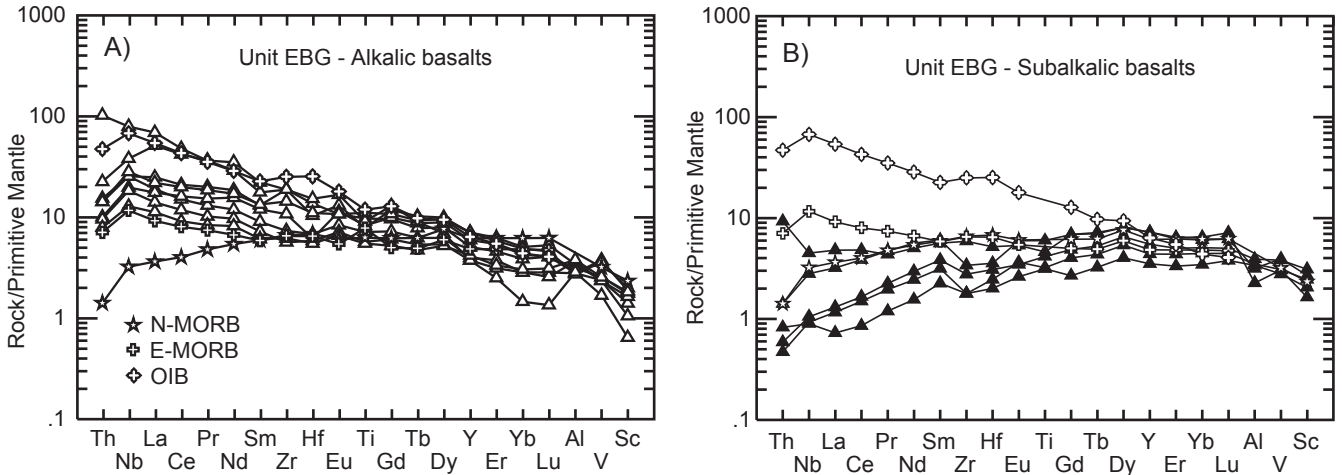
Figure 7. *Primitive mantle-normalized trace element plots for Cambrian mafic volcanic rocks of unit EBG. (A) Alkali, within-plate basalts that have a signature similar to OIB. (B) MORB-type basalts. Primitive mantle values, and N-MORB, E-MORB and OIB global values are from Sun and McDonough (1989). Symbols as in Figure 5.*
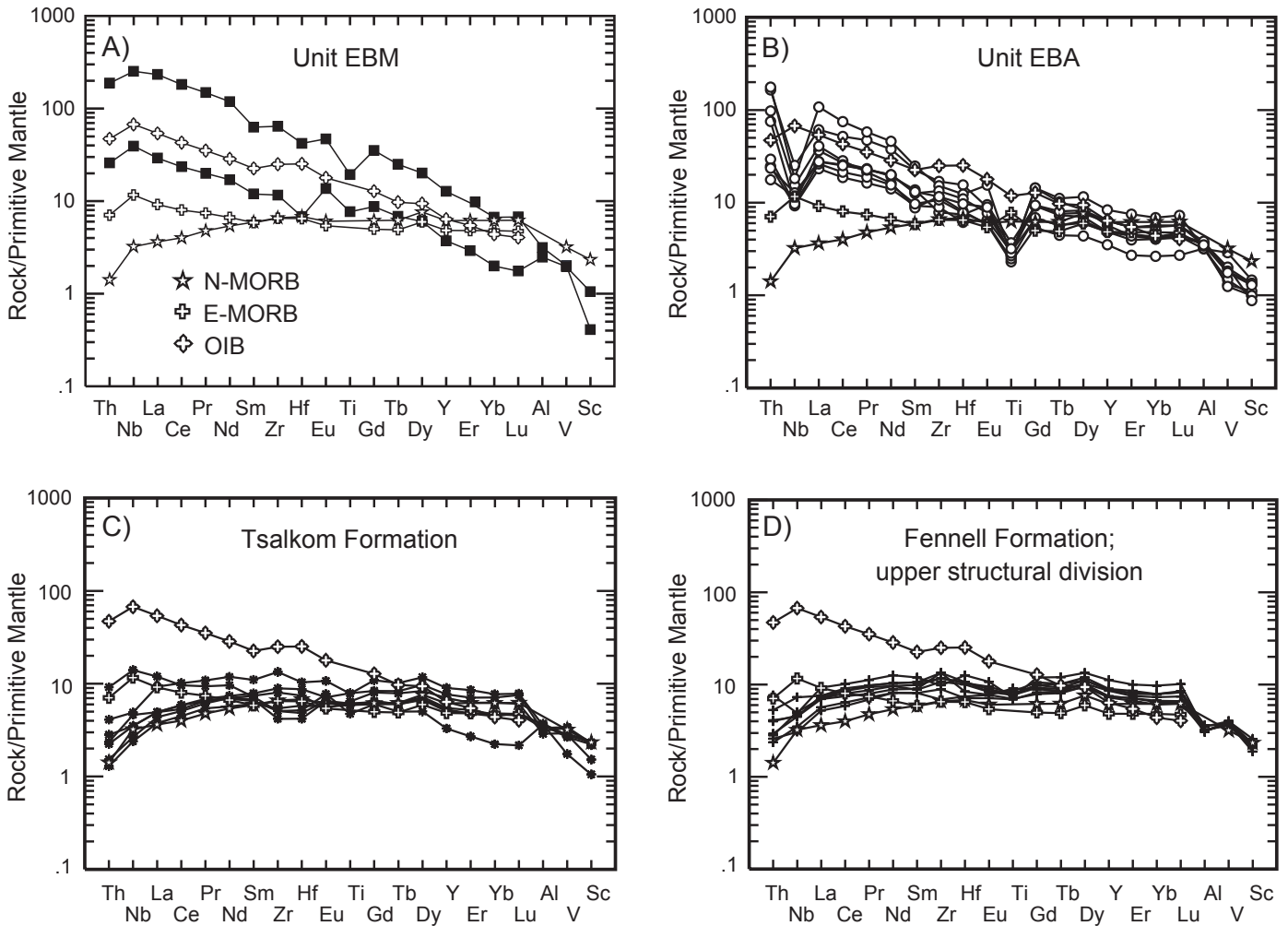

Figure 8. *Primitive mantle-normalized trace element plots for mafic volcanic rocks of: (A) unit EBM; (B) unit EBA; (C) Tsalkom Formation; and (D) upper Fennell Formation. Primitive mantle values, and N-MORB, E-MORB and OIB global values are from Sun and McDonough (1989). Symbols as in Figure 5.*

Tsalkom Formation

The mafic volcanic rocks of the Tsalkom Formation are subalkalic tholeiitic basalts that have similar compositions as the subalkalic basalts of unit EBG and the Fennell Formation (Fig. 5A). On the Ti *vs.* V diagram (Fig. 5B), the samples lie in the MORB-BABB field. On the various tectonic discrimination diagrams (Figs. 6A, B), they plot in the N-MORB field, which is consistent with their low HFSE content. Primitive mantle-normalized trace element plots are also similar to MORB with LREEs exhibiting depleted to slightly enriched patterns (La/Sm$_n$ = 0.41-1.65; Fig. 8C). The Nd isotopic composition of these basalts has yielded εNd_{360} values of +5.0 to +8.1 (Table 5).

Fennell Formation

Schiarizza and Preto (1987) described the geochemistry of the basalts of the Fennell Formation. They are subalkalic tholeiitic basalts (Fig. 5A) that plot in the N-MORB field in various diagrams (Figs. 5B, 6A, B). Primitive mantle-normalized trace element plots for the basalts of the upper structural division of the Fennell Formation are similar to N-MORB, with LREEs exhibiting depleted to slightly enriched patterns (La/Sm$_n$ = 0.61-0.81; Fig.8D). Schiarizza and Preto (1987) interpreted them as ocean-floor tholeiites that were deposited

in a deep oceanic basin at some unknown distance west from the Eagle Bay rocks. Beatty (2003) interpreted them as back-arc basin volcanic rocks, and Smith and Lambert (1995) suggested eruption on a spreading ridge in either a back-arc basin or a marginal oceanic basin. As shown in Figures 5, 6 and 8, the basalts have geochemical characteristics identical to basalts of the Tsalkom Formation. They yield εNd_{300} values of +8.1 to +8.7 (Table 5). Similar high εNd_{300} values (*e.g.*, 7.7 to 10.2) were obtained by Smith and Lambert (1995) for basalts of the Fennell Formation.

Geochemistry of Intermediate to Felsic Volcanic Rocks

Unit EBA

Results for unit EBA have been subdivided on the basis of volcanic and plutonic suites. Both suites have similar geochemical characteristics, except for Zr and Hf values that are slightly higher in the syn-volcanic intrusions. They have Zr/TiO$_2$ and Nb/Y ratios typical of rhyolite and dacite of subalkalic affinity (Fig. 9A; Table 7). They have moderate HFSE concentrations that are characteristic of arc rocks (Fig. 9B) with I-type affinity (Fig. 9C); and they also have moderate Zr/Nb and Zr/Y ratios (Figs. 10A, B), similar to published

Table 6. Summary of key major and trace element ratios for mafic volcanic rocks of the Eagle Bay assemblage and the Fennell Formation.

	Unit EBG Alkaline basalts (OIB)			Unit EBG Subalkaline basalts (N-MORB)			Unit EBM Alkaline basalts (OIB)		Unit EBA Subalkaline andesites-basalts (CAB)			Tsalkom Formation Subalkaline basalts (N-MORB)			Fennell Formation Subalkaline basalts (N-MORB)		
	Range	Ave. (n=8)	Ave. Dev	Range	Avg (n=6)	Ave. Dev	MC78-047	MC78-09l	Range	Ave. (n=14)	Ave. Dev	Range	Ave. (n=15)	Ave. Dev	Range	Ave. (n=19)	Ave. Dev
TiO$_2$ (wt.%)	1.19 - 2.40	1.74	0.32	0.68 - 1.30	0.88	0.17	4.21	1.67	0.50 - 3.57	0.94	0.47	0.56 - 2.18	1.41	0.30	1.36 - 2.34	1.72	0.20
Al$_2$O$_3$/TiO$_2$	5.25 - 14.71	9.01	2.65	10.50 - 23.14	19.44	4.72	3.47	6.89	4.03 - 29.66	21.75	7.05	6.88 - 26.96	12.34	3.40	6.24 - 10.66	8.67	0.98
FeMg/NaK	1.89 - 9.46	4.89	1.96	3.52 - 10.65	7.44	1.55	4.06	5.24	0.99 - 9.56	2.93	1.40	2.56 - 8.35	4.29	0.92	3.16 - 21.11	5.5	1.9
A-Index	21.0 - 61.0	42.1	10.2	25.8 - 62.3	41.3	7.8	39.2	36.8	20.7 - 61.8	36.9	9.3	23.1 - 42.0	34.4	4.7	25.2 - 48.5	36.0	5.0
Ser-Index	0.6 - 45.8	10.3	8.9	2.0 - 32.4	13.6	9.2	23.1	16.9	1.5 - 77.9	32.2	17.6	0.6 - 21.3	4.7	3.3	1.4 - 26.2	9.3	6.1
CCP-Index	65.4 - 90.4	79.8	7.3	77.9 - 91.4	86.9	3.2	80.2	84.0	49.7 - 90.5	69.4	9.0	71.9 - 89.3	80.1	2.7	76.0 - 95.5	82.2	3.9
Ti/V	34.1 - 85.6	50.3	11.8	15.2 - 24.2	18.2	3.3	153.0	62.2	18.7 - 54.5	29.2	8.2	16.6 - 66.7	33.8	7.9	27.8 - 66.4	34.7	5.4
Zr/Y	3.6 - 12.4	6.2	2.4	0.9 - 2.0	1.1	0.2	12.4	7.6	4.0 - 10.7	6.0	1.6	1.5 - 3.8	2.7	0.6	2.0 - 5.1	3.2	0.5
Zr/Nb	3.8 - 11.7	7.1	2.0	19.0 - 41.3	29.9	5.9	4.0	4.6	4.4 - 17.6	12.4	3.25	5.7 - 55.0	33.5	9.7	9.5 - 48.0	35.5	7.0
Zr/TiO$_2$	50.8 - 123.5	78.2	23.9	28.6 - 66.0	30.4	9.9	171.0	77.8	66.7 - 322.0	182	62.5	32.1 - 110.1	58.7	15.5	44.9 - 128.2	72.8	9.5
Nb/Y	0.48 - 1.75	0.94	0.38	0.03 - 0.10	0.04	0.02	3.10	1.65	0.26 - 1.64	0.61	0.36	0.05 - 0.67	0.12	0.07	0.06 - 0.54	0.11	0.05
Nb/U	10.6 - 58.7	43.4	11.6	6.4 - 50.0	28.7	13.8	46.2	54.9	2.8 - 41.8	12.3	8.5	1.7 - 50.0	24.3	9.2	10.7 - 44.4	25.4	5.6
Th/Nb	0.06 - 0.15	0.08	0.02	0.06 - 0.25	0.08	0.05	0.09	0.08	0.11 - 1.15	0.51	0.28	0.06 - 0.16	0.09	0.02	0.07 - 0.19	0.01	0.01
Nb/Yb	6.1 - 37.5	14.1	7.9	0.3 - 1.0	0.4	0.2	54.5	28.6	2.7 - 25.6	7.6	5.3	0.3 - 9.1	1.4	1.0	0.6 - 6.3	1.2	0.6
Zr/Yb	45.0 - 291.7	94.9	53.1	9.1 - 20.6	11.1	2.6	218.2	132.7	39.4 - 166.7	71.4	26.8	15.0 - 51.8	29.1	7.3	22.6 - 59.4	34.2	5.4
Th/Yb	0.40 - 3.44	1.20	0.92	0.02 - 0.25	0.03	0.06	4.85	2.24	0.56 - 7.14	2.92	1.59	0.03 - 0.71	0.12	0.08	0.05 - 0.47	0.11	0.04
Ta/Yb	0.34 - 2.22	0.83	0.46	0.02 - 0.06	0.03	0.01	3.64	1.53	0.16 - 1.56	0.45	0.33	0.02 - 0.55	0.01	0.06	0.04 - 0.38	0.08	0.03
La/Sm$_n$	1.46 - 3.89	2.13	0.48	0.32 - 0.85	0.43	0.15	3.69	2.44	2.11 - 4.63	2.92	0.52	0.41 - 1.65	0.76	0.16	0.61 - 1.78	0.80	0.12
La/Yb$_n$	3.68 - 34.87	9.83	7.18	0.21 - 0.74	0.35	0.17	34.78	14.64	4.64 - 25.28	10.15	4.81	0.42 - 5.35	1.19	0.56	0.72 - 3.59	1.10	0.28
Nb/Nb*	0.93 - 1.56	1.33	0.18	0.64 - 1.22	1.07	0.21	1.20	1.43	0.05 - 1.19	0.41	0.22	0.16 - 1.33	0.77	0.26	0.58 - 1.37	0.89	0.01
Mg#	32.82 - 68.20	53.52	9.40	51.56 - 65.71	61.50	4.55	40.02	58.78	31.48 - 66.65	45.86	8.26	33.65 - 67.45	54.26	6.35	37.15 - 60.07	53.69	4.73
εNd_T	+4.3 to +5.7			+8.2 and +8.3			N/A	N/A	-6.5 and -6.8			+5.0 to +8.1			+8.1 and +8.7		

FeO* = FeO+(0.89981xFe$_2$O$_3$) (total iron as FeO)
FeMg/NaK = FeO*+MgO/Na$_2$O+K$_2$O (Lentz, 1999)
A-Index = Ishikawa index 100x(MgO+K$_2$O)/(MgO+K$_2$O+Na$_2$O+CaO) (Ishikawa et al., 1976)
Ser-Index = sericite index = 100xK$_2$O/(K$_2$O+Na$_2$O) (Saeki and Date, 1980)
CCPI = chlorite-carbonate-pyrite index = 100x(MgO+FeO*)/(MgO+FeO*+K$_2$O+Na$_2$O) (Large et al., 2001)
La/Sm$_n$: ratio is normalized to chondritic values of Sun and McDonough (1989)
Nb/Nb* = 2xNb$_{pm}$/(Th$_{pm}$+La$_{pm}$); pm = primitive mantle values of Sun and McDonough (1989)

values for calc-alkalic to transitional rocks (Leat *et al.*, 1986; Barrett and MacLean, 1999). Their Nb/Ta ratios (7.8-16.85; average 13.27) vary between those of upper continental crust (~12) and mantle (~17; Green, 1995; Barth *et al.*, 2000).

Upper continental crust-normalized trace element plots are characterized by flat patterns with negative Ti, V, Sc, and variable Th, Nb anomalies (Figs. 11A, B), which are typical of rocks formed in arc environments (*e.g.*, Pearce and Peate, 1995). Some workers have shown however, that these negative anomalies and arc signatures in felsic rocks can also arise from remelting of rocks with arc parentage and upper crustal sources (*e.g.*, Whalen *et al.*, 1998; Morris *et al.*, 2000), or from the fractionation of HFSE-enriched accessory phases such as ferromagnesian oxide minerals (Lentz, 1999; Piercey *et al.*, 2001), regardless of their tectonic setting. Both cases are possible and are discussed in the section on Petrogenesis. εNd_{360} values for rocks of unit EBA range from –4.7 to –13.7 (T_{DM} = 1.43-2.17 Ga); and Nd concentrations (6.5-39.6 ppm) are low to moderate (Table 5).

Unit EBF

The quartz-feldspar-phyric and feldspar-phyric flows and tuffs of unit EBF have remarkable similarities in their geochemical characteristics regardless of their composition, and as such are treated geochemically as a common entity. They straddle the boundary between alkaline and subalkaline fields, plotting in the trachy-andesite and andesite-basalt fields (Fig. 9A). They have low to moderate HFSE concentrations that are characteristic of volcanic arc rocks having I-type affinities (Figs. 9B, C). Low Zr/Nb and Zr/Y ratios are also consistent with the transitional subalkaline-alkaline character of these rocks (Figs. 10A, B).

Upper continental crust-normalized trace element plots for most quartz-feldspar-phyric and feldspar-phyric flows and tuffs show relatively flat patterns with negative Nb, Zr, Hf and Ti anomalies, except for two quartz-feldspar-phyric samples, which have positive Nb, Ti and Sc anomalies (Fig. 11C, D). These two samples (SLB99-137 and SLB99-37) have high Na_2O/K_2O (10.9 and 6.5) and FeO^*+MgO/Na_2O+K_2O (1.9 and 2.2) ratios, which suggest that they are altered.

Table 7. Summary of key major and trace element ratios for intermediate and felsic volcanic and intrusive rocks of the Eagle Bay assemblage.

	Unit EBA Subalkaline felsic flows and tuffs			Unit EBA Subalkaline intrusions			Unit EBF Alkaline-subalkaline intermediate flows and tuffs			Unit EBAF Alkaline-subalkaline QFP dacite tuffs		
	Range	Ave. (n=22)	Ave.Dev	Range	Ave. (n=10)	Ave.Dev	Range	Ave. (n=24)	Ave.Dev	Range	Ave. (n=16)	Ave.Dev
Al_2O_3/TiO_2	28.84 - 125.00	54.73	22.84	35.12 - 65.22	48.04	6.57	25.18 - 56.90	38.66	9.23	20.65 - 70.00	29.79	6.22
FeMg/NaK	0.27 - 2.06	0.83	0.33	0.25 - 1.15	0.59	0.23	0.33 - 2.17	1.08	0.49	0.54 - 2.05	1.27	0.35
A-Index	32.4 - 97.2	65.0	18.1	26.6 - 64.1	46.5	9.6	22.0 - 92.8	41.8	10.7	23.6 - 76.9	44.1	11.2
SER-Index	23.7 - 96.1	73.5	22.5	28.0 - 64.3	47.8	9.5	8.4 - 98.5	42.2	19.7	15.1 - 79.2	41.9	18.5
CCP-Index	21.3- 67.3	42.5	10.7	20.3 - 53.4	35.9	8.0	24.7 - 68.5	49.5	11.1	35.3 - 67.2	54.2	7.9
Sc/Nb	0.22 - 3.13	0.74	0.42	0.26 - 0.82	0.48	0.15	0.24 - 3.52	1.01	0.66	0.77 - 2.41	1.41	0.35
Sc/Yb	1.40 - 16.15	3.92	2.11	1.62 - 5.57	2.93	1.05	2.79 - 15.83	7.93	4.09	3.81 - 15.56	9.31	2.67
Ti/Sc	128.5- 505.5	282.9	72.9	204.9 - 344.2	267.2	33.7	110.4 - 386.3	243.2	62.2	144.6 - 294.3	194.1	34.1
Zr/Y	5.2 - 16.0	8.7	2.0	5.6 - 24.3	10.6	3.2	4.7 - 9.3	6.7	0.8	3.5 - 13.5	8.4	1.7
Zr/Sc	5.2 - 77.8	31.9	13.0	23.1 - 53.7	36.9	6.9	3.7 - 34.0	15.2	7.5	4.6 - 20.9	10.0	2.7
Zr/Nb	10.0 - 22.0	15.8	2.3	10.9 - 38.6	17.2	4.3	6.3 - 13.6	9.7	1.9	6.84 - 20.91	13.1	2.5
Zr/TiO_2	244.4 - 1,400	663.1	239.7	439 - 1,360	858	225.7	200 - 562.5	349.5	98.1	173.3 - 505.3	307.1	57.7
Nb/Y	0.29 - 1.30	0.57	0.14	0.48 - 0.76	0.61	0.09	0.45 - 1.27	0.73	0.15	0.49 - 0.86	0.64	0.07
Nb/Ta	7.80 - 16.85	13.27	2.42	12.35 - 15.83	14.06	0.87	11.25 - 23.81	16.45	2.21	10.0 - 15.0	13.53	1.03
10^4xGa/Al	1.5 - 2.4	2.1	0.1	1.8 - 3.1	2.2	0.3	1.8 - 2.5	2.0	0.1	1.8 - 2.8	2.1	0.3
Th/Nb	0.46 - 2.19	1.34	0.55	0.83 - 2.05	1.30	0.19	0.53 - 1.71	1.26	0.20	0.43 - 1.32	0.79	0.25
Th/Ta	7.46 - 42.31	16.5	4.9	12.30 - 28.57	18.10	2.49	7.59 - 31.75	20.77	3.95	6.50 - 19.23	10.54	3.06
Nb/Yb	2.8 - 10.0	5.5	1.2	4.8 - 7.9	6.1	1.0	4.2 - 14.3	9.3	1.9	4.6 - 8.6	6.6	0.9
Zr/Yb	53.1 - 126.7	85.0	16.4	57.5 - 212.5	103.0	30.0	53.9 - 107.1	85.9	9.4	41.9 - 135.3	84.9	15.1
Th/Yb	1.44 - 14.00	7.41	3.38	5.00 - 11.25	7.75	1.54	3.67 - 19.29	11.99	3.74	3.24 - 8.18	5.03	1.31
Ta/Yb	0.18 - 0.94	0.45	0.15	0.30 - 0.55	0.44	0.09	0.27 - 0.93	0.58	0.14	0.39 - 0.66	0.49	0.05
La/Sm_n	1.71 - 10.25	5.25	1.65	2.62 - 6.63	4.82	0.83	3.63 - 6.00	4.95	0.50	3.23 - 6.23	4.30	0.46
La/Yb_n	2.75 - 20.56	12.85	3.95	5.38 - 18.01	13.35	3.14	7.17 - 49.31	27.50	8.64	6.24 - 19.44	10.66	2.43
Nb/Nb*	0.01 - 0.09	0.04	0.01	0.03 - 0.05	0.04	0.01	0.02 - 0.13	0.04	0.02	0.03 - 0.39	0.08	0.04
εNd_T	-4.7 to -13.7			-4.4 to -7.0			-3.3 to -4.2			-8.5 to -10.4		

$FeO^*=FeO+(0.89981xFe_2O_3)$ (total iron as FeO)
FeMg/NaK = FeO^*+MgO/Na_2O+K_2O (Lentz, 1999)
A-Index = Ishikawa index $100x(MgO+K_2O)/(MgO+K_2O+Na_2O+CaO)$ (Ishikawa et al., 1976)
Ser-Index = sericite index = $100xK_2O/(K_2O+Na_2O)$ (Saeki and Date, 1980)
CCPI = chlorite-carbonate-pyrite index = $100x(MgO+FeO^*)/(MgO+FeO^*+K_2O+Na_2O)$ (Large et al., 2001)
La/Sm_n: ratio is normalized to chondritic values of Sun and McDonough (1989)
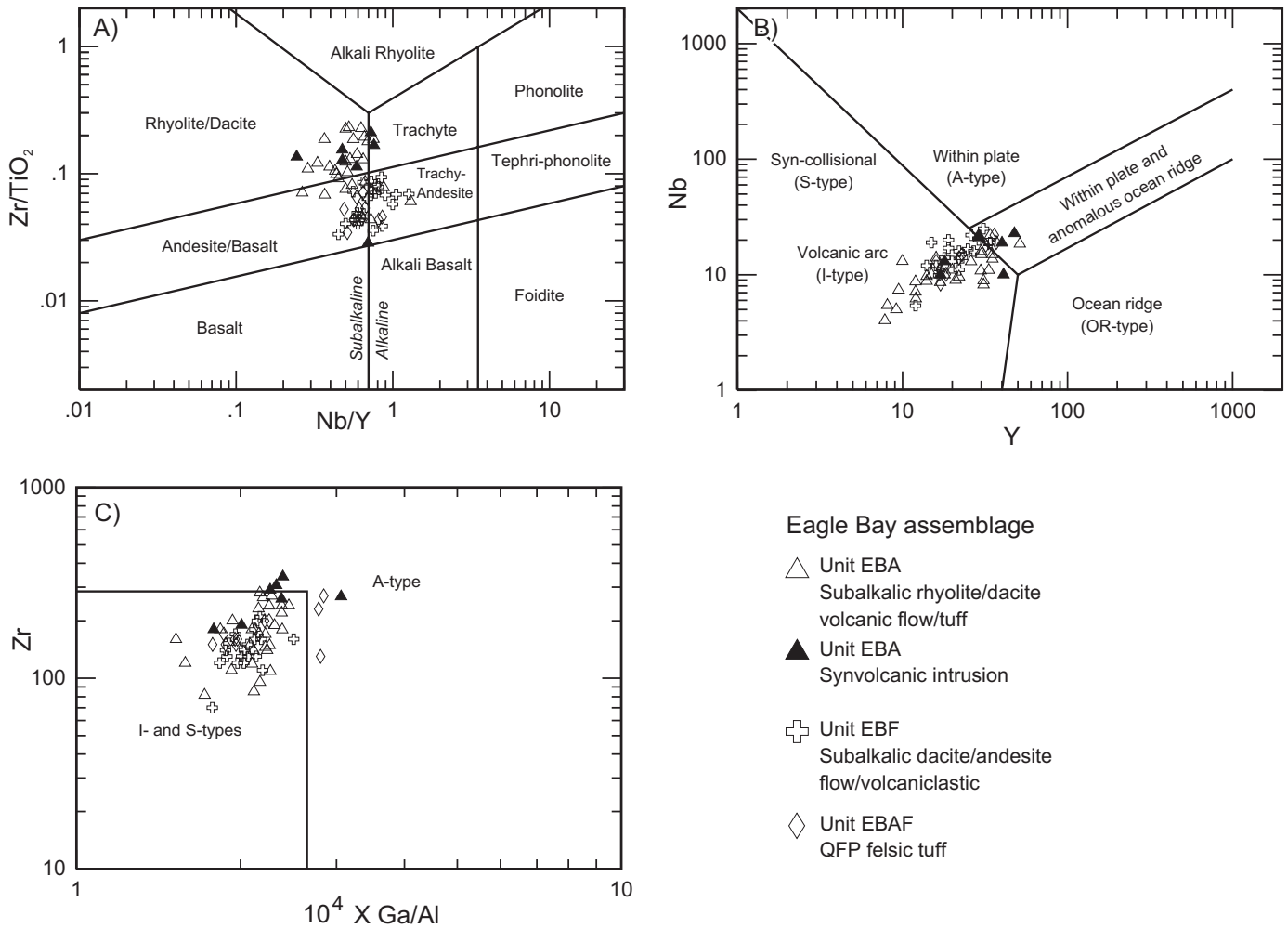Nb/Nb* = $2xNb_{pm}/(Th_{pm}+La_{pm})$

Figure 9. *Discrimination diagrams for felsic volcanic and intrusive rocks of the Eagle Bay assemblage. (A) Diagram of Pearce (1996; modified Winchester and Floyd, 1977). (B) Y-Nb plot of Pearce* et al. *(1984). (C) Ga/Al-Zr plot of Whalen* et al. *(1987).*
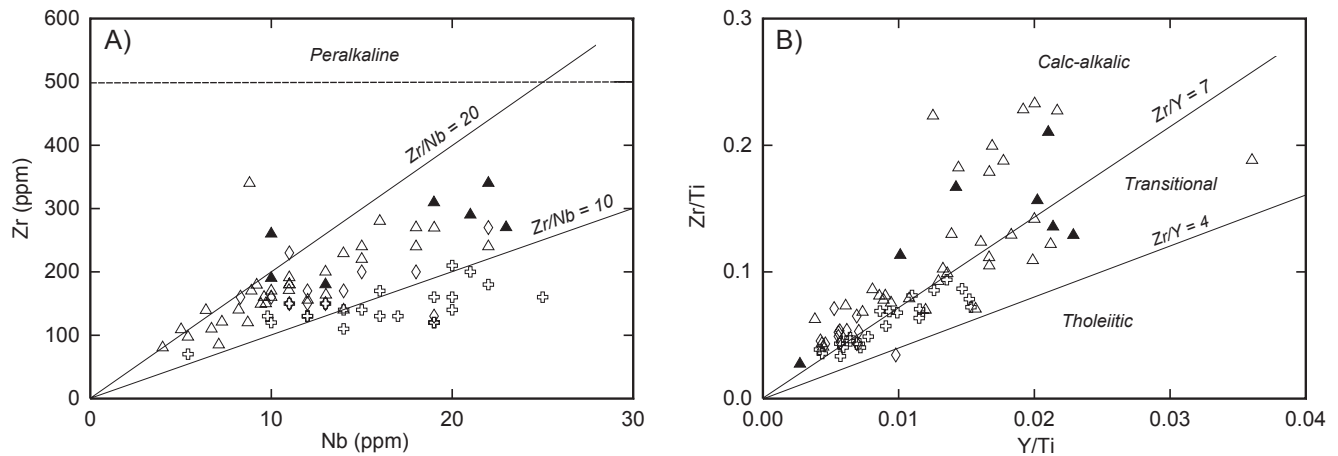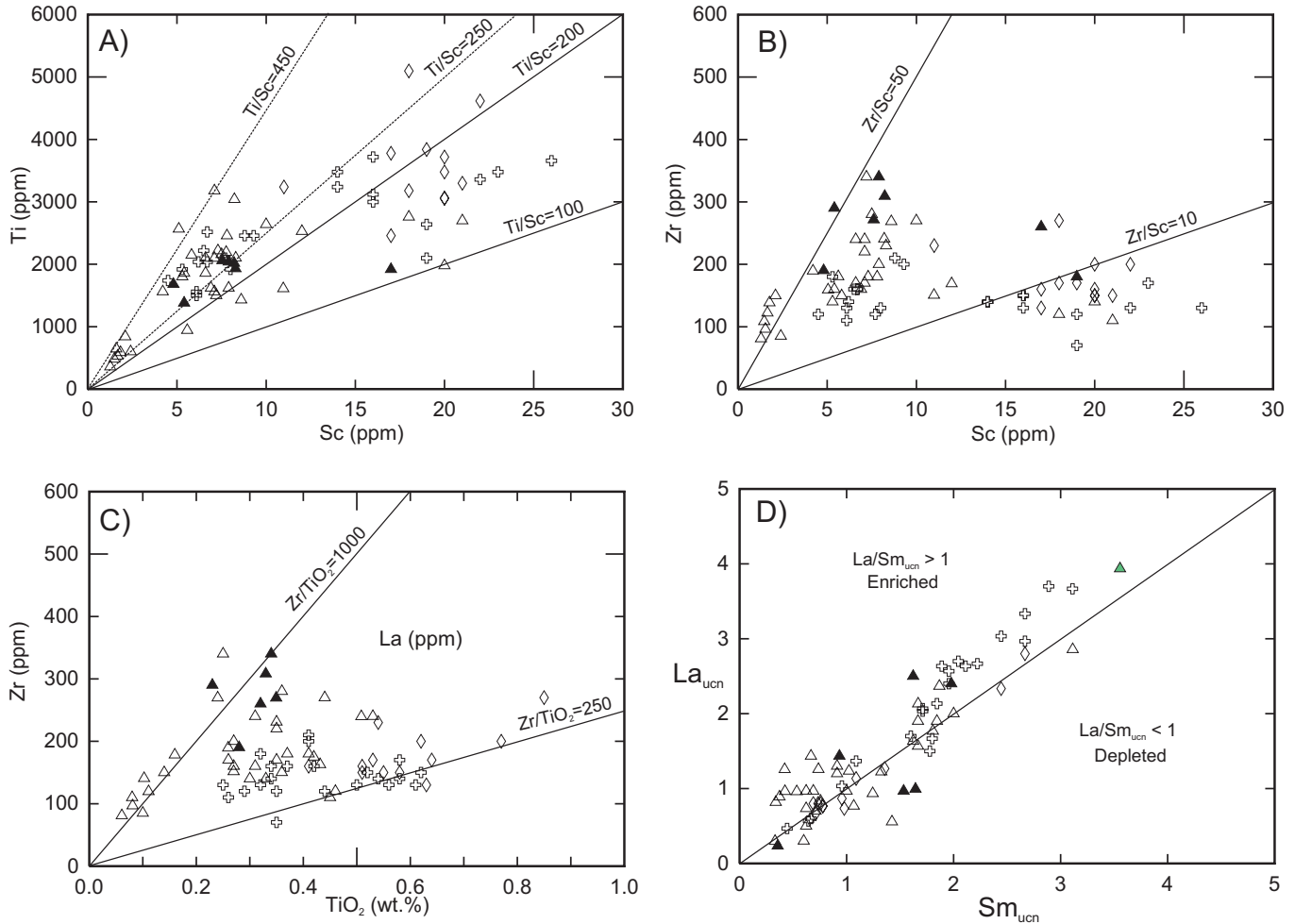

Figure 10. *High field strength element (HFSE) plots for the felsic volcanic and intrusive rocks of the Eagle Bay assemblage. (A) The Nb-Zr plot of Leat* et al. *(1986) illustrates the higher Zr/Nb ratios of the felsic volcanic and intrusive rocks of unit EBA in relation to unit EBF. (B) Y/Ti-Zr/Ti plot for deciphering the tholeiitic vs. calc-alkaline affinities of the felsic rocks (from Lentz 1998, 1999). Symbols as in Figure 9.*

EBA and EBF units have overall similar HFSE contents and ratios (*e.g.*, Nb/Y, Zr/Y, Zr/Nb, Ti/Sc, Th/Nb, Sc/Nb and Sc/Yb; Table 7), suggesting that they were derived from a common magmatic source (MacLean and Barrett, 1993). However, Zr and Hf values of felsic rocks of unit EBF are somewhat lower and Eu, Ti, Sc and V

values are higher when compared with felsic rocks of unit EBA (Figs. 10, 12; Table 4). εNd_{360} values for rocks of unit EBF range from -3.3 to -4.2 (T_{DM} = 1.22-1.36 Ga), and Nd concentrations (57.6-74.7 ppm) are relatively high (Table 5).
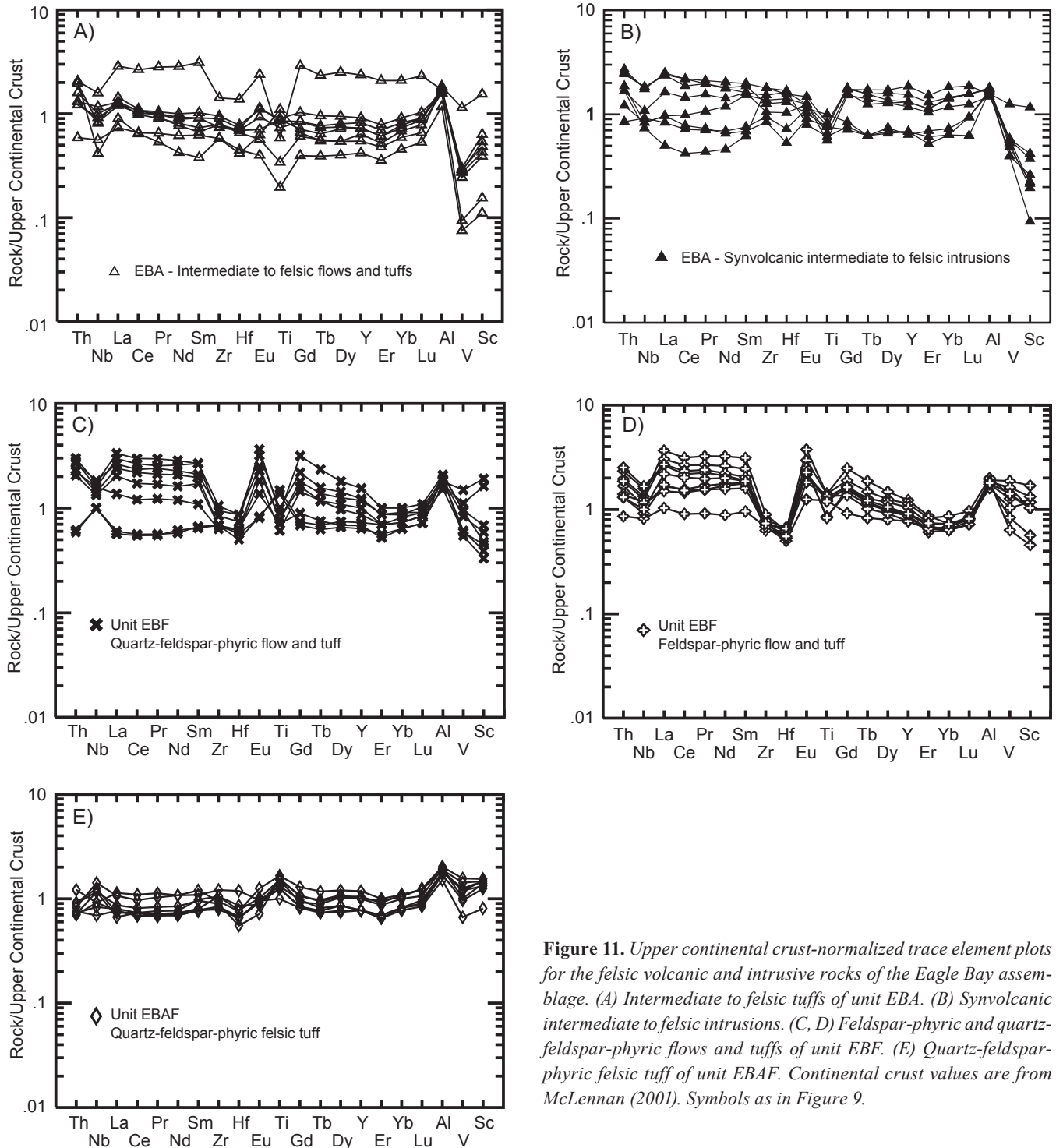
Figure 11. *Upper continental crust-normalized trace element plots for the felsic volcanic and intrusive rocks of the Eagle Bay assemblage. (A) Intermediate to felsic tuffs of unit EBA. (B) Synvolcanic intermediate to felsic intrusions. (C, D) Feldspar-phyric and quartz-feldspar-phyric flows and tuffs of unit EBF. (E) Quartz-feldspar-phyric felsic tuff of unit EBAF. Continental crust values are from McLennan (2001). Symbols as in Figure 9.*

Figure 12. *Key high field strength element (HFSE) and rare earth element (REE) plots for the felsic volcanic and intrusive rocks of the Eagle Bay assemblage. Although there is overlap, unit EBA samples have higher average Ti/Sc (A), Zr/Sc (B), and Zr/TiO$_2$ (C) ratios than unit EBF samples. (D) Felsic volcanic and intrusive rocks of the Eagle Bay assemblage plot on or close to the line with a slope of 1, equivalent to La/Sm$_{ucn}$ = 1. Upper continental crust values are from McLennan (2001). Symbols as in Figure 10.*

Unit EBAF

Unit EBAF consists of intermediate volcanic rocks that straddle the boundary between alkaline and subalkaline fields, plotting in the trachy-andesite and andesite-basalt fields (Fig. 9A). They have low to moderate HFSE concentrations characteristic of arc rocks (Fig. 9B) with I-type affinity (Fig. 9C), and low Zr/Nb and Zr/Y ratios (Figs. 10A, B) that are similar to published values for calc-alkaline to transitional rocks (Leat *et al*., 1986; Barrett and MacLean, 1999).

Upper continental crust-normalized trace element plots are characterized by flat patterns with variable Nb anomalies and slight negative Hf anomalies (Fig. 11E). HFSE concentrations and ratios of unit EBAF are similar to intermediate to felsic rocks of units EBA and EBF (Table 7). εNd$_{360}$ values range from –8.5 to –10.4 (T_{DM} =

1.77-1.93 Ga), and Nd concentrations (17.2-24.9 ppm) are moderate (Table 5).

DISCUSSION

Geochemical Systematics

Lower Cambrian magmatism within the Eagle Bay assemblage co-incided with eruption of alkalic within-plate basalts (OIB) and local eruption of subalkalic basalts (MORB). The alkalic basalts of unit EBG have a geochemical signature that resembles OIB or some continental intraplate basalts free of crustal contamination (Fig. 13A). Their geochemical characteristics suggest that they come from an incompatible element-enriched mantle source at low degrees of partial melting (*e.g.*, Laflèche *et al*., 1998). The OIB-like source for

these basalts is supported by their HFSE, REE and isotopic characteristics. They are enriched in Th/Yb, Ta/Yb and Nb/Yb, and plot between enriched mid-ocean-ridge basalt (E-MORB) and OIB end-members (Figs. 13B, C). Most EBG samples plot in the enriched mantle field of Figure 14. The Nb/Th$_{mn}$ *vs.* Nb/La$_{mn}$ diagram (Fig. 14) divides mafic rocks into those that have been contaminated by continental crust (*i.e.,* Nb/Th$_{mn}$ and Nb/La$_{mn}$ <1) and those that come from an enriched mantle source with inherited oceanic crustal component (*i.e.,* Nb/Th$_{mn}$ and Nb/La$_{mn}$ >1). The nature and origin of this enrichment is a matter of considerable debate: do alkalic within-plate basalts of unit EBG come from new upwelling enriched asthenospheric mantle sources (Sun and McDonough, 1989; van Staal *et al.*, 1991; Shinjo *et al.*, 1999), ancient subcontinental lithospheric

mantle sources (Pearce, 1983; McDonough, 1990; Hawkesworth *et al.*, 1990; Menzies, 1990), or enrichment processes involving crustal contamination? The geochemical characteristics of these basalts (*i.e.,* positive Nb anomalies relative to Th and La; moderate εNd$_{540}$ values of +4.3 to +5.7; low Th/Nb ratios of ≤1; and smooth trace element patterns) suggest minor interaction with continental crust. These geochemical attributes, coupled with geological characteristics such as a relatively minor volume of basaltic volcanic rocks compared to large igneous provinces of continental flood basalts, suggest derivation from subcontinental lithospheric mantle sources. Laflèche *et al.* (1998) also favoured a lithospheric origin for small volumes of intraplate alkalic magma with OIB characteristics from the Carboniferous Maritimes basin of eastern Canada.
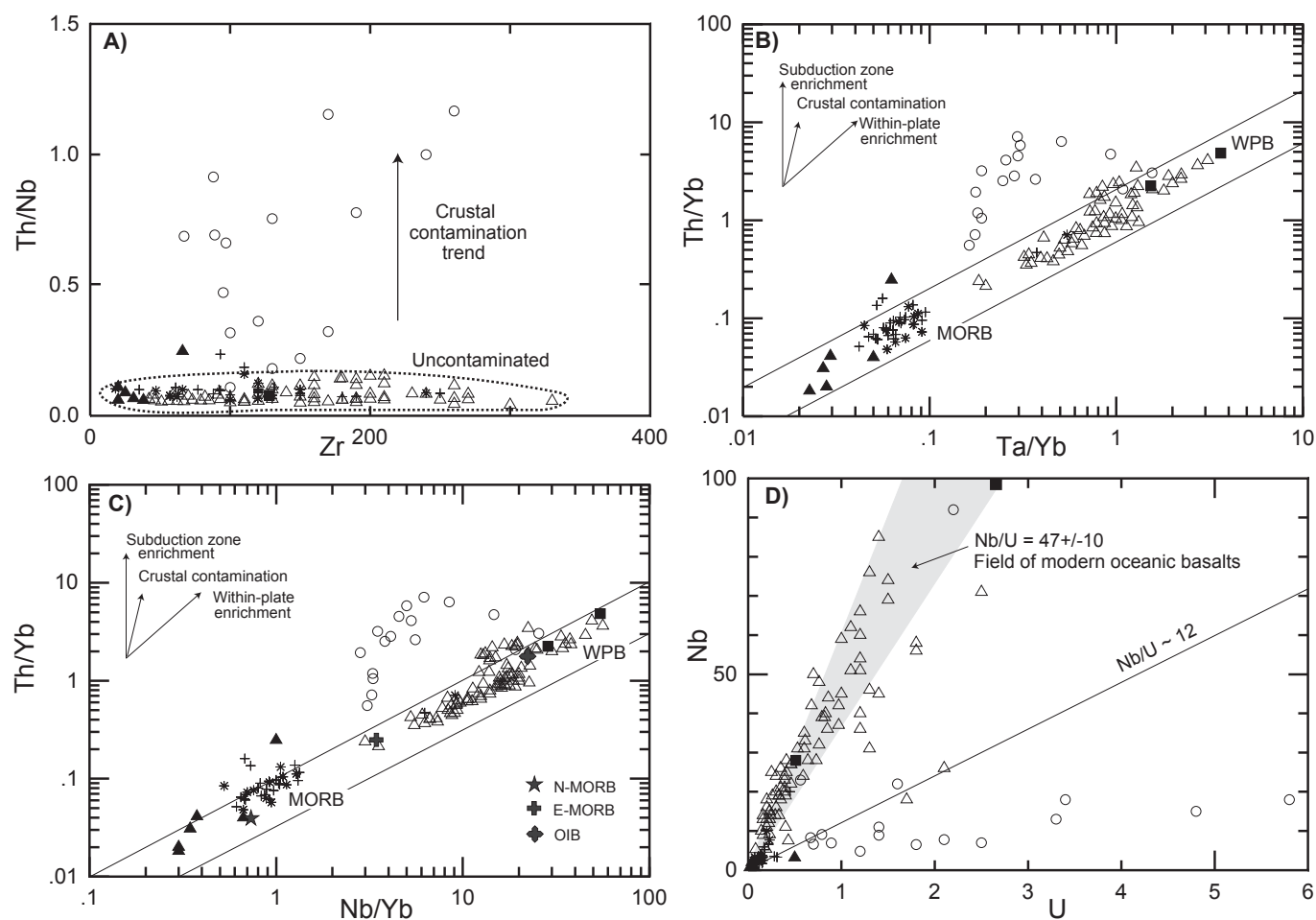
Figure 13. *Trace element diagrams that illustrate degree of crustal contamination in mafic volcanic rocks of the Eagle Bay assemblage and the Fennell Formation. (A) Th/Nb* vs. *Zr plot illustrates the crustal contamination trend of unit EBA samples. (B, C) The relationships between Th/Yb and Ta/Yb and Nb/Yb (modified from Pearce, 1983 and Stern* et al.*, 1995) illustrate potential crustal contamination in mafic volcanic rocks. Samples from unit EBG (subalkalic basalts - MORB), Tsalkom and Fennell formations plot close to the average values for N-MORB. Alkali basalts from unit EBG plot within a continuous array from average enriched mid-ocean-ridge basalt (E-MORB) and OIB values, reflecting their within-plate enrichment. Mafic volcanic rocks of unit EBA and a small group of samples from unit EBG exhibit a distinct crustally influenced trajectory. (D) The Nb/U ratios define two groups of samples, one that corresponds to most EBG samples with approximate ratio of 50 (field for modern oceanic basalts Nb/U~47 ± 10; Hofmann* et al.*, 1986), and the other with much lower ratio (Nb/U <12) that is consistent with crustal influence (Nb/U~12; McLennan, 2001). Global values for N-MORB, E-MORB and OIB are from Sun and McDonough (1989). Symbols as in Figure 5.*
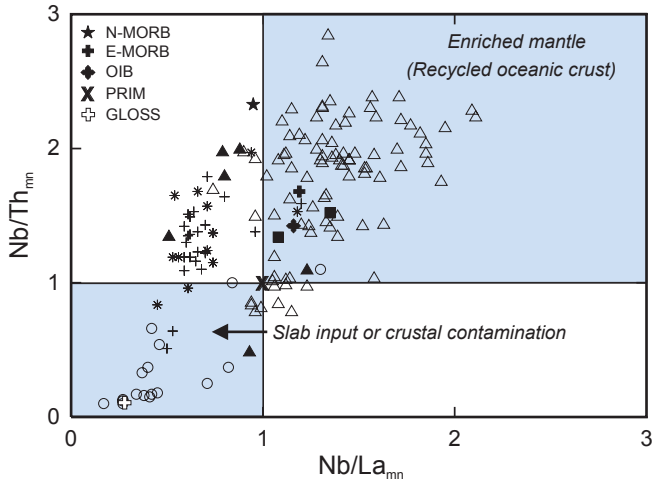
Figure 14. *Nb/La$_{mn}$ vs. Nb/Th$_{mn}$ for mafic rocks. Details of the diagram provided in the text. Diagram constructed by Piercey* et al. *(this volume) from the conceptual idea in Niu* et al. *(1999). Average values of mantle reservoirs are from Sun and McDonough (1989): N-MORB = Normal mid-ocean ridge basalt (depleted); E-MORB = Enriched mid-ocean ridge basalt; OIB = Ocean-island basalt; PRIM = Primitive mantle. GLOSS = Global subducted sediment (Plank and Langmuir, 1998). Symbols as in Figure 5.*

The subalkalic basalts of unit EBG have typical N-MORB geochemical characteristics. Their HFSE and REE contents and their εNd$_{540}$ values of +8.2 and +8.3 are similar to MORB elsewhere in the Canadian Cordillera (*e.g.*, Slide Mountain terrane, Smith and Lambert, 1995; Finlayson Lake district of the Yukon-Tanana terrane, Piercey *et al.*, 2004) and to global depleted mantle in Cambrian time (εNd$_{540}$ = +9.1; Goldstein *et al.*, 1984). The oceanic signature of the EBG subalkalic basalts is also consistent with their association with deep-ocean sedimentary rocks, such as banded chert, phyllite and argillite. Similar close association of MORB-type and OIB-type basalts has been documented in various ocean basins (*e.g.*, Le Roex *et al.*, 1989), including the northeast Pacific Ocean (Cousens *et al.*, 1995). The geochemical differences between the two basalt types (*i.e.*, MORB and OIB) require two mantle sources. The geochemistry of the alkalic within-plate basalts suggest that they derived from an enriched mantle source, similar to OIB, at low degrees of partial melting (*e.g.*, Laflèche *et al.*, 1998; Piercey *et al.*, 2002), whereas the subalkalic N-MORBs are derived from a depleted mantle source.

The Devonian-Mississippian igneous suite is characterized by geochemical diversity that includes subalkalic to alkalic basalts with arc, MORB and OIB affinities, and subalkalic intermediate to felsic volcanic and intrusive rocks of arc affinity.

The subalkalic basalts of the Late Devonian(?) Tsalkom Formation have typical N-MORB geochemical characteristics that are identical to basalts of the Late Devonian to Permian Fennell Formation, which were interpreted as ocean-floor tholeiites (N-MORB) by Schiarizza and Preto (1987), and Smith and Lambert (1995). Their HFSE and REE contents and their εNd values (εNd$_{360}$ = +5.0 - +8.1 for Tsalkom, εNd$_{300}$ = +8.1 - +8.7 for Fennell) generally

resemble modern MORBs. Two samples from the Tsalkom and Fennell formations plot between OIB and MORB (Figs. 13B, C) and are consistent with derivation from a slightly enriched mantle source. Overall, the identical geochemistry of the basalts from the Tsalkom and Fennell formations suggest derivation from the same depleted mantle source and tectonic setting, *i.e.*, a marginal oceanic basin or a back-arc basin (see below).

The alkalic within-plate basalts of unit EBM have HFSE and REE contents similar to OIB. As mentioned above, alkalic OIB-type basalts are commonly found in a variety of continental margin settings, including continental rifts (Goodfellow *et al.*, 1995) and continental arc rifts (van Staal *et al.*, 1991; Shinjo *et al.*, 1999). Both of these are plausible geodynamic environments for the southern Cordillera in Devonian-Mississippian time; however, the stratigraphic relationship between EBM and EBA favours a continental arc rift setting, because EBM basalts underlie unit EBA subalkalic volcanic-intrusive rocks of arc affinity.

The subalkalic mafic to felsic volcanic and intrusive rocks of units EBA, EBF and EBAF have geochemical characteristics of arc rocks. Their low abundances of Nb relative to Th and La on primitive mantle-normalized plots (Figs. 8B, 11A-E) are the hallmark of subduction-related rocks (*e.g.*, Pearce and Parkinson, 1993; Piercey *et al.*, this volume). Subalkalic andesite tuffs of unit EBA have low HFSE contents (Table 3) and are LREE-enriched (La/Sm$_n$ = 2.1-4.6) primitive mantle-normalized signatures with distinctive Nb and Ti anomalies (Fig. 8B). The tuffs plot in the arc fields on various tectonic discrimination diagrams (Figs. 6A, B). Their geochemical characteristics resemble other mafic to intermediate arc rocks of the Yukon-Tanana terrane (Simard *et al.*, 2003; Dusel-Bacon *et al.*, this volume) in terms of their overall negative slopes, Nb troughs, and absolute abundances on the primitive mantle-normalized plots. In addition, their field association with intermediate to felsic rocks of arc character supports their arc geochemical signature. However, the andesite tuffs have also high Th values (Figs. 13A-C), low Nb/U ratios (Fig. 13D), low Nb/Th$_{mn}$ and Nb/La$_{mn}$ ratios (Fig. 14), and evolved Nd isotopic signatures (εNd$_{360}$ values = -6.5 and -6.8), all of which imply an input of crustal material. The Th enrichment characteristic of these samples is either due to subduction slab metasomatism or crustal contamination. Crustal contamination is supported by Th/Nb *vs.* Zr systematics (Fig. 13A), with EBA andesites showing high Th/Nb ratios at a given Zr value, typical of magmas that have undergone some crustal contamination (Piercey *et al.*, 2002). The average Nb/U values (11.1) for the EBA andesites is between the upper crust value of 10.4 (Wedepohl, 1995) and lower crust value of 12.15 (Wedepohl, 1995). Primitive mantle normalized Nb/La and Nb/Th ratios of <1 (Fig. 14) are characteristic of subduction-related basalts with arc parentage, or basalts that have been crustally contaminated (Pearce and Peate, 1995; Niu *et al.*, 1999; Piercey *et al.*, this volume).

Intermediate to felsic volcanic and intrusive rocks of units EBA, EBF and EBAF have geochemical characteristics consistent with formation in a volcanic arc environment via melting of upper crustal sources (*e.g.*, Whalen *et al.*, 1998; Morris *et al.,* 2000) or via the fractionation of HFSE-enriched accessory phases such as ferromagnesian oxide minerals (Lentz, 1999; Piercey *et al.*, 2001). The ubiq-

uitous presence of inherited Proterozoic zircons in these rocks and in contemporaneous felsic rocks of the Yukon-Tanana terrane (Mortensen, 1992a, b; Grant, 1997; Piercey *et al.*, this volume), their evolved feldspar Pb-isotopic values, and their association with syngenetic volcanic-hosted massive sulphide (VHMS) deposits that have evolved Pb-isotopic signatures (Paradis, unpublished data) support derivation from an upper crustal source. Furthermore, they have evolved and variable Nd isotopic signatures with εNd_{360} values of -3.3 to -13.7 and T_{DM} ages of 1.22 to 2.17 Ga, which also suggests a significant role of crustal material in their genesis.

Tectonic Settings and Controls on Syngenetic Massive Sulphide Mineralization

Lower Cambrian Rocks of the Eagle Bay Assemblage

The geologic and geochemical signatures of the Lower Cambrian basalts, unit EBG of the Eagle Bay assemblage, suggest that they formed within a continental rift environment along the ancient western margin of the North American continent. The mafic volcanic rocks formed volcanic edifices, with fringing carbonate complexes, represented by the archaeocyathid-bearing Tshinakin limestone and its correlatives, and interlayered fine-grained clastic sedimentary rocks that host sulphide deposits (VSHMS or SEDEX). Felsic volcanic rocks are not known to be present in the Cambrian succession. The tectonic discrimination and multi-element normalized diagrams of Figures 6 and 7 illustrate the within-plate, OIB character for most of the EBG basalts and the MORB signature for some subordinate basalts. The OIBs host small VHMS mafic type deposits, however the MORBs do not host any known sulphide deposits. Their interlayered clastic sedimentary rocks host VSHMS or SEDEX-type deposits. This pattern differs from that observed in the Lardeau Group of the northern Selkirk Mountains, where MORBs and interlayered sedimentary rocks of the Index Formation are spatially associated with Besshi-type Cu-Zn and SEDEX deposits, and OIBs of the Index and Jowett formations lack association with sulphide deposits (Logan and Colpron, this volume).

The alkalic to subalkalic nature of the EBG mafic volcanic rocks, association with small VHMS deposits, and association with sedimentary rocks (*e.g.*, phyllite, chert, argillite) that host massive sulphide deposits of VSHMS or SEDEX types, support deposition in an intracontinental rift basin (Höy, 1999). Evidence of intermittent extension during Late Proterozoic to Cambrian time accompanied by extrusion of volcanic rocks of alkalic affinity and OIB chemical signature has been reported along the western North American continental margin (Poole *et al.*, 1992; Colpron and Price, 1995; Colpron *et al.*, 2002; Lund *et al.*, 2003; Sears and Price, 2003; Logan and Colpron, this volume). In the northern Canadian miogeocline, lower to middle Paleozoic alkalic volcanic rocks are concentrated along rift-parallel faults of the Selwyn basin, and are found spatially and temporally associated with SEDEX deposits (Goodfellow *et al.*, 1995). In the southern Canadian Cordillera, alkalic and subalkalic volcanic rocks of the Lardeau Group have also been interpreted to have erupted in an intracontinental rift setting (Logan and Colpron, this volume). Alkalic rocks also occur as Ordovician and Silurian

diatremes of ultrabasic composition in the Western and Main ranges of the southern Rocky Mountains (Pell, 1994).

The Lower Cambrian volcanic succession of the Eagle Bay assemblage appears to retain the lithogeochemical signature of an actively evolving continental rift environment with relatively thick alkalic within-plate OIB-type basalts and associated lesser MORB-type basalts, both of which show minor or no crustal contamination. This suggests that the mafic magmatic event took place over a relatively thin continental crust and occurred in response to continental margin extension, crustal thinning and rifting along inferred faults, which would induce decompression melting of the enriched lithospheric mantle resulting in the extrusion of the Eagle Bay assemblage OIBs. Further lithospheric extension would lead to asthenospheric mantle upwelling and local extrusion of the MORBs. Logan and Colpron (this volume) suggested the same tectono-magmatic events for the volcanic rocks of the Index and Jowett formations of the Lardeau Group in the Kootenay arc. Geological characteristics, such as the relatively minor volume of basaltic volcanism and the presence of an unconformity above the Lower Cambrian succession of the Eagle Bay assemblage, suggest an aborted rift that did not evolve to full seafloor spreading and creation of an oceanic basin, but instead only ruptured the crust.

Devonian-Mississippian Rocks of the Eagle Bay Assemblage

The tectonic settings in which felsic magmas are generated are much more difficult to establish than those for mafic magmas. For example, felsic magma generated in a non-arc setting can acquire an arc-like geochemical signature as a result of genesis in or contamination by crustal material. It can also form by blending of partial melt contributions from different continental lithologies (*e.g.*, Piercey *et al.*, 2001); and the abundance of some HFSE (*e.g.*, Ti, Zr, Hf) and REE are generally sensitive to fractionation of accessory minerals and removal from the melt. Consequently, our tectonic interpretation of felsic rocks in the Eagle Bay assemblage is based on a global analysis incorporating their geological, lithological and geochemical characters.

In the previous section, we have outlined the geochemical diversity of the Devonian-Mississippian igneous suite within the Eagle Bay assemblage and its associated units, which includes subalkalic MORBs of the Tsalkom formation and the oldest parts of the Fennell Formation, alkalic OIBs of unit EBM, and subalkalic arc-type mafic to felsic rocks of units EBA, EBF and EBAF. This geochemical diversity and certain geologic characteristics constrain the tectonic setting of these rocks to that of a continental arc complex with an adjacent back-arc oceanic basin along the ancient continental margin of western North America. Some of the geologic characteristics include abundance of volcaniclastic rocks *vs.* flows, abundance of clastic sedimentary rocks, abundance of felsic-intermediate magmatic rocks *vs.* mafic rocks, and presence of synvolcanic intermediate to felsic intrusions. Höy and Goutier (1986) and Höy (1999) also considered the Devonian-Mississippian rocks of the Eagle Bay assemblage to be the product of continental arc magmatism along the western edge of the North America margin. This arc magmatism

occurred in and on rocks that formed on or near the ancient continental margin of North America, and the fact that no contemporaneous subduction complex (*i.e.,* accretion complex) is found to the east of the arc complex(es) suggested to Monger and Price (2002) that the arc complex(es) reflect eastward subduction of oceanic lithosphere beneath the edge of North American plate.

Development of the arc sequences was dominated by relatively abundant felsic to intermediate magmatic rocks and associated clastic sedimentary rocks, and less abundant mafic rocks of arc signature. Based on stratigraphic relationships and correlations, we suggest that mafic magmatism commenced sometime during the middle Paleozoic, with extrusion of minor, alkalic OIB-type basalts of unit EBS (not described in this paper) within an environment of carbonaceous and siliciclastic sedimentation along or on the continental margin. This was followed by extrusion of more abundant alkalic OIB-type mafic volcanics of unit EBM in a similar tectonic setting, *i.e.*, continental rift or continental arc rift. It is possible that this period of alkalic within-plate volcanism on the continental margin occurred contemporaneously with the MORB-type volcanism represented by the Tsalkom, followed in late Paleozoic time by the Fennell formation, in a back-arc oceanic basin that developed along the continental margin. In other ancient continental margin settings of orogens in Canada, within-plate (rift associated) OIB-type magmatism commonly evolved through time into primitive MORB magmatism, indicating the development of oceanic crust in a back-arc setting (*e.g.*, the Bathurst Mining Camp, van Staal *et al.*, 1991; the Finlayson Lake district, Piercey *et al.*, 2002).

U-Pb geochronology documents an episode of arc activity in Late Devonian and Early Mississippian (*ca.* 360-346 Ma). Calc-alkaline to transitional felsic-intermediate arc magmatism of units EBA, EBF and EBAF occurred concurrently with less abundant transitional mafic arc volcanism of unit EBA. Involvement of crustal material is shown by the evolved εNd signatures and Proterozoic T_{DM} ages, inherited Precambrian zircons in these rocks, presence of quartzo-feldspathic sedimentary rocks containing Precambrian detrital zircons, and HFSE characteristics of the felsic-intermediate volcanic and intrusive rocks (Paradis and Nelson, 2000; Bailey, 2002).

Devonian-Mississippian arc magmatism, locally accompanied by back-arc basin generation and sulphide mineralization, has also been recognized elsewhere within the pericratonic terranes along the western North American margin from Alaska to northern British Columbia (Mortensen, 1992a; Piercey *et al.*, 2001, 2002, this volume; Dusel-Bacon *et al.*, this volume; Nelson *et al.*, this volume). Recent geological mapping and geochemical and isotopic studies corroborate episodic history of arc magmatism, rifting of the arc(s), development of back-arc basins, and formation of sulphide deposits in the Kootenay terrane (Bailey *et al.*, 2001; Bailey, 2002; Paradis *et al.*, 2003a, b) and the Yukon-Tanana terrane (Piercey *et al.*, 2001, 2002, this volume). Development of arc assemblages in the Kootenay terrane at the western edge of the North America margin is supported by the presence of a large amount of intermediate to felsic volcaniclastic rocks, coeval intrusive rocks and related clastic sedimentary rocks, and the geochemical signature of the volcanic and synvolcanic intrusive rocks, all of which indicate an arc environment.

The episode(s) of extension within the arc system coincided with the formation of VHMS deposits, such as Homestake, Rea Gold, Harper and Beca, in felsic volcanic rocks of units EBA and EBF, and SHMS deposits, such as Mount Armour and Fortuna, in clastic sedimentary rocks of unit EBS. Sillitoe (1982) recognized that VHMS deposits commonly form in bimodal volcanic sequences that are associated with extensional environments. In the Finlayson district of the Yukon-Tanana terrane, arc rifting, ensialic back-arc basin formation, and felsic magmatism coincided with genesis of VHMS deposits (Piercey *et al.*, 2001, 2002, this volume) and the initial opening of the Slide Mountain ocean between the pericratonic Yukon-Tanana terrane and the North American continent at about the Devonian-Mississippian boundary (Nelson, 1993; Nelson and Bradford, 1993; Creaser *et al.*, 1999). This period of arc rifting and felsic to intermediate volcanism in the pericratonic terranes is also coeval with extension, alkalic magmatism, and VHMS and SEDEX deposit formation in rocks of the North American miogeocline during the mid-Paleozoic (*e.g.*, Paradis and Nelson, 2000; Nelson *et al.*, 2002).

CONCLUSIONS

The diversity of geological characteristics and geochemical signatures of volcanic rocks of the Eagle Bay assemblage reflects a variety of continental margin settings and processes, including continental extension and rifting in Early Cambrian and volcanic arc and back-arc development in Devonian-Mississippian.

Most of the Lower Cambrian basalts of the Eagle Bay assemblage (unit EBG) have an alkalic, within-plate signature similar to that of ocean-island basalts (OIB) formed in continental rift setting. A suite of mid-ocean ridge basalts (MORB) forms a band 4.2 km in length within the OIB succession. The within-plate OIB-type mafic volcanic rocks and associated clastic sedimentary rocks host small VHMS mafic type deposits and VSHMS or SEDEX-type deposits, respectively. The geological and geochemical characteristics of the Lower Cambrian basalts suggest formation in a continental rift basin environment along the ancient continental margin of North America. The mafic volcanic rocks of the Tsalkom Formation have N-MORB geochemical characteristics that are identical to contemporaneous and younger mafic volcanic rocks of the Fennell Formation, which suggests genesis within the same tectonic setting. These rocks may have formed within a marginal oceanic basin or back-arc basin that developed along the continental margin during mid- to late Paleozoic time, and occurred concurrently with OIB-type volcanism on the margin. The latter is represented by alkalic within-plate basalts of unit EBM. MORB-type mafic volcanic rocks of the Fennell Formation host VHMS mafic-type sulphide deposits (*e.g.*, Chu Chua), whereas those of the Tsalkom formation do not host known syngenetic massive sulphide deposits.

The Upper Devonian to Lower Mississippian mafic tuffs of unit EBA are subalkalic transitional andesites-basalts typical of island arc environments. Their evolved Nd isotopic signature (εNd$_{360}$ values = -6.5 and -6.8) indicate a significant role of crustal material in their genesis. This Devonian-Mississippian mafic volcanism was accompanied by intermediate to felsic volcanic flows, tuffs and synvolcanic intrusions of units EBA and EBF, which have chemical characteris-

tics of an island arc setting, and variable and evolved Nd isotopic signatures (ϵNd_{360} values = -3.3 to -13.7). The arc-type felsic volcanic rocks of unit EBA and EBF host VHMS bimodal-felsic type polymetallic massive sulphide deposits. The geologic, geochemical and isotopic features of Devonian-Mississippian rocks record evidence of crustal contamination and deposition within an evolving arc built on continental crust along the western edge of ancestral North America.

ACKNOWLEDGEMENTS

REFERENCES

Bailey, S.L., 2002, Geology and geochemistry of the Eagle Bay assemblage in the Johnson Lake area, Kootenay terrane, south-central British Columbia: M.Sc. thesis, University of Victoria, Victoria, B.C., 201 p.

Bailey, S.L., Paradis, S. and Johnston, S.T., 2000, Geological setting of the Devonian-Mississippian, Rea and Samatosum VMS deposits of the Eagle Bay assemblage, Adams Lake area, south central British Columbia, in Geological Fieldwork 1999, B.C. Ministry of Energy and Mines, Paper 2000-1, p. 287-296.

Bailey, S.L., Paradis, S. and Johnston, S.T., 2001, New insights into metavolcanic successions and geochemistry of the Eagle Bay assemblage, south-central British Columbia: Geological Survey of Canada, Paper 2001-A8, p. 1-13.

Barrett, T.J. and MacLean, W.H., 1999, Volcanic sequences, lithogeochemistry, and hydrothermal alteration in some bimodal volcanic-associated massive sulfide systems, in Barrie, C.T. and Hannington, M.D., eds., Volcanic-Associated Massive Sulfide Deposits: Processes and Examples in Modern and Ancient Environments: Reviews in Economic Geology, v. 8, p. 101-131.

Barth, M.G., McDonough, W.F. and Rudnick, R.L., 2000, Tracking the budget of Nb and Ta in the continental crust: Chemical Geology, v. 165, p. 197-213.

Beatty, T.W., 2003, Stratigraphy of the Harper Ranch Group and tectonic history of the Quesnel terrane in the area east of Kamloops, British Columbia: M.Sc. thesis, Simon Fraser University, Burnaby, British Columbia, 168 p.

Campbell, R.B., 1964, Geology, Adams Lake, Seymour Arm, West Half, British Columbia: Geological Survey of Canada, Map 48-1963, 1:253,440.

Campbell, R.B. and Okulitch, A.V., 1973, Stratigraphy and structure of the Mount Ida Group, Vernon (82L), Adams Lake (82M W1/2), and Bonaparte Lake (92P) map-areas, British Columbia: Geological Survey of Canada, Paper 73-1, Part A, p. 21-23.

Campbell, I.H., Lesher, C.M., Coad, P., Franklin, J.M., Gorton, M.P. and Thurston, P.C., 1984, Rare-earth element mobility in alteration pipes below massive Cu-Zn sulfide deposits: Chemical Geology, v. 45, p. 181-202.

Carmichael, R.G., 1991, Final report on the Kamad property, Kamloops Mining Division, British Columbia: unpublished report, Kamal Silver Co. Ltd.

Colpron, M. and Price, R.A., 1995, Tectonic significance of the Kootenay terrane, southeastern Canadian Cordillera: An alternative model: Geology, v. 23, p. 25-28.

Colpron, M., Logan, J.M. and Mortensen, J.K., 2002, U-Pb zircon age constraint for late Neoproterozoic rifting and initiation of the lower Paleozoic passive margin of western Laurentia: Canadian Journal of Earth Sciences, v. 39, p. 133-143.

Cousens, B.L., Allan, J.F., Leybourne, M.I., Chalse, R.L. and Van Wagoner, N., 1995, Mixing of magmas from enriched and depleted mantle sources in the Northeast Pacific; West Valley segment, Juan de Fuca Ridge: Contributions to Mineralogy and Petrology, v. 120, p. 337-357.

Creaser, R.A., Erdmer, P., Stevens, R.A. and Grant, S.L., 1997, Tectonic affinity of Nisutlin and Anvil assemblage strata from the Teslin tectonic zone, northern Canadian Cordillera: Constraints from neodymium isotope and geochemical evidence: Tectonics, v. 16, p. 107-121.

Creaser, R.A., Goodwin-Bell, J.-A.S. and Erdmer, P., 1999, Geochemical and Nd isotopic constraints for the origin of eclogite protoliths, northern Cordillera; implications for the Paleozoic tectonic evolution of the Yukon-Tanana terrane: Canadian Journal of Earth Sciences, v. 36, p. 1697-1709.

Date, J., Watanabe, Y and Saeki, Y., 1983, Zonal alteration around the Fukazawa Kuroko deposits, Akita Prefecture, northern Japan, in Ohmoto, H. and Skinner, B.J., eds., Kuroko and Related Volcanogenic Massive Sulphide Deposits: Economic Geology, Monograph 5, p. 365-386.

Dickie, G.J., 1983, Geology of the Adams Plateau property, Adams Plateau, B.C., NTS 82M/4: B.C. Ministry of Energy, Mines and Petroleum Resources, Assessment Report 11521, 20 p.

Dusel-Bacon, C. and Cooper, K., 1999, Trace-element geochemistry of metabasaltic rocks from the Yukon-Tanana Upland and implications for the origin of tectonic assemblages in East-Central Alaska: Canadian Journal of Earth Sciences, v. 36, p. 1671-1695.

Dusel-Bacon, C., Hopkins, M.J., Mortensen, J.K., Dashevsky, S., Bressler, J.R. and Day, W.C., this volume, Paleozoic tectonic and metallogenic evolution of the pericratonic rocks of east-central Alaska and adjacent Yukon, in Colpron, M. and Nelson, J.L., eds., Paleozoic Evolution and Metallogeny of Pericratonic Terranes at the Ancient Pacific Margin of North America, Canadian and Alaskan Cordillera: Geological Association of Canada, Special Paper 45, p. 25-74.

Floyd, P.A. and Winchester, J.A., 1978, Identification and discrimination of altered and metamorphosed volcanic rocks using immobile elements: Chemical Geology, v. 21, p. 291-306.

Gabrielse, H., Monger, J.W.H., Wheeler, J.O. and Yorath, C.J., 1991, Morphological belts, tectonic assemblages, and terranes, in Gabrielse, H. and Yorath, C.J., eds., Geology of the Cordilleran Orogen in Canada: Geological Survey of Canada, Geology of Canada, v. 4, also Geological Society of America, Geology of North America, v. G-2, p. 15-28.

Goldstein, S.L., O'Nions, R.K. and Hamilton, P.J., 1984, A Sm-Nd isotopic study of atmospheric dusts and particulates from major river systems: Earth and Planetary Science Letters, v. 70, p. 221-236.

Goodfellow, W.D., Cecile, M.P. and Leybourne, M.I., 1995, Geochemistry, petrogenesis, and tectonic setting of lower Paleozoic alkalic and potassic volcanic rocks, northern Canadian Cordilleran miogeocline: Canadian Journal of Earth Sciences, v. 32, p. 1236-1254.

Grant, S.L., 1997, Geochemical, radiogenic tracer isotopic, and U-Pb geochronological studies of Yukon-Tanana terrane rocks from the Money klippe, southeastern Yukon, Canada: M.Sc. thesis, University of Alberta, Edmonton, Alberta, 177 p.

Green, T.H., 1995, Significant of Nb/Ta as an indicator of geochemical processes in the crust-mantle system: Chemical Geology, v. 120, p. 347-359.

Hawkesworth, C.J., Kempton, P.D., Rogers, N.W., Ellam, R.M. and van Calsteren, P.W., 1990, Continental mantle lithosphere, and shallow level enrichment processes in the Earth's mantle: Earth and Planetary Science Letters, v. 96, p. 256-268.

Heaman, L.M., Erdmer, P. and Owen, J.V., 2002, U-Pb geochronologic constraints on the crustal evolution of the Long Range Inlier, Newfoundland: Canadian Journal of Earth Sciences, v. 39, p. 845-865

Hofmann, A.W., Jochum, K.P. Seufert, M. and White, W.M., 1986, Nd and Pb in oceanic basalts: new constraints on mantle evolution: Earth and Planeraty Sciences Letters, v. 79, p. 33-45.

Hollings, P., 2002, Archean Nb-enriched basalts in the northern Superior Province: Lithos, v. 64, p. 1-14.

Hollings, P. and Kerrich, R., 2000, An Archean arc basalt-Nb-enriched basalt-adakite association: the 2.7 Ga Confederation assemblage of the Birch-Uchi greenstone belt, Superior Province: Contribution to Mineralogy and Petrology, v. 139, p. 208-226.

Höy, T., 1987, Alteration, chemistry and tectonic setting of volcanogenic massive sulphide-barite deposits at Rea Gold and Homestake, southeastern British Columbia, *in* Exploration in British Columbia 1986: B.C. Ministry of Energy, Mines, and Petroleum Resources, p. B-7-B-19.

Höy, T., 1991, Volcanogenic massive sulphide deposits in British Columbia: *in* Ore Deposits, Tectonics and Metallogeny in the Canadian Cordillera: B.C. Ministry of Energy, Mines and Petroleum Resources, Paper 1991-4, p. 89-123.

Höy, T., 1999, Massive sulphide deposits of the Eagle Bay assemblage, Adams Plateau, south-central British Columbia (082M 3, 4), *in* Geological Fieldwork 1998: B.C. Ministry of Energy and Mines, Paper 1999-1, p. 223-245.

Höy, T. and Goutier, F., 1986, Rea Gold (Hilton) and Homestake volcanogenic sulphide-barite deposits, southeastern British Columbia (82M/4W), *in* Geological Fieldwork 1985: B.C. Ministry of Energy, Mines and Petroleum Resources, Paper 1986-1, p. 59-68.

Kepezhinskas, P., McDermott, F., Defant, M.J., Hochtaedter, A., Drummond, M.S., Hawkesworth, C.J., Koloskov, A., Maury, R.C. and Bellon, H., 1997, Trace element and Sr-Nd-Pb isotopic constraints on a three-component model of Kamchatka Arc petrogenesis: Geochimica et Cosmochimica Acta, v. 61, p. 577-600.

Hughes, N.D., 2001, Tectonic significance of the Early Cambrian (and older?) Eagle Bay assemblage, Vavenby area, south-central British Columbia: M.Sc. Thesis, University of Montana, Missoula, Montana, 90 p.

Hughes, N.D., Sears, J.W. and Chamberlain, K.R., 2003, New Upper Devonian U-Pb date for Eagle Bay felsic volcanics in the distal Cordilleran miogeocline, Vavenby, British Columbia [abstract]: Geological Society of America, Abstracts with Programs, v. 35, no. 5, p. 3

Ishikawa, Y., Sawaguchi, T., Ywaya, S. and Horiuchi, M., 1976, Delineation of prospecting targets for Kuroko deposits based on modes of volcanism of underlying dacite and alteration haloes: Mining Geology, v .26, p. 105-117**.**

Laflèche, M.R., Camiré, G. and Jenner, G.A., 1998, Geochemistry of post-Acadian, Carboniferous continental intraplate basalts from the Maritimes Basin, Magdalen Islands, Quebec, Canada: Chemical Geology, v. 148, p. 115-136.

Large, R.R., Gemmell, J.B., Paulick, H. and Huston, D.L., 2001, The alteration box plot: A simple approach to understanding the relationship between alteration mineralogy and lithogeochemistry associated with volcanic-hosted massive sulfide deposits: Economic Geology, v. 96, p. 957-971.

Leat, P.T., Jackson, S.E., Thorpe, R.S. and Stillman, C.J., 1986, Geochemistry of bimodal basalt-subalkaline/peralkaline rhyolite provinces within the southern British Caledonides: Journal of the Geological Society of London, v. 143, p. 259-273.

Lefebure, D.V. and Ray, G.E., 1995, Selected British Columbia mineral deposit profiles, Volume I - Metallics and coal: B.C. Ministry of Energy, Mines and Petroleum Resources, Open File 1995-20, 136 p.

Lefebure, D.V. and Höy, T., 1996, Selected British Columbia mineral deposit profiles, Volume II - More metallic deposits: B.C. Ministry of Employment and Investment, Geological Survey Branch, Open File 1996-13, 172 p.

Lentz, D.R., 1998, Petrogenetic evolution of felsic volcanic sequences associated with Phanerozoic volcanic-hosted massive sulfide systems: the role of extensional geodynamics: Ore Geology Reviews, v. 12, p. 289-327.

Lentz, D.R., 1999, Petrology, geochemistry and oxygen isotopic interpretation of felsic volcanic and related rocks hosting the Brunswick 6 and 12 massive sulfide deposits (Brunswick belt), Bathurst Mining Camp, New Brunswick, Canada: Economic Geology, v. 94, p. 57-86.

Le Roex, A.P., Dick-Henry, J.B. and Fisher, R.L., 1989, Petrology and geochemistry of MORB from 25 degrees E to 46 degrees E along the Southwest Indian Ridge; evidence for contrasting styles of mantle enrichment: Journal of Petrology, v. 30, p. 947-986.

Logan, J.M. and Mann, R.K., 2000, Geology and mineralization in the Adams-East Barriere lakes area, south-central British Columbia, 82M/04: British Columbia Ministry of Energy and Mines, Open File 2000-7, 1:100,000.

Logan, J.M. and Colpron, M., this volume, Stratigraphy, geochemistry, syngenetic sulphide occurrences and tectonic setting of the lower Paleozoic Lardeau Group, northern Selkirk Mountains, British Columbia, *in* Colpron, M. and Nelson, J.L., eds., Paleozoic Evolution and Metallogeny of Pericratonic Terranes at the Ancient Pacific Margin of North America, Canadian and Alaskan Cordillera: Geological Association of Canada, Special Paper 45, p. 361-382.

Loughman, F.C., 1969, Chemical weathering of the silicate minerals: American Elsevier, New York.

Lund, K., Aleinikoff, J.N., Evans, K.V. and Fanning, C.M., 2003, SHRIMP U-Pb geochronology of Neoproterozoic Windermere Supergroup, central Idaho: Implications for rifting of western Laurentia and synchroneity of Sturtian glacial deposits: Geological Society of America Bulletin, v. 115, p. 349-372.

MacLean, W.H., 1990, Mass change calculations in altered rock series: Mineralium Deposita, v. 25, p. 44-49.

MacLean, W.H. and Barrett, T.H., 1993, Lithogeochemical techniques using immobile elements: Journal of Geochemical Exploration, v. 48, p. 109-133.

Maniar, P.D. and Piccoli, P.M., 1989, Tectonic discrimination of granitoids: Geological Society of America Bulletin, v. 101, p.635-643.

McDonough, W.F., 1990, Constraints on the composition of the continental lithospheric mantle: Earth and Planetary Science Letters, v. 101, p. 1-18.

McLennan, S.M., 2001, Relationships between the trace element composition of sedimentary rocks and upper continental crust: Geochemistry, Geophysics, Geosystems, v. 2, Paper 2000GC000109.

Menzies, M.A., 1990, Archean, Proterozoic and Phanerozoic lithospheres, *in* Menzies, M.A., ed., Continental Mantle: Oxford Monographs on Geology and Geophysics, Oxford Press, Oxford, p. 67-86.

Meschede, M., 1986, A method of discriminating between different types of mid-ocean ridge basalts and continental tholeiites with the Nb-Zr-Y diagram: Chemical Geology, v. 56, p. 7-218.

Monger, J.W.H., 1993, Canadian Cordilleran tectonics, from geosynclines to crustal collage: Canadian Journal of Earth Sciences, v. 30, p. 209-231.

Monger, J.W.H. and Price, R.A., 2002, The Canadian Cordillera: Geology and tectonic evolution: Canadian Society of Exploration Geophysicists, Recorder, v. 27, no. 2, p. 17-36.

Monger, J.W.H., Wheeler, J.O., Tipper, H.W., Gabrielse, H., Harms, T., Struik, L.C., Campbell, R.B., Dodds, C.J., Gehrels, G.E. and O'Brien, J., 1991, Part B. Cordilleran terranes, Upper Devonian to Middle Jurassic assemblages (Chapter 8), *in* Gabrielse, H. and Yorath, C.J., eds., Geology of the Cordilleran orogen in Canada: Geological Survey of Canada, Geology of Canada, no. 4, also Geological Society of America, The Geology of North America, v. G-2, p. 281-327.

Morris, G.A., Larson, P.B. and Hooper, P.R., 2000, 'Subduction style' magmatism in a non-subduction setting: the Colville igneous complex, NE Washington State, USA: Journal of Petrology, v. 41, p. 43-67.

Mortensen, J.K., 1992a, Pre-mid-Mesozoic tectonic evolution of the Yukon-Tanana terrane, Yukon and Alaska: Tectonics, v. 11, p. 836-853.

Mortensen, J.K., 1992b, New U-Pb ages for the Slide Mountain terrane in southeastern Yukon Territory, *in* Radiogenic Age and Isotopic Studies: Report 5: Geological Survey of Canada, Paper 91-2, p. 167-173.

Nelson, J.L., 1993, The Sylvester allochthon: Upper Paleozoic marginal-basin and island-arc terranes in northern British Columbia: Canadian Journal of Earth Sciences, v. 30, p. 631-643.

Nelson, J.L. and Bradford, J.A., 1993, Geology of the Midway-Cassiar area, northern British Columbia: B.C. Ministry of Energy, Mines and Petroleum Resources, Geological Survey Branch, Bulletin 83, 94 p.

Nelson, J. L., Paradis, S., Christensen, J. and Gabites, J., 2002, Canadian Cordilleran Mississippi Valley-type deposits: A case study for Devonian-Mississippian back-arc hydrothermal origin: Economic Geology, v. 97, p. 1013-1036.

Nelson, J.L., Colpron, M., Piercey, S.J., Dusel-Bacon, C., Murphy, D.C. and Roots, C.F., this volume, Paleozoic tectonic and metallogenic evolution of the pericratonic terranes in Yukon, northern British Columbia and eastern Alaska, *in* Colpron, M. and Nelson, J.L., eds., Paleozoic Evolution and Metallogeny of Pericratonic Terranes at the Ancient Pacific Margin of North America, Canadian and Alaskan Cordillera: Geological Association of Canada, Special Paper 45, p. ??.

Niu, Y., Collerson, K. D., Batiza, R., Wendt, J. I. and Regelous, M., 1999, Origin of enriched-type mid-ocean ridge basalt far from mantle plumes: The East Pacific Rise at 11°20′N: Journal of Geophysical Research, v. 104, p. 7067-7087.

Okulitch, A.V., 1974, Stratigraphy and structure of the Mount Ida Group, Vernon (82L), Seymour Arm (82M), Bonaparte Lake (92P) and Kettle River (82E) map-areas, British Columbia: Geological Survey of Canada, Paper 74-1A, p. 25-30.

Okulitch, A.V., 1975, Stratigraphy and structure of the western margin of the Shuswap metamorphic complex, Vernon (82L), and Seymour Arm (82M) map-areas, British Columbia: Geological Survey of Canada, Paper 75-1A, p. 27-28.

Paradis, S. and Nelson, J.L., 2000, The Devonian-Mississippian metallogenetic history of Western Canada, from plate margin to continent interior [abstract]: Volcanic Environments and Massive Sulfide Deposits, International Conference and Field Trip, Hobart, Tasmania, November 2000, Program with Abstracts, p. 139.

Paradis, S., Bailey, S.L., Hughes, N.D., Piercey, S.J. and Höy, T., 2003a, Geochemistry and paleotectonic settings of the Eagle Bay VHMS and SEDEX deposits, British Columbia [abstract]: Geological Association of Canada, Program with Abstracts, v. 28, Abstract 60.

Paradis, S., Nelson, J.L., Piercey, S.J., Bailey, S.L., Höy, T., Murphy, D.C. and Peter, J., 2003b, Devonian-Mississippian sulphide deposits of western Canada as an expression of continent margin tectonics [abstract]: Geological Association of Canada, Program with Abstracts, v. 28, Abstract 59.

Pearce, J. A., 1983, Role of sub-continental lithosphere in magma genesis at active continental margins, *in* Hawkesworth, C.J. and Norry, M.J., eds., Continental Basalts and Mantle Xenoliths: Shiva Publications, Nantwich, U.K., p. 230-249.

Pearce, J.A., 1996, A user's guide to basalt discrimination diagrams, *in* Wyman, D.A., ed., Trace Element Geochemistry of Volcanic Rocks: Applications for Massive Sulphide Exploration: Geological Association of Canada, Short Course Notes, v. 12, p. 79-113.

Pearce, J. A. and Parkinson, D., 1993, Trace element models for mantle melting: applications to volcanic arc petrogenesis, *in* Prichard, H.M., Alabaster, T., Harris, N.B.W. and Neary, C.R., eds., Magmatic Processes and Plate Tectonics: Geological Society of London, Special Publication 76, p. 373-403.

Pearce, J. A. and Peate, D. W., 1995, Tectonic implications of the composition of volcanic arc magmas: Annual Reviews of Earth and Planetary Science, v. 23, p. 251-285.

Pearce, J.A., Harris, N.B.W. and Tindle, A.G., 1984, Trace element discrimination diagrams for the tectonic interpretation of granitic rocks: Journal of Petrology, v. 25, p. 956-983.

Pell, J., 1994, Carbonatites, nepheline syenites, kimberlites and related rocks in British Columbia: B.C. Ministry of Energy, Mines and Petroleum Resources, Bulletin 88, 136 p.

Piercey, S.J., Paradis, S., Murphy, D.C. and Mortensen, J.K., 2001, Geochemistry and paleotectonic setting of felsic volcanic rocks in the Finlayson Lake volcanic-hosted massive sulfide (VHMS) district, Yukon, Canada: Economic Geology, v. 96, p. 1877-1905.

Piercey, S.J., Mortensen, J.K., Murphy, D.C., Paradis, S. and Creaser, R.A., 2002, Geochemistry and tectonic significance of alkalic mafic magmatism in the Yukon-Tanana terrane, Finlayson Lake region, Yukon: Canadian Journal of Earth Sciences, v. 39, p. 1729-1744.

Piercey, S.J., Murphy, D.C., Mortensen, J.K. and Creaser, R.A., 2004, Mid-Paleozoic initiation of the northern Cordilleran marginal backarc basin: Geologic, geochemical, and neodymium isotope evidence from the oldest mafic magmatic rocks in the Yukon-Tanana terrane, Finlayson Lake district, southeast Yukon, Canada: Geological Society of America Bulletin, v. 116, p. 1087-1106.

Piercey, S.J., Nelson, J.L., Colpron, M., Dusel-Bacon, C., Roots, C.F. and Simard, R.-L., this volume, Paleozoic magmatism and crustal recycling along the ancient Pacific margin of North America, northern Cordillera, *in* Colpron, M. and Nelson, J.L., eds., Paleozoic Evolution and Metallogeny of Pericratonic Terranes at the Ancient Pacific Margin of North America, Canadian and Alaskan Cordillera: Geological Association of Canada, Special Paper 45, p. ???.

Plank, T. and Langmuir, C.H., 1998, The chemical composition of subducting sediment and its consequences for the crust and mantle: Chemical Geology, v. 145, p. 325-394.

Poole, F.G., Stewart, J.H., Palmer, A.R., Sandberg, C.A., Madrid, R.J., Ross, R.J. Jr., Hintze, L.F., Miller, M.M. and Wrucke, C.T., 1992, Latest Precambrian to latest Devonian time; development of a continental margin, *in* Burchfiel, B.C., Lipman, P.W. and Zoback, M.L., eds., The Cordilleran Orogen: Geological Society of America, Geology of North America, v. G-3, p. 9-56.

Saeki, Y. and Date, J., 1980, Computer application to the alteration data of the footwall dacite lava at the Ezuri Kuroko deposits, Akito Prefecture: Mining Geology, v. 30, p. 241-250.

Schiarizza, P., 1989, Structural and stratigraphic relationships between the Fennell Formation and Eagle Bay assemblage, western Omenica belt, south-central British Columbia: Implications for Paleozoic tectonics along the paleocontinental margin of western North America: M.Sc. thesis, University of Calgary, Calgary, Alberta, 343 p.

Schiarizza, P. and Preto, V.A., 1987, Geology of the Adams Plateau-Clearwater-Vavenby area: B.C. Ministry of Energy, Mines and Petroleum Resources, Paper 1987-2, 88 p.

Sears, J.W. and Price, R. A., 2003, Tightening the Siberian connection to western Laurentia: Geological Association of America Bulletin, v. 115, p. 943-953.

Shervais, J.W., 1982, Ti-V plots and the petrogenesis of modern and ophiolitic lavas: Earth and Planetary Science Letters, v. 59, p. 101-118.

Shinjo, R., Chung, S-L, Kato, Y. and Kimura, M., 1999, Geochemical and Sr-Nd isotopic characteristics of volcanic rocks from the Okinawa Trough and Ryukyu Arc: Implications for the evolution of a young, intracontinental back arc basin: Journal of Geophysical Research, v. 104 (B5), p. 10591-10608.

Sillitoe, R.H., 1982, Extensional habits of rhyolite-hosted massive sulphide deposits: Geology, v. 109, p. 403-407.

Simard, R.-L., Dostal, J. and Roots, C.F., 2003, Development of late Paleozoic volcanic arcs in the Canadian Cordillera: an example from the Klinkit Group, northern British Columbia and southern Yukon: Canadian Journal of Earth Sciences, v. 40, p. 907-924.

Smith, A.D. and Lambert, R.St.J., 1995, Nd, Sr, and Pb isotopic evidence for contrasting origin of Late Paleozoic volcanic rocks from the Slide Mountain and Cache Creek terranes, south-central British Columbia: Canadian Journal of Earth Sciences, v. 32, p. 447-459.

Stern, R.A., Syme, E.C., Bailes, A.H. and Lucas, S.B., 1995, Paleoproterozoic (1.90-1.86 Ga) arc volcanism in the Flin Flon Belt, Trans-Hudson Orogen, Canada: Contributions to Mineralogy and Petrology, v. 119, p. 117-141.

Sun, S. and McDonough, W.F., 1989, Chemical and isotopic systematics of oceanic basalts: implications for mantle composition and processes, *in* Saunders, A.D. and Norry, M.J., eds., Magmatism in the Ocean Basins: Geological Society of London, Special Publication 42, p. 313-345.

Thompson, R.I. and Daughtry, K.L., 1998, Stratigraphic linkages across Vernon map area, British Columbia: Geological Survey of Canada, Paper 1998-A, p. 181-187.

Thompson, R.I., Nelson, J.L., Paradis, S., Roots, C.F., Murphy, D., Gordey, S.P. and Jackson, L.E., 2000, The "Ancient Pacific Margin" NATMAP Project: Year One: Geological Survey of Canada, Paper 2000-A14, p. 1-10.

Thompson, R.I., Glombick, P., Acton, S., Heaman, L., Freidman, R., Daughtry, K., Erdmer, P. and Paradis, S., 2002, New constraints on the age and distribution of the Chase Quartzite, Vernon (82L) and Lardeau (82K) map areas: Regional implications, *in* Cook, F. and Erdmer, P., eds., Slave-Northern Cordillera Lithospheric Evolution (SNORCLE) and Cordilleran Tectonics Workshop: Lithoprobe Report No. 82, p. 92-94.

Thompson, R.I., Glombick, P., Erdmer, P., Heaman, L.M., Lemieux, Y. and Daughtry, K.L., this volume, Evolution of the ancestral Pacific margin, southern Canadian Cordillera: Insights from new geologic maps, *in* Colpron, M. and Nelson, J.L., eds., Paleozoic Evolution and Metallogeny of Pericratonic Terranes at the Ancient Pacific Margin of North America, Canadian and Alaska Cordillera: Geological Association of Canada, Special Paper 45, p. ????.

Valsami, E. and Cann, J.R., 1992, Mobility of rare earth elements in zones of intense hydrothermal alteration in the Pindox ophiolite, Greece, *in* Parson, L.M., Murton, B.J. and Browning, P., eds., Ophiolites and their Modern Oceanic Analogues: Geological Society of London, Special Publication 60, p. 219-232.

van Staal, C.R., Winchester, J.A. and Bédard, J.H., 1991, Geochemical variations in Middle Ordovician volcanic rocks of the northern Miramichi Highlands and their tectonic significance: Canadian Journal of Earth Sciences, v. 28, p. 1031-1049.

Wasserburg, G.J., Jacobsen, S.B., DePaolo, D.J., McCulloch, M.T. and Wen, T., 1981, Precise determination of Sm/Nd ratio, Sm, Nd isotopic abundances in standard solutions: Geochimica et Cosmochimica Acta, v. 45, p. 2311-2323.

Wedepohl, K.H., 1995, The composition of the continental crust: Geochemica et Cosmochimica Acta, v. 59, p. 1217-1232.

Whalen, J.B., Currie, K.L. and Chappell, B.W., 1987, A-type granites: geochemical characteristics, discrimination and petrogenesis: Contributions to Mineralogy and Petrology, v. 95, p. 420-436.

Whalen, J. B., Rogers, N., van Staal, C. R., Longstaffe, F. J., Jenner, G. A. and Winchester, J. A., 1998, Geochemical and isotopic (Nd, O) data from Ordovician felsic plutonic and volcanic rocks of the Miramichi Highlands: petrogenetic and metallogenic implications for the Bathurst Mining Camp: Canadian Journal of Earth Sciences, v. 35, p. 237-252.

Wheeler, J.O. and McFeely, P., 1991, Tectonic assemblage map of the Canadian Cordillera and adjacent parts of the United States of America: Geological Survey of Canada, Map 1712A, 1: 2,000,000.

White, G.P.E., 1985, Hilton massive sulphide discovery (Rea Gold), Johnson Creek – Adams Lake Area (82M/4W), *in* Geological Fieldwork 1984: B.C. Ministry of Energy, Mines, and Petroleum Resources, Paper 1985-1, p. 77-83.

Whitford, D.J., McPherson, W.P.A. and Wallace, D.B., 1989, Geochemistry of the host rocks of the volcanogenic massive sulfide deposit at Que River, Tasmania: Economic Geology, v. 84, p. 1-21.

Winchester, J.A. and Floyd, P.A., 1977, Geochemical discrimination of different magma series and their differentiation products using immobile elements: Chemical Geology, v. 20, p. 325-343.

Wood, D.A., 1980, The application of a Th-Hf-Ta diagram to problems of tectonomagmatic classification and to establishing the nature of crustal contamination of basaltic lavas of the British Tertiary Volcanic Province: Earth and Planetary Science Letters, v. 50, p. 11-30.

APPENDIX 1 – U-PB ANALYTICAL TECHNIQUES

The samples selected for U-Pb geochronology were prepared and analyzed at the University of Alberta Radiogenic Isotope Facility, following procedures outlined by Heaman *et al.* (2002). Approximately 3-4 kg of samples was crushed with a steel jaw crusher and powdered to <300 µm using a Bico disk mill. Heavy mineral fractions were collected using a Wilfley table and zircons isolated using standard magnetic and heavy mineral fraction separation techniques. Individual zircon crystals were selected from mineral concentrates for U-Pb analysis based on clarity and grain morphology using a binocular microscope. Zircon crystals with fractures, alteration or inclusions were generally avoided during the selection process. The selected zircon fractions were spiked with a ^{205}Pb- ^{235}U tracer solution, dissolved in an HF/HNO$_3$ mixture, and purified U and Pb aliquots isolated using anion exchange chromatography. The isotopic compositions of U and Pb were determined on a solid source thermal ionization VG 354 mass spectrometer. All ages are calculated using the decay constants: ^{238}U - 1.55125x10^{-10}/yr and ^{235}U - 9.8485 x 10^{-10}/yr determined by Jaffey *et al.* (1971) and uncertainties reported at one sigma (see Table 2).

APPENDIX 2 – GEOCHEMICAL AND ISOTOPIC SAMPLES: ANALYTICAL TECHNIQUES AND PRECISIONS

Weathered surfaces of samples were removed with a diamond saw. The samples were crushed to 1.5 cm in a steel jaw crusher, and pulverized in a Bico ceramic disc grinder followed by reduction to <100 mesh powder in a ceramic ball mill. Final product is a 20g vial of representative powder suitable for acid dissolution or fusion. Powdered whole rock samples were analyzed for major and trace element compositions using fused bead X-ray fluorescence (XRF), acid dissolution inductively coupled plasma mass spectrometry (ICP-MS) and inductively coupled plasma emission spectrometry (ICP-ES) techniques at the Geological Survey of Canada's (GSC) analytical laboratories. The major elements (except H$_2$O, CO$_2$, FeO) were determined on fused beads by X-ray fluorescence (XRF). H$_2$O and CO$_2$ were analyzed by infrared spectroscopy, and FeO was analyzed by modified Wilson titration. The trace elements were analyzed by a combination of inductively coupled plasma emission spectrometry (ICP-ES: Cr, Ni, Co, Cu, Zn, Ba, La, Pb, Sc, Sr, V, Y, Yb and Zr if >100 ppm) and inductively coupled plasma mass spectrometry (ICP-MS: remaining REE, Cs, Rb, Th, Nb, U, Ga, Hf, Ta and Zr if <100 ppm) on totally dissolved samples using a combination of nitric, perchloric, and hydrofluoric acids, with a lithium metaborate flux. Further details on the methodology can be obtained from the GSC analytical chemistry lab website at http://gsc.nrcan.gc.ca/labs/chem_e.php.

Analytical precision and accuracy were calculated from repeat analyses of rock samples with matrices similar to those in this study. They were calculated from repeat analyses of internal felsic and mafic samples and details of the methods are available in Piercey *et al.* (2001, 2002).

Thirty-one samples were analyzed for their Nd isotopic composition at the University of Alberta Geochronology and Radiogenic Isotope Facility following the methods of Creaser *et al.* (1997). Whole rock powders accurately weighed, dissolved in concentrated HF and HNO$_3$, and spiked with a known amount of mixed ^{150}Nd-^{149}Sm tracer solution. The isotopic composition of Nd is determined in static mode by multi-collector Inductively Coupled Plasma Mass Spectrometry (MC-ICP-MS). All isotope ratios are normalized for variable mass fractionation to a value of ^{146}Nd / ^{144}Nd = 0.7219 using the exponential fractionation law. The ^{143}Nd/^{144}Nd ratio of samples is presented relative to a value of 0.511850 for the La Jolla Nd isotopic standard and is monitored by analysis of a cross-calibrated Alfa Nd isotopic standard during each analysis session. Sm isotopic abundances are measured in static mode by TIMS, and are normalized for variable mass fractionation to a value of 1.17537 for ^{152}Sm/^{154}Sm also using the exponential law. The mixed ^{150}Nd-^{149}Sm tracer solution used is calibrated directly against the Caltech mixed Sm/Nd normal described by Wasserburg *et al.* (1981). Using this mixed tracer, the measured ^{147}Sm/^{144}Nd ratios for the international rock standard BCR-1 range from 0.1380 to 0.1382, suggesting a reproducibility for ^{147}Sm/^{144}Nd of <± 0.1% for real rock powders. The value of ^{147}Sm/^{144}Nd determined for BCR-1 is within the range of reported literature values by isotope dilution methods. The initial εNd values for the samples were calculated at 300, 340, 360 and 540 Ma (see Table 5).